UNIVERSITY OF CATANIA

CIVIL ENGINEERING - ARCHITECTURE DEPARTMENT

Ph. D. COURSE
"EVALUATION AND MITIGATION OF URBAN AND LAND RISKS"
XXXII CYCLE

BIOTA IMPACT ON LEVEE STABILITY

ECOHYDRAULIC EVALUATION OF LEVEE FAILURE MECHANISMS AND REMEDIATION TECHNIQUES

Ph.D. Student

PENNISI VALERIA

Esame finale anno 2020

Tutor:

Prof. Ing. ENRICO FOTI

Prof. Ing. Antonio Cancelliere

Prof. Ing. Rosaria Ester Musumeci

Tutor of University of Hull:

Prof. Stuart McLelland

Industrial Tutor of TREVI S.p.A.:

Ing. Andrea Gunnella

La borsa di dottorato è stata cofinanziata con risorse del Programma Operativo Nazionale di Ricerca e Innovazione 2014-2020 (CCI 2014IT16M2OP005), Fondo Sociale Europeo, Azione I.1 "Dottorati Innovativi a caratterizzazione industriale" in partnership con l'Univerisità di Hull (UK) e la TREVI S.p.A.

We ourselves feel that what we are doing is just a drop in the ocean. But the ocean would be less because of that missing drop.

[Mother Teresa]

ABSTRACT

The greatest civilizations in human history have always developed near water and, in order to increase arable land, have built serval types of river structures to control the flow. Levees (also known as dikes), for instance, are simply man-made embankments built to keep a river from overflowing its banks. However, river flooding is a natural phenomenon so that it is not rare that rivers overflow their banks and flood the surrounding landscape causing considerable damages.

Researchers, technicians, land managers, and other stakeholders have attempted to overcome the problems of river flooding. However, the flood protection systems are complex, and their failure mechanisms are not yet completely understood. Additionally, contrary to past practices, it is not possible to investigate levee failure mechanisms only from the hydraulic and geotechnical perspectives. Levees are inserted in fluvial ecosystems where animals and vegetation play key roles. Indeed, levees are a habitat for animals, which often dig tunnels and holes inside these soil structures, altering their performance and possibly triggering failure phenomena.

The present dissertation operated in this framework of the failure levee induced by the presence of animals. This thesis aims to contribute to the flood risk mitigation in river ecosystem through the understanding of levee failure mechanisms induced by burrowing animal activities. Specifically, the main aspect of this work is to overcome the traditional approach used to study levee failures, to develop an eco-hydraulic approach, and to define a suitable remediation technique. To achieve these goals, after building a consistent view of the state of art, the research is divided into three main components.

The first part studies a flood that occurred in Sicily in 2012. In particular, the performance of the levees during this event and the probable levee failure mechanisms are investigated. Then levee structures are investigated in order to describe the main geometric characteristics of animal burrows. Specifically, after a visual inspection of the activity of burrowing animals, and after measuring the dimensions of the hole

entrances, a Ground Penetrating Radar (GPR) survey was carried out to investigate depths and paths of these dens.

The second part studies the effects derived from the presence of holes on the levee stability. In collaboration with the University of Hull, an eco-hydraulic analogue model and an image analysis procedure were designed. To look the effect that some geometrical paraments of holes have on the levee performance, the density, the position, and the length of the burrows are investigated. The results from comparing erosion in undisturbed levee with the case of weakened levees (i.e. with burrows) indicate that the erosion mechanism changes as a function of the vertical position of the burrows: the burrows above water level increase the total erosion, while the burrows located under the water level seem to reduce it. Moreover, the not orthogonal burrows related to the flow direction produce a greater surface erosion.

The third part is focused on industrial applications. To reduce soil permeability and to increase levee stability, in collaboration with Trevi S.p.A. engineering society, some remediation techniques were studied and selected. The research showed that a geotextile is the most suitable technique in order to reduce the levee instability. Indeed, this material is proper to different kind of morphological and geotechnical characteristics of soil conditions, and its application and maintenance are easy. Furthermore, it could be covered by natural vegetation to achieve a rapid regeneration of river flora on the levees.

CONTENTS

1. INTRODUCTION

1.1. Background

Flooding is probably the natural hazard with the highest occurrence in time and space across the world, causing every year a considerable amount of damage in terms of loss of lives and property [Jonkman and Vrijling, 2008; Loat, 2009]. Major floods in China, for example, killed about 2 million people in 1887, nearly 4 million in 1931, and about 1 million in 1938 [Mohamed Elmoustafa, 2012].

Flood levees are among the most ancient and widely used defense structures against river flooding in the world [Michelazzo, 2014]. It is estimated that there are several hundreds of thousands of kilometers of levees in Europe and the USA alone [CIRIA, 2013]. The U.S. National Flood Insurance Program (NFIP) defines a levee in Title 44, Chapter 1, Section 59.1 of the Code of Federal Regulations (44 CFR 59.1) as "a man-made structure, usually an earthen embankment, designed and constructed in accordance with sound engineering practices to contain, control, or divert the flow of water so as to reduce risk from temporary flooding."

Levees are barriers (earthen dikes or embankments) built on the banks of a river in order to prevent it from flooding the lateral areas [Michelazzo, 2014]. They have also the function of decreasing the surface area that a river would naturally flood thus extending human activities. This increases the flooding hazard by reducing lateral flood storage and hence the river capacity for laminating the flood wave; additionally, the amount of potential damages induced by flooding is dramatically increased in flood prone areas because these are now occupied by vulnerable elements (human lives, buildings, infrastructures, activities).

Unfortunately, the failure of levees or earth fill dams is not a rare event and it has caused a lot of damage. Following levee collapses, many countries in the world have experienced extensive and frequent losses of life and property [Jonkman and Vrijling, 2008; Loat, 2009]. In 1977, the failure of Laurel Run Dam (Pennsylvania, USA)

resulted in $ 5.3 million in damage; in 1997, the collapse of the Klamath levee (north California, USA) caused $350 million in losses; in 1997, the failure of Anita Dam (milk River, Montana, USA) produced $10.000 of ravages [FEMA, 2005]. In 2014, the breach of the Secchia earth levee (Italy) resulted $500 million of damage [Orlandini et al., 2015]. This kind of damages may take place in less than half an hour, but the losses are enormous.

In order to reduce flooding hazards through the use of adequate mitigation measures, it is necessary to evaluate the flood risk beforehand. To this end, most countries conduct flood mapping, to show the flood extent and assess human activities at risk. Nevertheless, the delineation of flooding-prone areas and the related hydraulic hazard mapping, taking account of uncertainty, are usually developed with scarce consideration of the possible occurrence of levee failures along the investigated river channel [Apel et al., 2008; Mazzoleni et al., 2014].

Flood protection systems are complex, interconnected, adaptive engineered systems where failure at one location means failure of the system, and failure at different locations may result in flooding of different areas. The levee failure mechanisms are usually studied as hydraulic or geotechnical phenomena. For these reasons, until now, all traditional approaches used to define vulnerability consider only the hydraulic and geotechnical characteristics of the levee.

Moreover, due to the large physical extent of such systems along rivers and canals and their varying age, and in the absence of as-built documentation, soil investigation data are at best available at scattered intervals along a levee length. Consequently, analyses carry a high level of uncertainty, and can be inconsistent, unreliable, or incomplete, depending on when and by whom the investigation was carried out [Saadi et al., 2013]. Accordingly, traditional studies of levee failure mechanisms are typically performed by assuming that levee systems are undamaged before the flood event occurs [Camici et al., 2017].

This is not always a true and faithful picture of the most common situation, though. Frequently, levees are ideal habitats for animals, which often dig tunnels and

holes inside these earth structures for habitat or in search for food or prey. The vegetation at the inner side of the dike and the isolation of the levee from human presence attract the animals [Taccari et Van Der Meij, 2016]. Thus, levees offer an ideal environment for the dispersal of different species of burrowing animals, such as badgers, porcupines, coypus (nutrias) and red swamp crayfishes.

Most of the detrimental activities of animals result in altering external and internal geometry and integrity of earth levees. Nevertheless, most classical geotechnical engineering textbooks and specific technical reports [e.g., Terzaghi et al., 1996; Resio et al., 2011] do not even mention wildlife activity among the relevant factors causing the failure of earthen dams and levees. Only a few seminal works have explicitly and mechanistically connected seepage, piping, and erosion responsible for the failure of earth structures to preferential flow extending along paths developed by burrowing animals [Carroll, 1949; Masannat, 1980; Bayoumi and Meguid, 2011].

Even though the impacts of biota activities are still rarely acknowledged by engineers, technicians, and land managers as a potentially serious threat to dam and levee stability, in recent years the topic has become more relevant in the scientific and technical community. A multidisciplinary approach is needed that involves all the relevant stakeholders, as engineers, ecologists, geologists and managers of water resources.

1.2. Aim of the work

Failure of river levees is one of the most frequent causes of riverine flooding and the technical-scientific community is interested in this phenomenon because of the low predictability and incomplete understanding of its mechanisms.

The objective of the present work is to contribute to flood risk mitigation in river systems through a better understanding of the levee failure mechanisms induced by animal activities, and the development of methodologies and technologies that take

the interactions between such faunal bioturbation, levees stability and the consequent flood risk into account.

The traditional study of levee failures is based on hydraulic and geotechnical approaches and, in many cases, this flood risk assessment may not be sufficient. Indeed, structural deterioration could lead to the failure of an earth structure, and it may be due not just to hydraulic and geotechnical changes, but also to animal bioturbation effects. Animal's activities cause cracks and macropores, which compromise the stability of earth structures. Nevertheless, such biological impacts are not easy to evaluate and, although the need to take the interaction between earth structures and fauna activities into account is widely recognized, the scientific research is still in its infancy and there are not shared methodologies to address the problem.

Consequently, the most important aspect of this research is to overcome the traditional methodology for the study of levee failure mechanisms, which is based only on hydraulic and geotechnical approaches. Thus, a new multidisciplinary approach is proposed, based on eco-hydraulic methodologies, intending to understand the main factors trigger levee failures in the presence of faunal components, namely of burrowing animals. For this, it is important to evaluate the levee state of health, to understand animal behaviour and to define their most common burrow configurations. This knowledge will be useful in order to define parameters to be investigated as regards the tendency of triggering the failure mechanisms.

Specific objectives are, first, to propose methods to evaluate the presence of burrowing animals in levee structures, then to estimate the tendency of burrow to trigger the failure process and, last but not least, to propose some remediation techniques. Indeed, the geometries of animal burrows and the recognition that some configurations are prone to cause failure give important information that allows for appropriate remediation techniques and simplifying the choice of interventions.

1.3. Methodology

In order to evaluate the role played by biota in past flooding events, numerical and analytical approaches are adopted. A flood event is selected as a case study. The area where the event occurred is evaluated for possible burrowing animal activity. Using rainfall-runoff and flood propagation modelling, the flow rate of the historical flood event is estimated, and consequently flooding stages are assessed. Considering the flood hydrograph and assuming that levees were undamaged, an evaluation of overtopping and possible seepage phenomena is carried out. In particular, to evaluate the overtopping phenomenon, flow profiles are simulated using the HEC-RAS software. Marchi's (1961) and Green-Ampt's (1911) analytical models are used to evaluate seepage vulnerability of levees associated to the emergence of the phreatic line along the landside of the levee. Nevertheless, analyses showed that the flow profile was not too high to justify overtopping and seepage did not occur, so that an assessment of the levee status is conducted. In particular, the potential presence of burrows on the case-study levees is surveyed using a Ground Penetrating Radar (GPR). Through these field analyses, knowledge about burrow configurations is acquired.

An experimental approach is applied for evaluating the impact of biota. The direct interaction between flow characteristics and animal burrows is the main element to evaluate the failure mechanisms. Thanks to the collaboration with researchers at the University of Hull, a simplified methodology to study biota impacts was planned and developed. After analysing real burrow configurations, simple parameters are defined to represent them. The selected burrow configurations are investigated in a physically-based analogue model at the Laboratory of Physical Geography, University of Hull. This experimental approach has become to be a valuable analogue to natural landscapes, if analysed correctly [Paola et al., 2009; Kleinhans at al., 2014]. The scale of these experiments is such that they do not provide a geometrically scaled version of what to expect in reality. Regardless, these experiments exhibit a range of processes and associated morphologies that could occur in natural landscapes, and

that could give the idea of biota impact on levee stability. The experimental campaign conducted consisted of 110 experiments, in addition to a rather wide range of calibration tests to individuate the optimized soil composition, which allows the proper trade-off between the medium time of erosion and burrow stability.

In order to propose potential remediation techniques that are successful, innovative, and eco-friendly, we collaborate with Trevi S.p.A., a worldwide leader in underground engineering, which has been actively involved in solving seepage problems in existing levees (with a specific focus on water-tightness of the levee body, walls and bottom). Thanks to the advanced knowledge and expertise of the company, as well as the time working at Trevi's building sites, different technologies were observed and studied. In particular, in order to reduce natural permeability and surface erosion, special technologies and systems to set up "impermeable" screens, as well as soil treatment or geotextile products, are considered.

Different intervention techniques are examined, as well as the equipment, times and site organization necessary for their application. All these engineering methods are evaluated and studied for the purpose of re-establishing levee functions.

1.4. Limits

Research limitations are an important and unavoidable aspect of any study. For this reason, it is not only relevant to identify and acknowledge the shortcoming of a piece of work, but also to understand how these limitations affect the results.

The novel multidisciplinary approach used, based on eco-hydraulic methodologies, is quite innovative and it is not supported by an extensive literature. Indeed, the correlation between presence of burrows and levee failure has not yet been unequivocally demonstrated.

For these reasons, in order to discover the hydrodynamic and morphodynamic parameters that regulate the complex system of levee failures, the experimental approach at the laboratory scale was a physically-based analogue model. Obviously,

the model simplified some of the relevant geometrical parameters; nevertheless, it allowed us to obtain physical information on eroded systems in the presence of burrows.

As regards the analytical and numerical analyses, computational limits and difficulties in determining suitable boundary conditions implied the need for further simplifying hypotheses of the problem. All such limitations are discussed in the appropriate section of the work.

However, although the abovementioned limitations impose constraints on the possibility of obtaining a complete vision of the studied processes, it is believed that the present work may constitute a promising approach from a scientific point of view, and that it provides useful recommendations from an engineering perspective.

1.5. Organization of the work

To achieve the objectives, a systematic research organized step-by-step is found to be indispensable. The first step of the research is an overview of the relevant scientific literature on the subject aimed at building a unitary, consistent view of the state of art. During this phase, the driving forces and the possible mechanisms that trigger failure are studied (Section 2). The research focuses on specific failure mechanisms, such as seepage, piping and internal erosion (Section 2.3) and on recognized assessment methodologies (Section 2.4).

In Chapter 3, the relationship between failure mechanisms and not always obvious biota activities are investigated. In particular, the importance of an eco-hydraulic investigation, as a suitable interdisciplinary approach to study the present issue, is discussed in Section 3.2. Then an overview of the behavior of different burrowing animals (Section 3.3) and of the state of art of the topics (Section 3.4) are summarized.

The next part of the work is divided into three closely interlinked themes: the first is focused on a historical flood event and corresponding field survey; the second

is concentrated on the physical modelling; the last is focused on identifying the best, if possible eco-friendly, remediation techniques and practical applications.

In Chapter 4, an investigation of a real flood event is presented. First, a description of the study site is offered (Section 4.2). Then, a hydrological analysis is performed (Section 4.3) in order to reconstruct flood hydrographs of the 2012 event and to investigate the mechanisms that triggered the levee failure. A control and non-destructive investigation of levee structures is performed by means of GPR (Section 4.4). As, the investigated zone is indeed inhabited by burrowing animals, important information about burrow configuration is collected.

In Chapter 5, the eco hydraulic experimental analyses are presented and the importance of setting an analogue model are highlighted (Section 5.2). In particular, the setup of the experiment (Section 5.3), the experimental procedures (Section 5.5), the preliminary test on levee material (Section 5.6), the analysis procedure (Section 5.7) and the investigated parameters (Section 5.9) are presented. A total of 110 number of experiments were carried out at the University of Hull.

The experimental activities aim to understand the connection between burrow configuration and the surface erosion development, comparing the failure mechanisms of undisturbed levees with those of weakened levees. All the analysis results are summarized in Chapter 6. In particular, the difficulties encountered using a 40 cm long levee are described in Section 6.2. Then, the surface erosion analyses of 100 cm long undisturbed levees (Section 6.3) and 40 cm long undisturbed levees (Section 6.4) are discussed. These results are the most suitable benchmark for the analysis of burrows' impact on the surface erosion phenomenon, considering both 40 cm long levee (Section 6.5) and 100 cm long levee (Section 6.6).

Chapter 7 describes the remediation techniques that can be used to solve the problems of seepage and surface erosion on earth structures. The research is made in collaboration with Trevi S.p.A., leader in the field of geotechnical engineering. Particular attention is paid to different techniques of soil consolidation, such as cased secant piles (Section 7.2), jet grouting (Section 7.3), and micropiles (Section 7.4), as

well as soil sealing, like cement and chemical grouting (Section 7.6). Some building sites where these technologies were applied are described. Moreover, in order to propose an eco-friendly solution, a less invasive and suitable technology is presented in Section 7.8. Specifically, it is a geotextile product able to enhance levee stability without changing the soil composition.

The dissertation is concluded with a discussion of the main results, of the practical implications, and of future research lines.

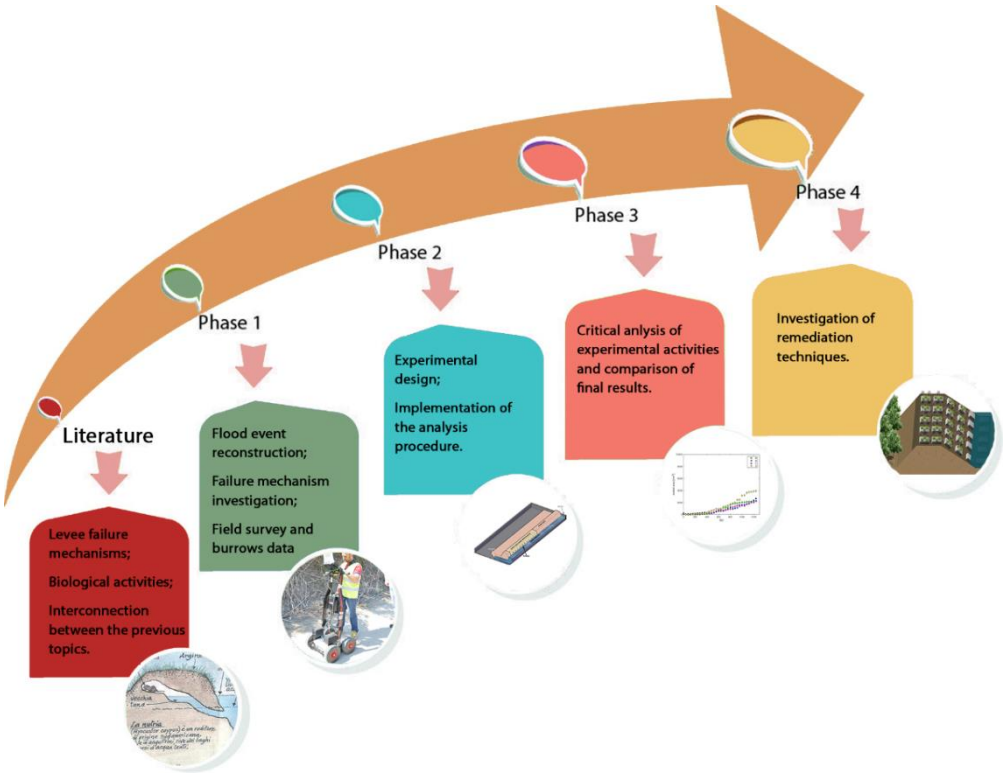

Figure 1-1:Sketch of the organization of dissertation work.

2. MECHANISMS OF LEVEE FAILURE

2.1. Overview

Past and current disasters and the increased frequency of devastating flood events have triggered many governments around the globe to invest in comprehensive flood risk management initiatives, such as flood control schemes, early warning systems and evacuation planning [Black et al., 2019].

As the recent flood in Arkansas shown in Figure *2-1*, numerous flood events are the consequence of levee failure, the retaining structures, parallel to the flow, designed to contain or guide river flow.

Figure 2-1: Flood waters from the Arkansas River rush trough a broken levee 1st June 2019 [Thomas Metthe - Arkansas Democrat Gazette 31st May 2019].

Levee failures are frequent and are not always predictable. The scientific community has studied and analyzed different mechanisms, the trigger causes, and has attempted to define distinct phases of their development.

Unfortunately, there is no single vision of levee failure mechanism that everyone agrees on and this is perhaps due to the differences in failure processes and in material and structures types. Indeed, all the processes could be quite different as a function of soil type and state of the levee. Moreover, the complexity of levee failure mechanisms are heightened by the manifold interactions between structure, soil and water.

In the following sections a brief description of the main mechanisms of levee failure is presented, with a special focus on the seepage phenomenon and on the typical methodologies of hazard assessment.

2.2. Physical mechanisms of levee failure

A river levee not only protects lower lands from flooding but is also an environmentally important link between the land and rivers. Global climate change and urbanization have increased the incidences of abnormal floods exceeding the design flood discharge, so that river levees have become more vulnerable to flood damage [Ko et Kang, 2018].

Levee instability may be due to many reasons, but the consequence are always huge losses of both lives and properties. In order to reduce flood risk, it is first necessary to understand the mechanisms that trigger the failure phenomena.

A levee is typically constructed of compacted earth drawn from locally available sources. The central core is usually built of clay or silty clay, which has a high degree of workability and a low permeability that guarantees a good protection against seepage. Usually, a river levee is about 3-6 m high and its crest is 3-4.5 m wide. The cross section is commonly trapezoidal, with side slopes ratio of about 2 horizontal distance units every 1 vertical rise (2H:1V). The geometries of flood protection levees vary considerably, based on the level of intended protection and local experiences

with successful levee construction. Figure *2-2* shows a typical geometry of a levee for primary flood protection.

Levee response and performance are dependent on the hydraulic conditions (river flow), as well as the levee geometry and the properties of its materials and foundation soils [Saadi et al., 2013]. For example, the use of different materials may change levee performance: non cohesive fill, cohesive fill and rock fill materials lead to different erosion mechanisms [Morris, 2009]. However, levees are typically built from locally excavated soil, thus the construction material choice is conditional upon the cost-benefit analysis. Moreover, soil compaction during construction and its moisture content are significant factors for the durability of the structures.

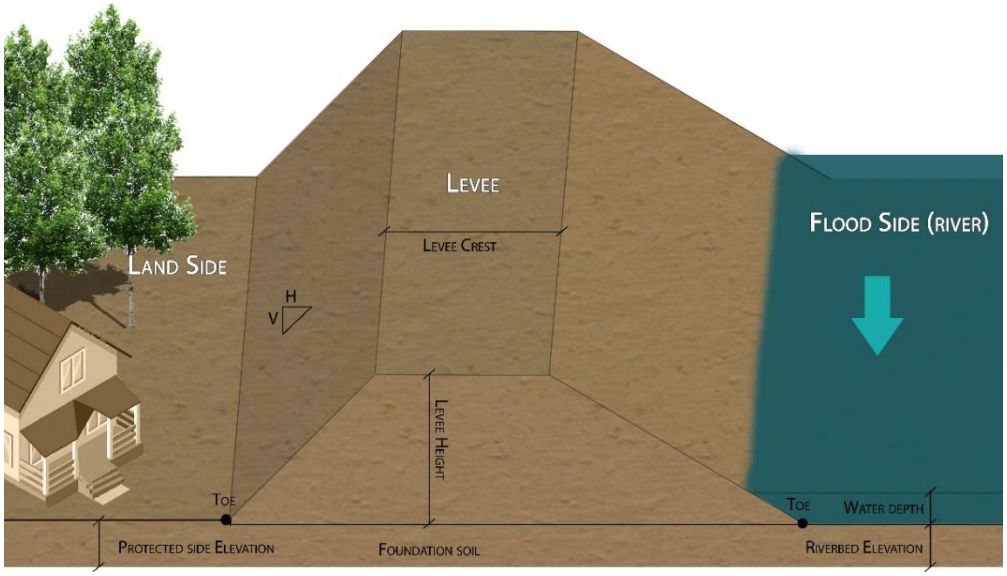

Figure 2-2: Definitions of terms associated with river levees

Furthermore, river flow conditions significantly affect levee durability. Indeed, water levels, flow velocity and water volumes, as well as flood duration, which are constantly changing, generate continuous variations in total stress within levee slopes. Interaction between the structure and water levels generates hydrodynamic and hydro-

geotechnical processes and erosion mechanisms which may lead to the initiation of a failure mechanism.

The main failure mechanisms can be grouped into three main categories: causes involving surface degradation, structural causes, and hydraulic causes.

Surface degradation of the levee includes different types of surface erosion caused by surface water flowing over or against the surface of the levee [Yang et Wang, 2015]. The most common causes of surface degradation are: overtopping (Figure 2-3/1a), overtopping and jetting (Figure 2-3/1b), surface erosion (Figure 2-3/3), and wave impact (Figure 2-3/5).

Structural cases of levee failures are mainly dependent on the strength of the soil. For example, sliding (Figure 2-3/4), physical objects that collide with the levee (Figure 2-3/6), tree damage (Figure 2-3/9), and slope failure (Figure 2-3/10) are classified as structural mechanisms. An example of a catastrophic structural levee failure was the 17th Street breach during Hurricane Katrina, where 200 ft of the levee failed due to sliding [Heerden, 2005].

Hydraulic causes are connected to water that flows through or under the levee body. This form of failure includes seepage/internal erosion/piping (Figure 2-3/2), liquefaction (Figure 2-3/7), and piping of substratum (Figure 2-3/8).

Although all above mechanisms can contribute to levee failure, overtopping and seepage are among the most frequent causes that initiate the breaching process of a levee [Horlacher et al., 2005; Nagy and Tòth, 2005; Nagy, 2006; Morris et al., 2007].

Overtopping occurs when the river stage exceeds the crest of the levee so that water spills over it. Because of the levee's relatively steep landside slopes, water moves rapidly down the landside, initiating erosion in locally weak spots where the flow tends to concentrate the erosive forces [Saucier et al., 2009].

Actually, surface erosion, referred to as a continuous degradation of a levee's surface over a wide area, leads to substantial reduction in levee cross section and loss of its function as a protection system. Thus, the overtopping could be a consequence of excessive surface erosion.

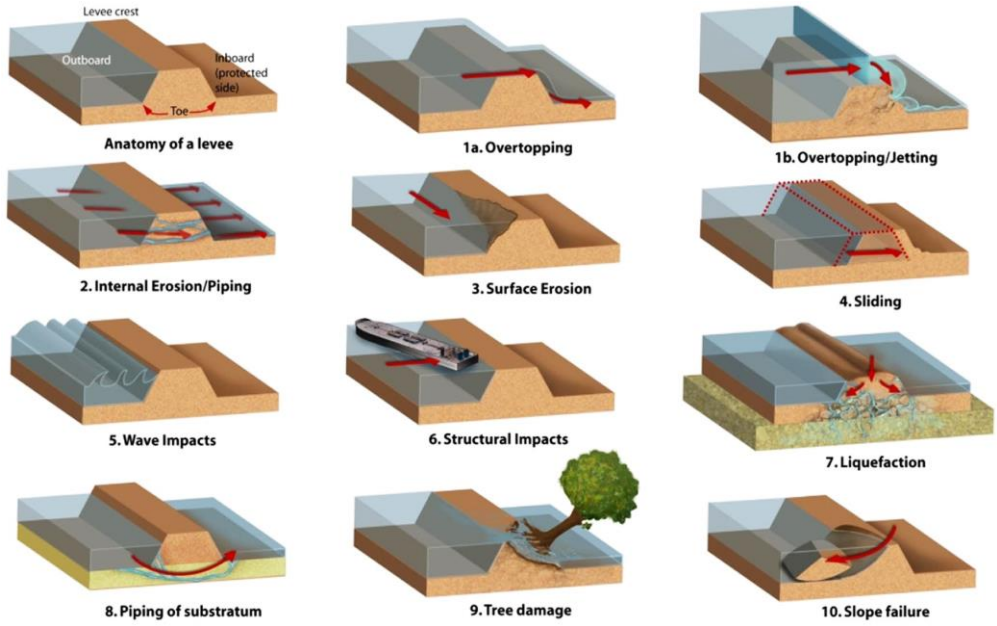

Figure 2-3: Failure mechanisms of earth levees [Deretsky, 2010].

Generally, both hydraulic and surface degradation mechanisms generate a levee breach because an erosion phenomenon is triggered. Indeed, among various failure mechanisms that cause levee breaches, soil erosion is found to be one of the most important factors [Kamalzareet al., 2013, Seed et al., 2008].

Nevertheless, even though predicting soil erosion and scour generation is very important in order to design stable levee and floodwalls, this task is not easy. The main variables affecting levee slope erosion are velocity, shear stress, and the significant displacement of sediment mass. Unfortunately, computing shear stresses involves major difficulties and most of the existing shallow water erosion models do not resolve the dynamic bed deformation [Cantero-Chinchilla et al., 2019].

While overtopping can lead a levee to breach because external erosion mechanisms take place, seepage of water through and under a levee during times of flood may become a matter of concern for the safety of a levee when internal erosion

mechanisms occur [Ozkan, 2003]. Indeed, the seepage phenomenon could initiate motion of soil particles from the inner core of a levee or from its foundation layer. This mechanism triggers internal erosion and causes piping. The problem of internal soil stability when particles are subject to drag forces resulting from reservoir seepage is one of the major concerns regarding the safety of embankment dams [Arulanandan et Perry, 1983]. Seepage of water through and under a levee during a flood may become a matter of concern for the safety of a levee when internal erosion mechanisms occur [Ozkan, 2003].

The following section presents a brief description of seepage phenomena and of the most common methodology used for assessing it.

2.3. Seepage phenomenon

In recent years, the number of levee failures has increased dramatically along several Italian embanked rivers with catchment areas ranging from a few dozen to more than 1500 km^2, meaning that this problem is now of critical importance at a national scale [Barbetta et al., 2015]. Most such levee collapses shared a similar failure mechanism of internal erosion without overtopping, as, for instance the levee failures on the river Po [Mazzoleni et al., 2014] and the river Serchio [Cosanti et al., 2011]. This phenomenon is called seepage.

Usually, the seepage phenomenon is generated from changing hydrostatic levels due to varying river discharges. Specifically, a local increase in gradient may capture more seepage flow, intensifying erosion [Hagerty, 1992] so that the soil particles are moved, and the earth structure is weakened.

Terzaghi et al. (1996) showed that the moving of a mass of soil as a result of seepage forces takes place if the average hydraulic gradient i_{av} downstream of the structure exceeds the critical gradient i_c. The value i_{av} is calculated by considering the average hydraulic gradient in the prism of soil adjacent to the toe. The critical gradient corresponds to the quicksand condition, which occurs when the effective stress in the

soil is reduced to zero. If all the forces acting on a unit volume of soil through which seepage occurs are considered, i_c can be calculated as:

$$i_c = \gamma'/\gamma_w \quad (1)$$

where γ' indicates the submerged unit weight of soil and γ_w the unit weight of water.

Actually, seepage of water through and under a levee during passage of a flood is a natural phenomenon. However, a failure mechanism often triggered by seepage is piping.

When flow lines concentrate towards the open exit, the local hydraulic gradient increases and the seepage pressure exceeds the submerged weight of the soil grains, so that internal erosion is triggered within the levee. At that moment, seepage becomes a matter of concern for the safety of the structure. The erosion of soil particles from the internal core damages the levee and/or its foundation, resulting in settlements or collapses [Ozkan, 2003]. Actually, the internal erosion of sandy soil creates approximately cylindrical conduits, or "pipes." Consequently, this form of erosion has been called "piping," defined by Mears (1968) as ". . . subterranean erosion initiated by percolating waters which remove solid particles [...] to produce tubular underground conduits" [Hagerty et al., 1992].

In short, piping refers to the development of pipes, but also it is referred by the occurrence of channels at the landside of the levee structure where the flow lines converge [Sellmeijer, 1988]. The subsequent erosion process develops backwards as a headcut and, if the process continues, the structure may collapse in the end.

For internal erosion to produce cavities, there must be a free face or external plane from which seepage outflow can first remove soil particles. A source of water must be available to supply the requisite flow; the source need not be constant since the mechanism can operate intermittently. Generally, flow must be concentrated in order that the intensity of exfiltration, characterized by the exit hydraulic gradient, will be sufficient to remove soil particles. If piping is to occur, the exit gradient must produce seepage forces sufficient to overcome all the forces and factors that tend to keep particles in place: interlocking with other particles, which interferes with

movement; inter-particle friction, which resists motion; cohesion between grains derived from physicochemical attraction including capillary forces; cementation; binding by roots; and, in some cases, gravity forces [Hagerty et al., 1992].

The detrimental effects of concentrated seepage outflow in cohesionless soils have long been recognized [Terzaghi, 1929]. Instability in soil embankments caused by seepage-related internal erosion was described by Casagrande (1936), and the importance of this erosion mechanism to the safety of dams has been repeatedly demonstrated [Reuss et Schattenberg, 1972; Sherard et al., 1972].

In order to reduce levee failures due to seepage, a well-designed earth structure should contain the phreatic line within its body, and the possibility of seepage flow from the landside of the levee should be avoided or, at least, controlled and limited to small values. That condition in which the phreatic line reaches the landside is in itself a hydraulic failure of the levee performance and represents a dangerous situation that affects the levee reliability, as it may lead to consequent critical conditions for erosion of soil particles [Michelazzo et al., 2016]. The importance of this condition is also stated by Camici et al. (2017) and it is verified in a case study, as, for instance, the levee breach of the river Secchia that was triggered by the emergence of seepage flow on the landside slope during the 2009 event [Bonanni et al., 2010; Cosanti et al., 2011].

The propensity of a levee to undergo seepage processes without overtopping, that is its seepage vulnerability, is recognised as a key point to assess the reliability of flood defence systems.

2.4. Assessment of the seepage phenomenon

Until now, all traditional approaches used to define seepage vulnerability only consider the hydraulic and geotechnical characteristics of a levee. The aim of vulnerability assessment is to find the critical condition for which the process may produce extreme erosion, that is, piping in the levee resulting in its inevitable collapse [Camici et al., 2017]. These approaches generally compare the time scales of the

seepage process to the persistence of flood levels in the river. The time scale of the through-seepage process associated with the state of the phreatic line reaching the landside surface is addressed as a typical condition that may lead to successive failures, as stated previously.

Different analytical models have been proposed in order to describe seepage through the body of a levee, but they all start from two main assumptions: i) homogenous and isotropic geotechnical properties of the soil composing both the levee body and its foundation, in terms of hydraulic conductivity k and porosity n; ii) trapezoidal shape of the levee's cross-section.

As previously mentioned, the critical condition is found when the phreatic line reaches the landside slope of the levee cross-section, which leads to internal erosion mechanisms and, thus, to a quick development towards a full breach in the levee system. Michelazzo et al. (2016) states that the comparison between Marchi's (1961) and modified Green–Ampt's [Pistocchi et al., 2004] methods allow one to evaluate a conservative prediction that can be implemented in a straightforward way for long reaches of embanked rivers. Indeed, these two models give a different prediction of the phreatic line positions. Marchi's model tends to give reliable results for the seepage flow in the lower region of the levee body, whereas it underestimates the position of the saturation line in the region near the levee crest. Instead, an adapted Green-Ampt's model, described by Michelazzo et al. (2016), appears to be more realistic for the seepage flow in the region near the levee crest and is not affected by undisturbed water table level.

Marchi's model, by combining the continuity principle with Darcy's equation, provides an analytical expression for the phreatic line through the levee body, is given by the envelope of the seepage front forced by the river water level. The spatial domain of resolution starts from the highest point on the riverside slope (Point B in Figure *2-4*), and from a geotechnical point of view Marchi's model requires some further assumptions. Indeed, this approach neglects the occurrences of a capillary fringe, assumes Dupuit's hypothesis, simulates the seepage as a plane flow, and

assumes that the aquifer thickness is huge as compared with the seepage depth. The flood hydrograph is a schematic rectangular characterized by a flood duration T and a steady flood stage h_0. As shown in Figure *2-4*, L is the horizontal distance between A (levee toe) and B. H_f is the thickness of the aquifer.

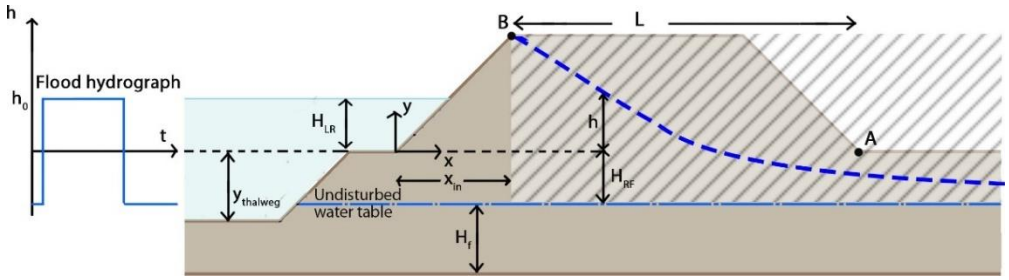

Figure 2-4: Spatial domain of Marchi's model and relevant parameters used [adapted from Michelazzo et al., 2016].

Considering a deep phreatic aquifer, which is when H_f > L, the linearized analytical solution proposed by Marchi is:

$$hx+HRFh0+HRF=2\pi\ arctgkTn(x-xin) \qquad valid\ for\ x>xin\ and-HRF<y<HLR \qquad (2)$$

The second model is based on the infiltration equation by Green and Ampt (1911), adapted to the case of horizontal seepage flow. The model assumes that infiltration takes place through the levee body along horizontal planes that are independent from each other. The location of the phreatic line is identified by coupling the continuity and Darcy's equations: the integration of the flood hydrograph at different levels y provides the position of the seepage front through the levee (as depicted in Figure *2-5*). In this a model, capillary action is neglected together with the interchanges of water along the vertical direction. This may be a questionable assumption since the real seepage process through a homogeneous and isotropic levee takes place as a phreatic front that is hydraulically connected along the vertical

direction. However, the model solves for the phreatic line position within the entire levee body, so that the spatial domain matches the real geometry of the levee.

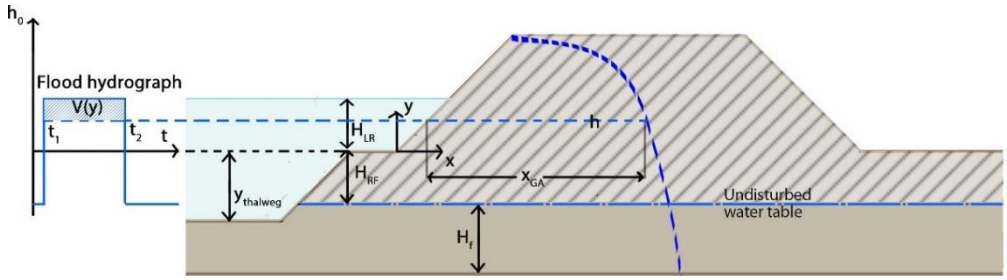

Figure 2-5: Spatial domain of Green-Ampt's adapted model and relevant parameters used [adapted from Michelazzo et al., 2016].

The formulation of this model is:

$$\begin{cases} x_{GA}(y) = \sqrt{\dfrac{2k}{n} V(y)} \\ V(y) = \displaystyle\int_{t_1}^{t_2} [h_0(t) - y]\, dt \end{cases} \tag{3}$$

where $x_{GA}(y)$ is the horizontal distance between the phreatic line and the riverside level slope at level y, V(y) is the flood hydrograph volume above level y, and t_1 and t_2 are the initial and final time of the defined flood level, respectively.

Pistocchi et al. (2004) used some similar models to predict the phreatic line through the body of levee: they demonstrated that the solution obtained as the envelope of the two models gives a good approximation of that predicted by a more detailed numerical model which solves the Richards' equation by means of a finite volume technique.

The emergence of the phreatic line can occur either in the upper or lower part of the landside slope, according to the envelope of the two models. Thus, the results of

both models could be implemented in order to find the critical combinations of river water level and its persistence (duration) for which the levee body is unable to contain the phreatic lines. Using the aforementioned models, Michelazzo et al. (2016) defined a critical time T_{cr}, for which the flood water level h_0 lasts enough to make the phreatic line reach the toe of the landside slope, and a vulnerability index i_{seep} for the seepage mechanism as the ratio $\Delta T/T_{cr}$ where ΔT is the hydrological time scale for the persistence of river flood level.

2.5. Discussion

The results of these analyses can easily be applied to long river reaches, in order to elaborate seepage-hazard maps and locate those levees that are more vulnerable to seepage failure. Actually, using studies such as those mentioned previously, flood hazard maps for levee failure could be developed considering not only overtopping, but also seepage and piping phenomena. These maps, together with overtopping and seepage hazard maps, provide a fundamental guidance for flood-risk assessment and for maintenance operations, as well as for monitoring and surveillance during flood events.

For instance, Camici et al. (2017) applied Marchi's model in order to study levee failure along the Foenna stream (Tuscany region, central Italy) which occurred during the flood of 1st January 2006. In particular, the authors assessed the levee vulnerability to seepage through a procedure based on vulnerability index value I_v defined for a dimensionless geometry of levee body. The probability of occurrence of the levee seepage was described by 'fragility curves', which describes a relationship between the vulnerability index, I_V, and the hydraulic conductivity parameter, K, and the soil porosity, n. Then, they collected data on the flood event, in terms of maximum stage recorded at a gauged section close to the failure locations, status of the levee from geophysical surveys, and evolution of the failure events. Finally, the vulnerability index was applied. The study provides evidence that for the hydraulic conditions

characterizing this flood event the investigated levees should not have failed. They reasonably assumed that the levee body was damaged, so that its structural integrity was affected by discontinuities. The outcome of a geo-electrical tomography indicated the presence of cavities in the embankment most likely caused by the activity of wild animals, like porcupines. Thus, the analysis showed that the failure was probably due to the presence of porcupine burrows Indeed, the burrows located at middle height of riverside levee drawing the flow into the embankment, so that seepage phenomenon is triggered.

Similar to Camici et al. (2017), Orlandini et al. (2015) studied the failure mechanisms of the Secchia and Panaro river levees, in 2014. Likewise, they strongly believed that the levee failures could be ascribed to animal bioturbation.

In the last years, an increasing number of levee failures are believed to be linked to the presence of animal burrows. Consequently, numerous scholars have attempted to analyse the connection between levee failure and the presence of such burrows. In the following chapter 3, we present an overview on key studies on the relationship between levee failure and presence of burrowing activities.

3. INFLUENCE OF BURROWING ANIMALS ON LEVEE WEAKENING

3.1. Overview

Up to this point, the difficulty of estimating the hydraulic parameters and, thus, of describing with sufficient accuracy the failure mechanisms of levees implies that studies are typically carried out by assuming that the levee system is undamaged during the flood event [Camici et al., 2017].

Nevertheless, burrowing animals may compromise the hydraulic performance and the structural integrity of earth levees leading to mass removal and subsequent deformation [Saghaee et al., 2017] as well as enhanced seepage pathways that can accelerate piping mechanisms. It is widely recognized that the complex interaction between levee failure phenomena and biota activities are fundamental to understanding and managing of the environment. For instance, in many cases removal or alteration of communities of organisms can have severe consequences for the functioning of environments by changing geomorphic, hydraulic and biogeochemical process [Coleman &Williams, 2002].

Accordingly, vulnerability assessment of earth structures must be performed also taking into account the presence of biota. Nevertheless, the actual knowledge on this complex interaction is very limited.

In this chapter, the principles of eco-hydraulic modelling and experimentation are summarized. Then, an overview of burrowing animal behavior is presented and the current state-of-the-art, regarding biota impacts on levee stability is described.

These are the starting points for the subsequent development of the research.

3.2. Eco-hydraulic modelling and experimentation

In order to study freshwater aquatic systems, hydraulic and geotechnical modelling are often simplified and regarded as an abiotic process. Indeed, numerical modelling are not always able to evaluate the faunal bioturbation. Frostick et al. (2014) highlights that the field of experimental and numerical hydraulic modelling frequently reduces the complex consequences of biota interaction with flows to a passive effect on bed roughness.

Actually, the river environment is not only a system of hydraulic and geotechnical forces; animals and plants interact with physical processes and environments at all spatial and temporal scales. Indeed, incorporating animals into hydraulic experiments is an essential step in gaining insight into their importance for modifying the flow and sediment transport in the natural environment and their response to given flow and sediment transport regimes [Frostick et al., 2014]. Sediment transport, for instance, continues to be predominantly regarded as an abiotic process driven by the conversion of potential energy derived from relief to kinetic energy across elevation gradients. Nevertheless, Rice et al. (2016) demonstrated that contrary to what is currently thought, the crayfish burrowing activity has an important impact on sediment transport during base flow periods. In addition to direct sediment entrainment by bioturbation, crayfish burrowing supplies sediment to the channel for mobilization during floods so that the total geomorphic effect of crayfishes is potentially greater than documented. The results presented by Rice et al. (2016) demonstrated that bioturbation in rivers could entrain significant quantities of fine sediment into suspension, with implications for the aquatic ecosystem and base flow sediment fluxes.

As Nikora (2014) says, although the importance of eco-hydraulics in developing better management strategies for aquatic ecosystems is widely recognized, the actual knowledge of hydrodynamic effects of flow-biota interactions remains very limited. Probably this depends on the complexity of the topics. Indeed, in order to thoroughly

understand and manage the total aquatic environment, a knowledge of the complex interactions between aquatic organisms and physicochemical processes is essential.

Physical models help in the understanding of phenomena that are as yet unknown or are so complicated that it is difficult or impossible to derive a numerical solution [Frostick et al., 2014]. Moreover, physical modelling using laboratory flume experiments provides a specific example of essential cross-disciplinary knowledge because the information of eco-hydraulics, bio-geomorphology and ecological engineering are key in a design of successful eco-hydraulic flume experiments.

Obviously, also in experimental researches it is not always easy to introduce biological components and to model all relevant variable, as they would exist in the natural environment. In general, experiments focus on the interactions between animals and their environment must account for, and in many case replicates, the environmental and ecological context of the species and process being studied [Frostick et al., 2014]. For these reasons, all physical modelling approaches have to incorporate elements of simplification and scaling. Therefore, the choice of facility material, and measurement equipment is the first step of every physical experimental model and it requires careful consideration.

Moreover, when mobile animals are studied, added restrictions are introduced and disentangling the direct impacts of macro-fauna and their often-complex relationship with meio-fauna is challenging [Frostick et al., 2014]. Mobile animals, in particular macro-fauna, alter stability through direct disturbance associated with burrowing, the flushing of burrow sediments, and the grazing of stabilizing microbial biofilms [De Backer et al., 2010]. As Frostick et al. (2014) explain, macro animals mix sediments, altering their structure and having substantial impact on bed stability. This is associated with local alterations in packing, porosity, compacting, and rigidity in the vicinity of burrows [Aller et Yingst, 1980], which increase the spatial heterogeneity of sediment structures and can alter properties over large areas (<10 m^2) [Frostick et al., 2014].

Most laboratory studies have attempted to study faunal impact by allowing animals to colonize sediment beds in the lab. However, this methodology has some limitations. In such cases, animals are isolated from biological interactions, such as predation or feeding, allowing for unrealistic behaviors. Moreover, artificial sediments rarely replicate the structural complexity of natural soil, and in fine-grained systems it is also important to use water obtained from the field site because water chemistry exerts an important control on the erosion of cohesive sediments [Winterwerp et Van Kesteren, 2004].

Furthermore, even if a physical model enables direct observation of phenomena and mechanisms, which may not be possible otherwise, it is necessary that such observations are validated. Thus, Frostick et al. (2014) state that "the corollary of this decision-making process [for an ecohydraulic approach] is the need for a *nested approach* where results from field studies, laboratory experiments, and numerical models are used in parallel to address the objectives of any study. Each of these approaches to studying eco-hydraulics is essential to informing and refining the results of the other fields of study".

With regards to the present research topic, in order to achieve an effective eco-hydraulic experimentation and modelling, an "interdisciplinary" overview of the issue is essential. The investigation of earth structure failures due to burrowing animal activities is not sufficiently developed yet. The scientific literature indicates only that there is a connection between failure mechanisms and animal activities. Nevertheless, current knowledge on the impact of biota on earth structures is scarce, so that the topic requires further investigation considering different levee deterioration levels. Moreover, as highlighted by Bayoumi et al. (2011), burrowing activities of wildlife in earth structures are sophisticated biophysical processes, that are generally difficult to observe during routine levee management.

Despite all these difficulties, it is clear that the two main factors that should be simultaneously considered to understand these phenomena are the following: hydraulic parameters (dynamic change of river stage that could initiate of failure

processes) and biological parameters (bio-induced modification of levee structures that accelerates these processes). Moreover, both of these two factors include in themselves many other variables.

The first step toward achieving the established goals is to understand the state of the art of faunal behaviors. Subsequently, in the following sections burrowing animal behaviors and analysis on their typical burrows are described. Then, studies on eco-hydraulic approach to understand the connection between animal bioturbation and levee failure are summarized.

3.3. Burrowing animals

Past studies indicate that there is a connection between levee failure mechanisms and animal activities. Nevertheless, they do not give sufficient indications as to how to quantify such impact. This lack of information is partially due to the fact that development of leave breach and/or the failed material covers up the evidence of their origin.

Burrowing animals often dig tunnels and holes inside earth structures, either for habitat or foraging, and also flatten levee slopes while manoeuvring, or when search for food or preys. Their tunnels may have different shapes and dimensions depending on what animal does the digging. Most of these activities alter the external and internal geometry of earthen structures and are thus detrimental to their integrity. Damage caused by wildlife in earthen hydraulic structures is typically associated with internal and external erosion, and sometimes with boils [Bayoumi et al., 2011].

For some species the shelters are simple, consisting of the shade of a tree or the lee of a rock. Many other species, however, construct elaborate dens, nest, or burrows [Reichman et Smith, 1990]. The vegetation at the inner side of the dike and the isolation of levees from human presence attract the animals [Taccari et al., 2016]. Thus, levees offer an ideal environment for the diffusion of different species of burrowing animals, such as badgers, porcupines, coypus (nutrias), and crayfish.

In order to capture the effects of animal burrowing in levees of different composition in different environments, Roa et al. (2014), in collaboration with the California Department of Water Resources, assessed the extent and the architecture of burrow networks. First, they identified active burrows, classified "based on the presence of material ejected downslope of the entrance, food waste and/or footprints in the vicinity of the entrance". Then, they injected cement-bentonite grout into the burrows, with a chemical grout to fill remaining void space. A Lidar survey was carried out. Using a combination of compressed air powered wand, hand labor and backhoe operation, the levee was excavated. Figure 3-1 shows the results of Roa et al.'s (2014) investigation, which is a burrow complex system made by California ground squirrels inside an earth levee. Such results give an idea of the relevance of the problem.

Nevertheless, California ground squirrel is not the only burrowing animals capable of achieving this kind of complex tunnel systems. The Federal Emergency Management Agency reported twenty-three main species among those posing a threat to earthen dams [FEMA, 2005]. Many of these species share common characteristics, but the pattern and size of burrows and severity of damage they cause to earthen structures could substantially vary [Bayoumi at al., 2011].

Bayoumi et al. (2011) summarized, for each animal species, the typical damage and burrow shape and activity indicators. For instance, regarding crayfish, they say that these animals burrow extensive tunnels inside earth levees, that may cause internal erosion and structural integrity losses.

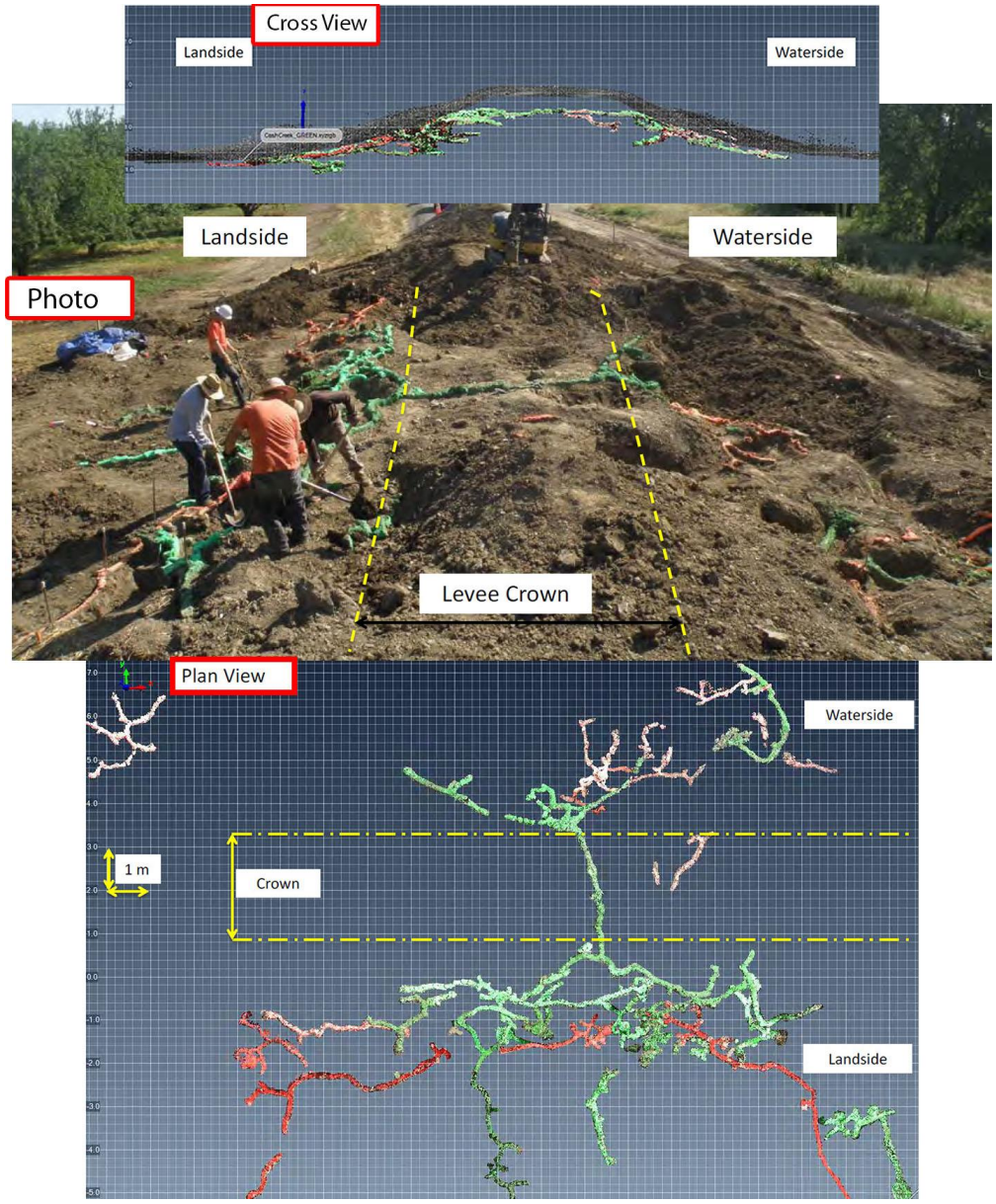

Figure 3-1: Cross section view, plant view and a view of completely penetrating burrow in the levee [adapted from Roa et al., 2014]

Crayfish resemble miniature lobsters, with over 300 species of various sizes, shapes, and colours. Most crayfish dig burrows to use as a refuge from predators and

as a resting habitat during molting and inactive periods. Actually, these animals stay in their burrows or in mud bottoms during cold weather but emerge once the water warms up [Helfrich et al., 2001]. Moreover, they burrow on both the landside and waterside slope of the levee, along the shore line their tunnels are 0,60 to 5,00 cm in diameter with a cone-shaped mound, known as a "chimney", plugging the burrow, as shown in Figure 3-2.

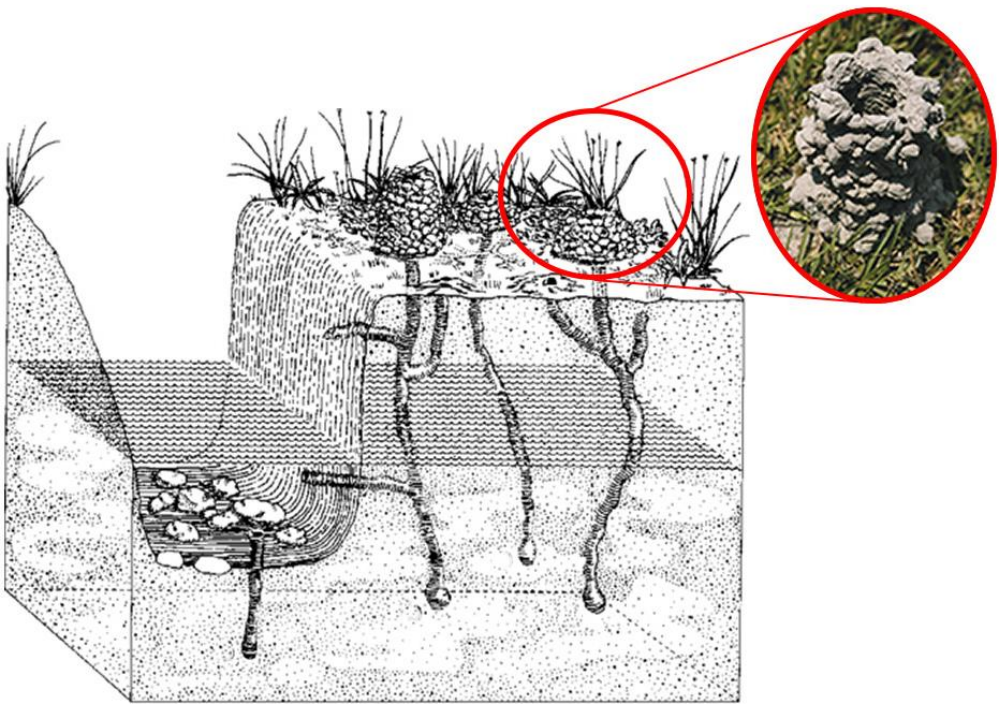

Figure 3-2: Crayfish burrows and the typical "chimney" made with mud pellets [adapted from Hobbs et Lodge, 2010].

To increase the knowledge of crayfish so that it is possible to develop levee structures that are less vulnerable to the presence of Procambarus clarkii (North American crayfish), Haubrock et al. (2019) conducted some experiments. Specifically, to assess the shape, volume, and structure of its burrows and the associated behavior inside earth levees, they introduced two size-matched adult

crayfish into an artificial setup and video-recorded their behavior for 96 h. At the end of each replicate, they retrieved casts of excavated burrows made with polyethylene foam. As shown in Figure 3-3, the authors observed that, in the absence of shelter, crayfish began digging rapidly and realized two types of burrows: a complex burrow with entrances at the water line commencing straight into the levee and in some cases with a central chamber, which volume can contribute to almost 50% to the overall excavation volume of the burrows, and a considerable number of short burrows constructed u-shaped and placed near the ground in the first basal layer of the levee. The recorded burrowing activity led to a total amount of excavation up to 4% of the levee, that can directly affect levee stability. Nevertheless, the authors believed that the observed excavation values are likely an underestimation, especially because in the field a higher abundance of crayfish is present, and the number of burrows increases over time.

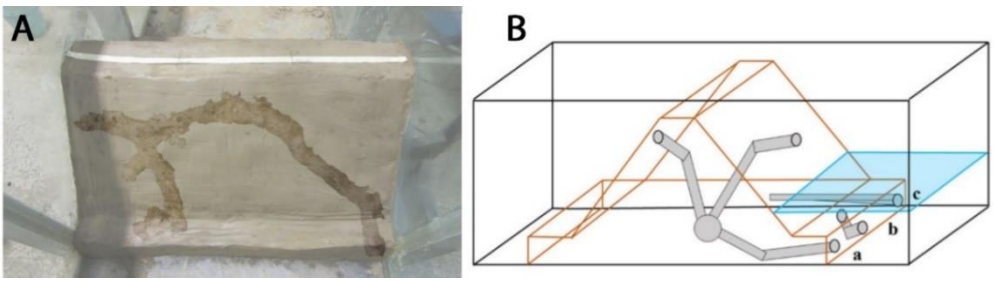

Figure 3-3: Reconstructed model of the levee after the experiment, showing the position and the excavated volume of burrows [Haubrock et al., 2019]:
A) Observed burrows as positioned inside the levee;
B) model of all differing types of burrow structures observed during the experiments: a) complex structure with chamber; b) u-shaped burrow; c) blind tunnel.

Another burrowing animal, which is considered an invasive species, is the coypus, also called nutria. This animal is held responsible for some of the major main levee failures that have occurred in Italy [Camici et al., 2010]. It constructs extensive burrows and shelters preferably on the riverside slope, which weaken the earth structures to the point of collapse.

With an average weight of 6 kg and a body length of 60 cm (tail adds an additional 40 cm), nutria is larger than muskrat, but much smaller than beaver [FEMA, 2005]. Unlike muskrat or beaver, a nutria's tail is round with scant hair, the whiskers are long (around 10 cm) and whitish, and nutria has prominent red-orange incisors [FEMA, 2005]. This amphibian animal is considered an invasive species, which can adapt to a variety of habitats. It prefers a semi-aquatic environment, particularly the zone between land and permanent water, where aquatic vegetation abounds. Actually, nutria are ground-dwellers during the summer, preferring to live in dense vegetation, while the rest of the year they live in burrows they have dug, or that have been abandoned by other animals.

Nutria burrows may be very complex, with several tunnels, compartments, and entrances at different levels in the bank. In general, the entrances are hidden in vegetated banks of dams and waterways; a bank that has a slope greater than 45 degrees, maybe due to toe erosion, is a preferred location [Hygnstrom et al., 1994]. Figure 3-4 shows the structure of a nutria burrow composed of several tunnels, although if a den is inhabited by a single animal, it will be composed only by one tunnel not longer than 3 m.

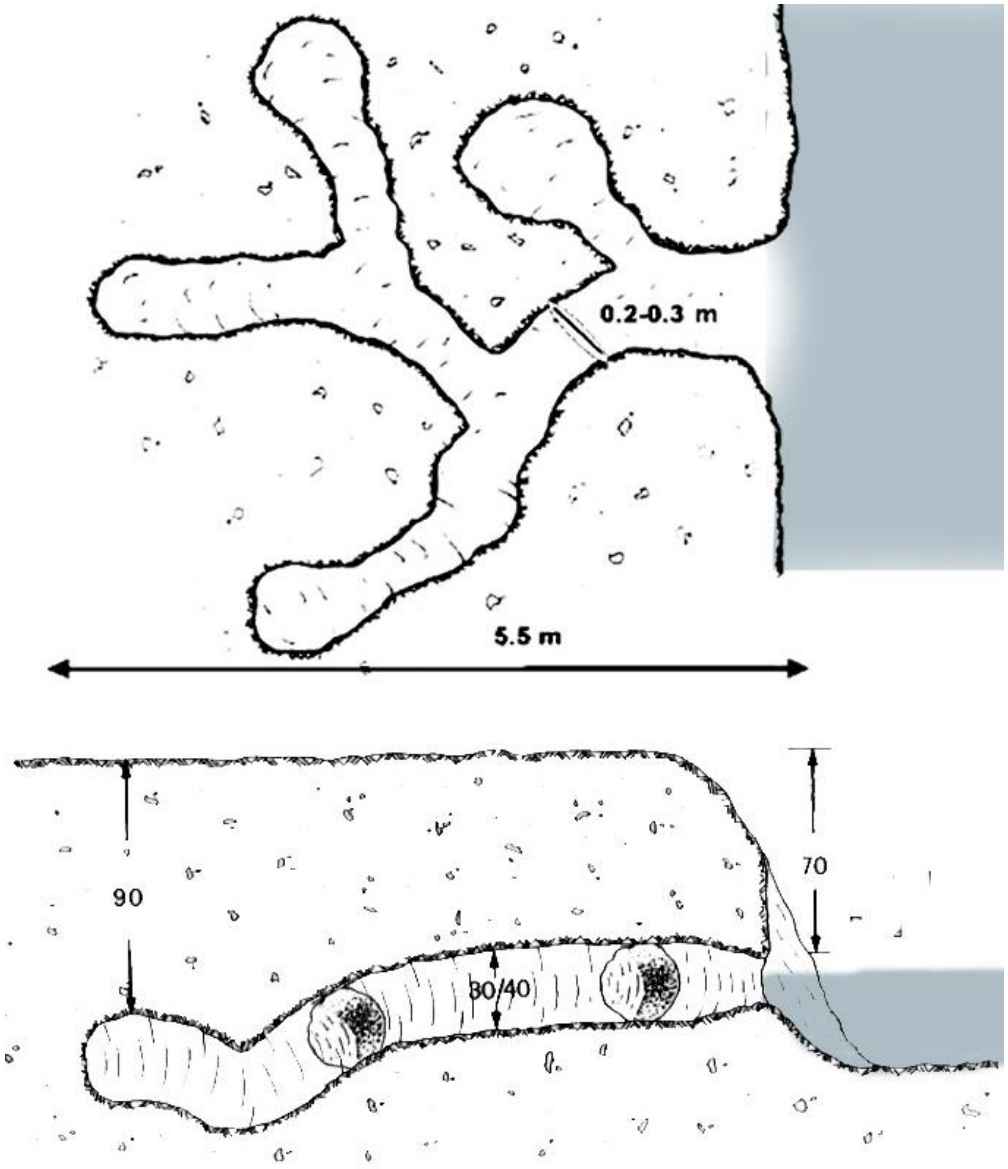

Figure 3-4: A typical complex nutria burrow [Tocchetto, 2000].

3.4. Previous studies of biota impact on levee failure mechanisms

Little research concerning the connection between levee failures and the presence of burrows has been published in the peer-reviewed literature. These researches originate from the necessity of understanding the geophysical interactions between water flows and disturbed levees, the triggers for the failure mechanisms, and the impacts of biota on hydraulic and geotechnical function of earth structures.

Some studies attempt to demonstrate that the presence of burrows is one of the main triggering mechanisms causing real events of levee failure.

The first paper reporting the hypothetical impact of animal burrows on an actual levee failure was published in 2015 by Orlandini et al. Thanks to a detailed 2D numerical modelling of rainfall, river flow and variably saturated flow in the levee, they explored the hydraulic and geotechnical mechanisms which lead to the levee failure of Panaro and Secchia Rivers. First, they reconstructed the 2014 flood hydrographs by developing a level pool routing model and a dynamic wave model. This analysis showed that the maximum stage reached by the river in that month was about 1.5 m below the top of the levee and that this peak water surface elevation as well as the duration of high river stages along the Secchia River were smaller than observed in previous events. Moreover, an extensive field inspection and terrain analysis conducted after the disaster revealed the positions of the animal burrows and, in some cases, they found levee areas where intensive internal erosion was developed around animal dens, as shown in Figure 3-5. In that case, the levee top was collapsing, and it was rapidly repaired, preventing a second disaster.

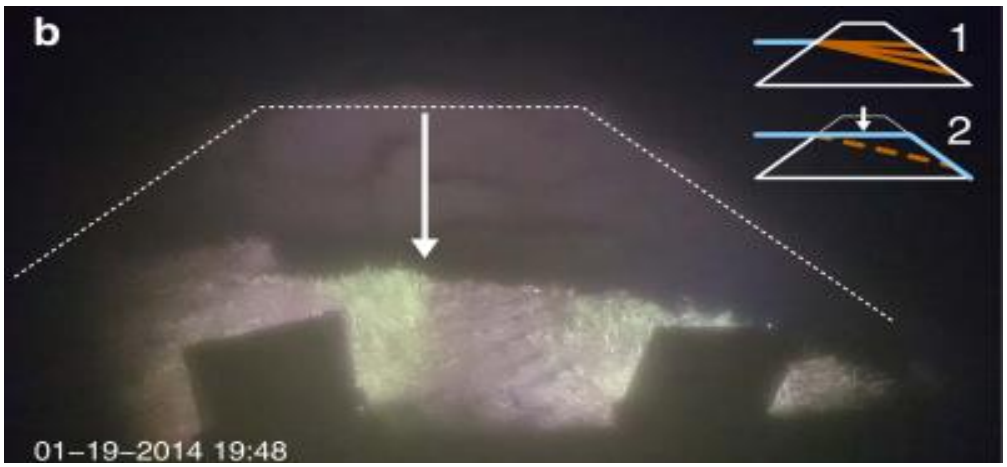

Figure 3-5: Collapse of the levee top over the gallery formed by internal erosion, at 19:48, Panaro levee [Orlandini et al. 2015]

The authors suggested three competing hypotheses for failure triggers. The first hypothesis was that of direct inflow into the den system simply due to increasing river stage (pipe flow only). This would have triggered internal flow and erosion processes by direct river inflow into the riverside entrance of the den system. This could be considered consistent with the reconstructed elevations of the observed burrows. The second was the collapse of the riverside den entrance under the effects of direct rainfall on the levee surface and simultaneous river stage raising. Unfortunately, numerical simulations reveal that no levee instabilities and/or critical sliding surface occurred by considering a realistic configuration of the tunnel extending from the riverside den entrance into the levee. Finally, it was hypothesized that there was an internal den chamber 1 m under the den entrance and 1m distant form levee riverside slope and that, since burrowing animals typically excavate in soils that are easy to dig [Vleck, 1979; Roper, 1992], a weak soil portion is assumed to exist around the den entrance. However, the numerical modeling of the system reveals that no critical soil saturation occurs around the den chamber when applying the actual hydroclimatic conditions.

In conclusion, Orlandini et at. (2015) revealed the role played by burrowing animals in the disastrous levee failure along the Secchia River at San Matteo, on 19th

January 2014 and, thus, raises the distinct possibility that other levee failures in Italy may have been connected to the activity of burrowing animals [e.g., Camici et al., 2017]. Actually, the collected evidence suggested that it is quite likely that the levee failure on the Secchia River was of a similar mechanism as that observed on the Panaro River [Orlandini et al., 2015].

Taccari et Van Der Meij (2016 - A) investigate the contribution of burrowing animals to the initiation of a levee failure. The research considers a series of historical failures caused by internal erosion due to animal burrowing: San Pedro River -Arizona (1940) [Carrol, 1949], Lower Stichcomb, Georgia (1978), Big Sand Creek Str Y032032, Mississippi (1996), Mallard Lake, Tennessee (1996), Prospect Reservoir Dam, Colorado (2002), and San Matteo 2014 [Taccari et Van Der Meij, 2016 - A]. They investigated the effects of burrowing activities by three mechanisms: macro-instability, internal erosion, and micro-instability. They did this by simulating several scenarios of tunnels and burrows entrances with the software PLAXIS 2D and 3D, which is a finite element computer program used to perform deformation and stability analyses for several geotechnical applications.

Their results show that the phreatic surface changed with the presence of burrows. The possible failure mechanism was given by the position of the burrow entrance and the risk increased as the distance between two entrances was lower. In particular, the authors believe that the burrows reduce the shearing resistance and can cause macro-instability of the inner slope. Moreover, they assumed that the burrows on the river slope result in bigger effects to the three failure mechanisms than the landside burrows, even if they can all increase the phreatic line. Finally, they concluded that burrows placed above the water level have no influence on levee safety. Figure 3-6 summarizes the paper results:

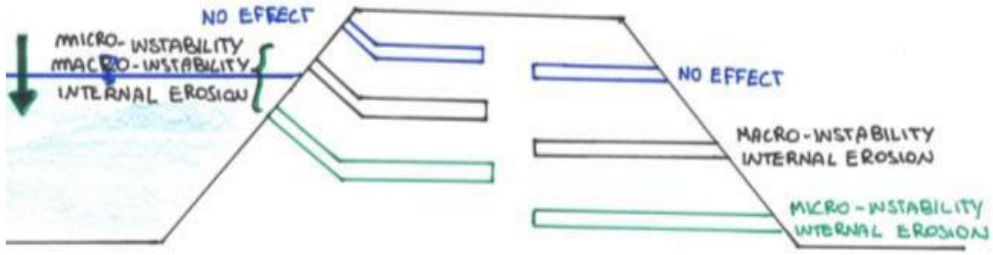

Figure 3-6: Influence of burrows to the failure mechanisms according to their position along the levee [Taccari et Van Der Meij, 2016 - A].

Furthermore, Taccari et Van Der Meij (2016-A) investigated the influence of animal burrows on pore water pressures, to predict the failure mechanism for the Secchia river. Using PLAXIS 2D, groundwater flow analyses were performed., including information on soil stratigraphy and properties, increase and decrease of rainfall, and changing water levels. Moreover, the simulations were performed considering the actual burrow geometries and entrance positions. The analysis showed that, even with burrows, the macro-instability and the micro-instability phenomena did not occur. Concerning internal erosion, the authors applied the approach derived by the Hole Erosion Test (HET) [Bezzazi et al., 2010] which estimates the evolution of the inner tube radius as a function of time. This test was applied for the levee of San Matteo for the conditions that led to the breach. When the water level in the river covers the lower burrow entrance at the outer slope and the burrow is connected to the inner slope, a pressure difference develops between the outer and inner side. If then this pressure difference overcomes the critical shear stress, internal erosion starts and causes the hole to increase. Taccari et al. (2016-A) concluded that the internal erosion was the only mechanism that leads to failure with realistic soil parameters. The interconnected underground system inside the levee and the fact that the entrance to one of the burrows was located below the maximum stage created the conditions for water to fill the burrow and erode the tunnels in the whole network. In view of the performed analyses, they found that hole erosion after animal burrowing is a most suitable explanation for the collapse of the San Matteo levee.

Palladino et al. (2019) also studied the seepage paths and the hydraulic head profile of both intact and damaged levees, using the 2D numerical model SEEP/W. First, they studied the sensitivity of the seepage line to geotechnical parameters, such as hydraulic conductivity, volumetric compressibility, water table depth and aquifer depth. Then, different burrow configurations on the riverside levee were simulated, examining the effects of the vertical position of the burrows, as well as their lengths. The numerical investigations indicated that the seepage probability increases proportionally with burrow length. However, when keeping the length of the burrow constant and varying its vertical position, no specific trend was found. As previous authors, Palladino et al. (2019) believe that burrows located above the water level do not affect seepage paths. They conclude that "the presence of burrows reduces the critical time of saturation for the levee, thereby inducing collapse of a levee even for flood durations shorter than the critical time of undamaged levees."

Actually, all of these studies were motivated by the need to justify the mechanisms behind actual failures. However, numerical simulations can only answer some specific questions, but are not able to provide a complete description of the phenomena triggering levee failures. Specifically, the papers mentioned above demonstrate that the presence of animal burrows can speed up internal erosion processes. Nevertheless, they provide no evidence that other failure mechanisms may have been triggered before or at the same time to the internal erosion phenomenon.

Physical models allow insight into phenomena that are as yet unknown or are so complicated that it is difficult or impossible to derive a numerical solution [Frostick et al., 2014]. For this reason, a physical model is probably able to increase knowledge about this extremely relevant topic. An interesting experimental programme to investigate the impacts of burrows on levee stability is described in the next part of this section.

Saghaee et al. (2017) investigated the impact of different configurations of animal burrows on the integrity and geotechnical performance of earth levees.

They conducted a series of centrifuge tests on homogenous, scaled-down, 1 horizontal : 1 vertical (1H:1V) levee models built from silty sand material in a controlled environment, taking into account a scaled acceleration level. In particular, they investigated the impact of location and elevation of animal burrows. Both waterside and landside burrow positions were closely examined by monitoring the surface movement, global deformation, and changes in pore pressure distribution due to the introduction of cylindrical burrows. Figure 3-7 shows the model configuration and the burrows distributions. When the initial acceleration started to increase, the water level on the waterside was gradually raised using a water pump.

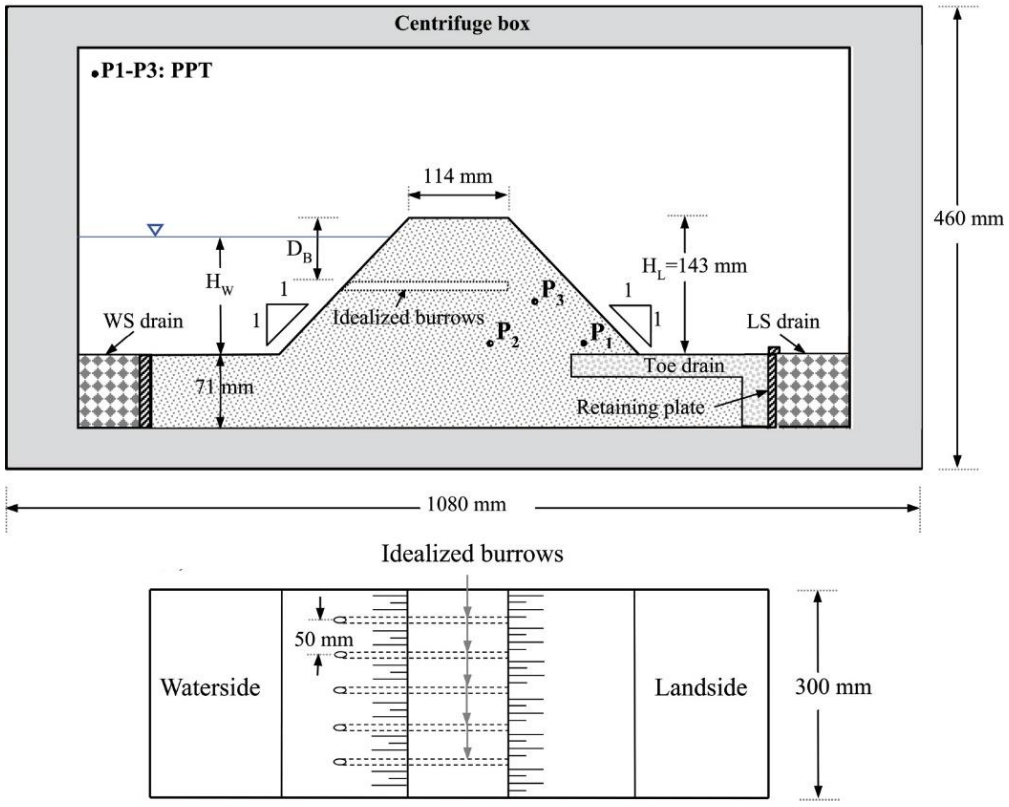

Figure 3-7: Model configurations: geometry, location of pore pressure transducers and planview of the model with waterside burrows [Saghaee et al., 2017].

In order to support their hypotheses as to alterations to the phreatic surface and failure mechanisms of the deteriorated levees, three-dimensional (3D) finite element (FE) analyses were carried out.

The experimental results showed, as expected, that the deteriorated levee exhibited an excessive and abrupt settlement, followed by rapid failure, while the intact levee did not show any distress sign, up to the end of the experiment. Moreover, although they appear similar, the displacements for the waterside burrow model suggested higher settlement than for the landside burrow model. The authors concluded that the waterside and landside burrows generated different failure mechanisms, as shown in Figure 3-8.

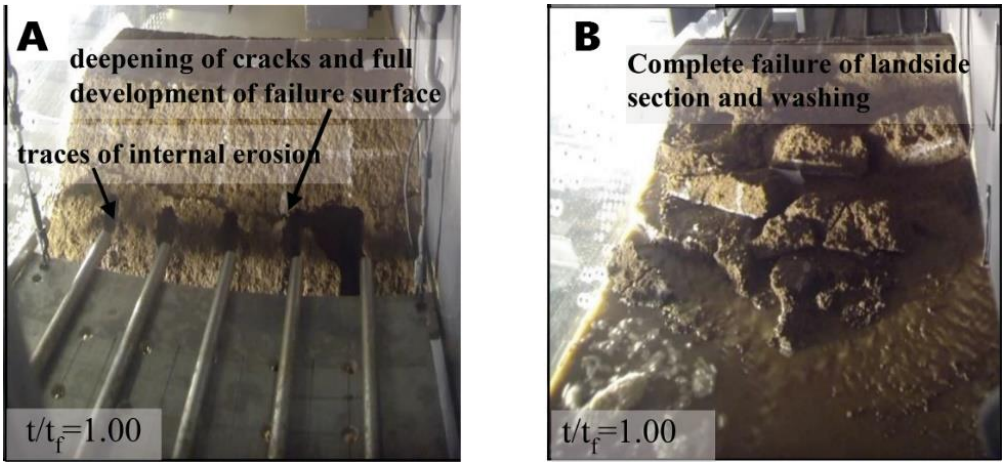

Figure 3-8: Levee failure at the end of experimental activities: A) Landside burrow model and b) Waterside burrow model [Saghaee et al., 2017].

Regarding the hydraulic response to the experiment, the authors used pore pressure transducers in order to define the phreatic surface for each configuration. Comparing to the intact case, the hydraulic gradients in the deteriorated models were higher. Indeed, matching the seepage path, it was altered by the presence of cavities, and the phreatic surface was parallel to the burrows within the levee prior to running parallel to the landside slope toward the landside toe. Specifically, from this point of

view, the waterside burrows allowed direct access to water with minimal head loss along their length, causing greater hydraulic gradients than those in levees with landside burrows.

Using PLAXIS 3D software, numerical simulations of the seepage and stress analysis was performed to further support the visual observations of the physical model. The seepage analysis assumed a homogenous, isotropic material under steady-state conditions. The stress and stability analyses were carried out using the Mohr–Coulomb failure criterion. The numerical results were in fair agreement with the experimental observations. They suggest that the adverse effect of the cavities is not limited to a specific geometry (different levee slopes were considered), and the reduction in the safety factor depends on how far the burrows extend into the levee.

In conclusion, Saghaee et al. (2017) demonstrated that the subsidence in deteriorated levees is triggered by the combined effect of cavity destruction and loss of strength. Crest settlement can cause failure in deteriorated levees, which is indicative but does not provide a comprehensive view of the structural integrity. The levees' apparent intactness before failure could be misleading. This has significant bearing on levee systems management, because the damage (size of cavities) of concealed burrow systems within a levee section could be much larger than what the visible openings suggest [Bayoumi and Meguid, 2011]. However, as the authors stated their results are limited by the ranges in the investigated parameters, including the levee and burrow geometries and the size and density of the burrows.

4. LEVEE FAILURE MECHANISMS AND NON-DESTRUCTIVE INVESTIGATION OF SICILIAN RIVER LEVEES

4.1. Overview

On March 11th, 2012, a heavy rainfall event affected Sicily, causing a flood on the near Acate River, on the South coast. The resulting flash flood and the releases from Ragoleto Dam, located in the upper reaches of the river, rapidly increased the river discharge. The Dirillo River levee failed at different points, causing 2 million euros worth of damages throughout the area downstream of the SS115 Road Bridge. In the following sections, a description of the site is presented, and the 2012 flood event is investigated. In particular, the mechanisms that triggered the levee failures during this flood event are studied.

Overtopping and seepage are among the most frequent hydraulic causes of levee failure mechanism. However, the numerical simulations to reconstruct the overtopping phenomenon and the analytical models applied to evaluate seepage showed that the 2012 flood may not justified considering only hydraulic failure mechanisms: if the levees had been intact, probably the failure would not have occurred.

As well as numerous failures of earth structures described in the previous chapter, this flood event may be due to an emerging levee failure mechanism connected to burrowing animal activities. Indeed, based on a questionnaire sent by the Region, nutrias were present at the Irminio River (Sicily) until the flood event of 2012, but were not seen afterwards. Nevertheless, to date the whole island is still inhabited by burrowing animals, such as crested porcupine.

During the summer of 2019, several inspections were carried out along levees of Sicilian rivers, finding that levees on the Dirillo River are adversely impacted by the presence of animal burrows. In order to evaluate the distribution of faunal burrows

and their configuration, a control of levee structures and non-destructive investigations were performed, whose results as well as analyses of the possible causes of failure mechanisms, are discussed in the present chapter.

4.2. Site descriptions

The Dirillo River basin is located in the SW of Sicily Island and outflow into the Mediterranean Sea. It flows from the NE to the SW, from 986 m a.s.l. to 0 m a.s.l., and its channel divides the border between Caltanissetta and Ragusa districts. Its mouth is near the city of Gela. The river is 54 km long with a 740 km^2 catchment area; the average flow rate is 4 m^3/s. Figure 4-1 shows the catchment area of Dirillo River.

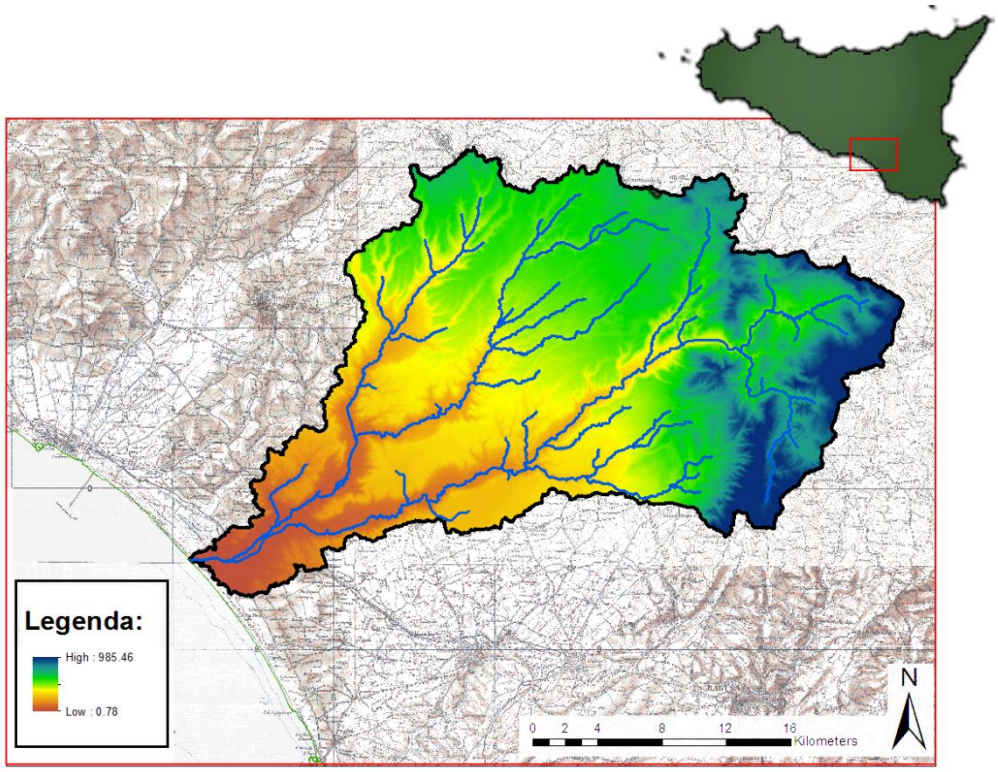

Figure 4-1: Catchment area of Dirillo River.

In the headwaters area, the valley slopes are steep, made up of lithotypes (calcarenites and sands); instead, the lower part is characterized by clay-sandy soils. Currently the erosive process is concentrated on the slopes further upstream, while alluvial material settles in the valley areas. However, generally the territorial structure has a stable structure, with limited and localized evolutionary phenomena. A delta environment with an estuary characterizes the outlet to the sea. Due to the reduction of incoming sediment, there is a trend of coastline regression [PAI, 2004].

Downstream of SS115 road, the land near the river is protected by earth levees (Figure 4-2) and is predominantly under agricultural use, mainly in greenhouses.

Figure 4-2: Current situation of Dirillo earth levees – field survey on the 2nd July 2019.

In the 1930s, the first protection structures along the Dirillo River (levees) were built in order to defend works of great public interest, prevent flooding and overflow. The areas with hydraulic works are identified in Figure 4-3. The levees were constructed and built from a local material consisting of a mixture of sand, silt and clay.

Figure 4-3: Map of authorized hydraulic works to protect the Dirillo River valley in 1930s [adapted from Consorzio Idraulico Fiume Dirillo-Acate, Comune Vittoria].

In 1948, 1949 and 1951 the earth levees were destroyed by flood events but were subsequently re-built. Figure 4-4 shows a typical section of the river and its earth levees. The defence structures were designed considering a maximum flow rate of 200 m^3/s.

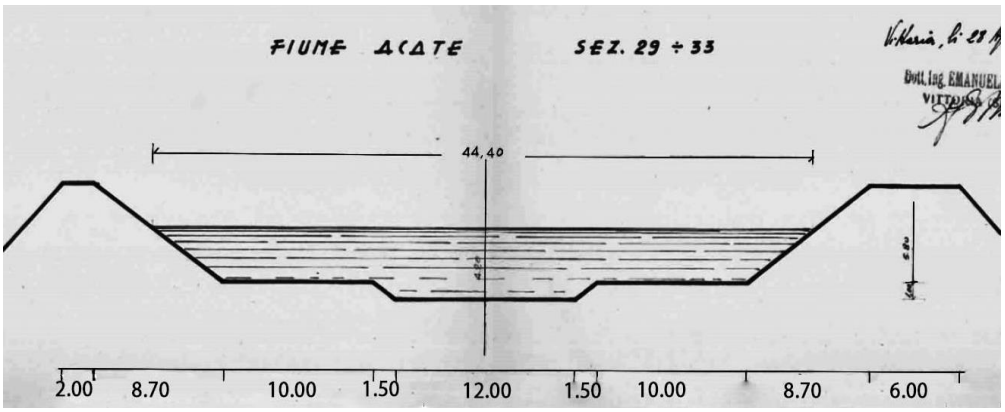

Figure 4-4: Earth Levee section built in 1950s [adapted from Consorzio Idraulico Fiume Dirillo-Acate, Comune Vittoria].

More recently, flooding events occurred in 2005, 2006, and 2012. During a flood, in 2005, the levees broke on the left side of the river, while in 2006 and 2012, overtopping resulted in levee failures at different sections along the river.

As evidenced by historical analyses, the last repair works (2008) were aimed at removing deposited sediments, but the sections of the levee were not substantially changed. In fact, Figure 4-5 shows that surveyed levee transects are the same as those of original project. The huge accumulation of debris, which were removed, is depicted in yellow. The evaluation of levee height variation is more complicated because over the years they may have suffered subsidence.

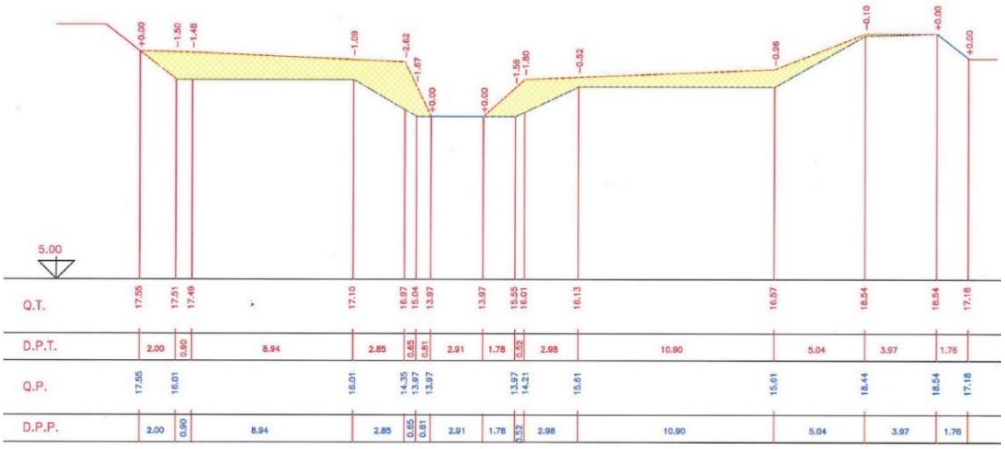

Figure 4-5: Levee restored according to '50s project depicting sediment accumulations that were removed during 2008 works [Genio Civile Ragusa and ICARO Ecology s.r.l. of Gela 8th May 2008].

Today, the levees of the Dirillo river are covered with vegetation, but they are also burrowing animal sites. In fact, a series of burrows were identified along the river. Although vegetation hides the burrows, maintenance works conducted by private farmers has allowed us to find some relevant burrows. Those animal dens may be considered critical points for levee stability, and apparently, they may develop on the whole levee.

4.3. Analysis of the 2012 flood event

From historical analyses, the Dirillo River floodplain is considered a zone at a high risk of flooding. Indeed, the river has flooded several times, causing extensive damage and in 2014 the Department of Civil Protection of Sicily Region identified Acate Valley as a recurring flood event area, as shown in Figure 4-6.

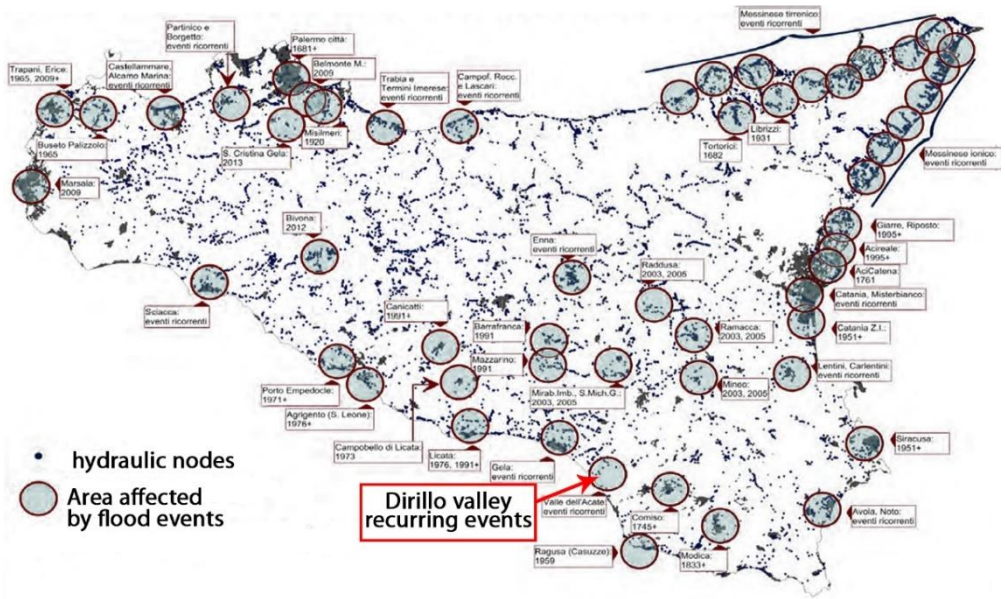

Figure 4-6: Map of main flood events in Sicily [Preliminary Report on Hydraulic Risk in Sicily and releases in the Civil Protection System – prot.38651-10th April 2014].

To make things worse, it is likely that the presence of animal burrows deteriorates these flood protection structures, thereby endangering their resistance.

In 2012, a flood event occurred, causing tremendous physical damage as well as economic and social disruptions. The stream broke the river levees at different points. Using the landowners' historical memory and consulting reports drafted by the Civil Protection Department, those locations with levee overflows were determined along the river, as shown in Figure 4-7.

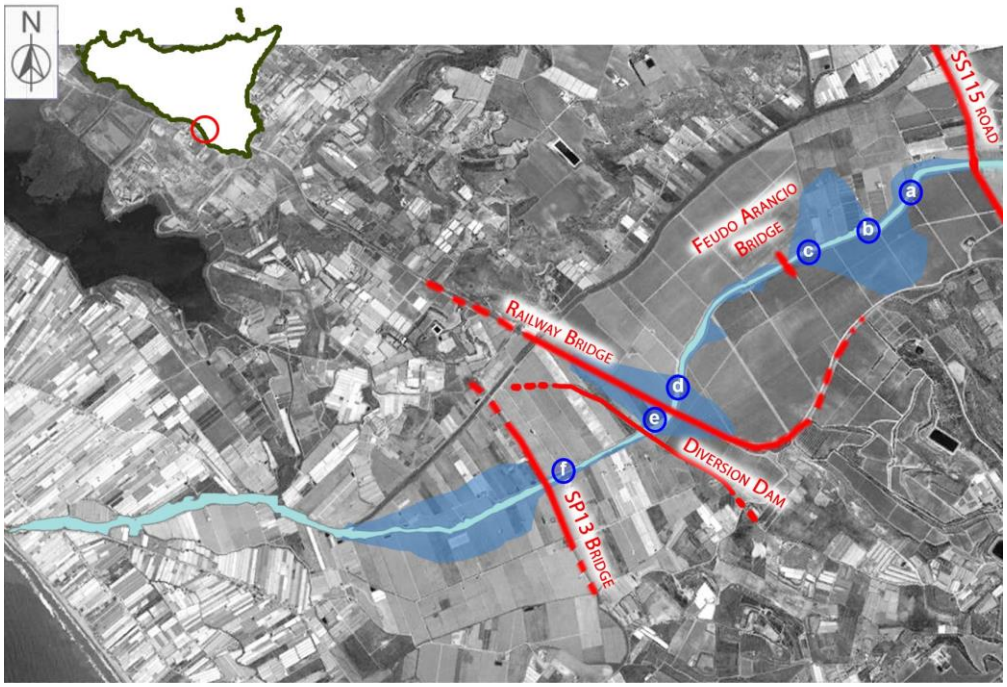

Figure 4-7: Reconstruction of the 2012 Flood of the Dirillo River and determination of levee failure points –A, B, C, D, E, F.

This chapter describes the 2012 flood event and investigates the probable mechanisms of levee failure. Starting with a reconstruction of the flow rate during the event, the vulnerability to overtopping and seepage is examined for the case of an undisturbed levee.

Some considerations on the possibility that the levee failure mechanisms could have been influenced by presence of burrows are exposed.

4.3.1. *Derivation of flood hydrograph using rainfall-runoff analysis*

Rainfall-runoff modelling is series of a methods that convert local information on rainfall to a flood peak or flood hydrograph at a basin's outlet.

The area studied is located below the SS115 road bridge. In fact, this is the only part of Dirillo River with levees. The overtopping and seepage mechanisms were evaluated considering the discharge coming from the upstream basin. Thus, the SS115 road bridge is the downstream limit of the catchment area, in other words the outlet of the basin, and the flood hydrograph is estimated in reference to it.

The upstream presence of the Ragoleto Dam represented a discontinuity on the whole basin, preventing the direct flow of the water towards the valley. Nevertheless, its hydrological effects had to be considered for the following analysis.

Figure 4-8 shows the catchment area of SS115 road outlet (A) and the basin bounded by the Ragoleto Dam.

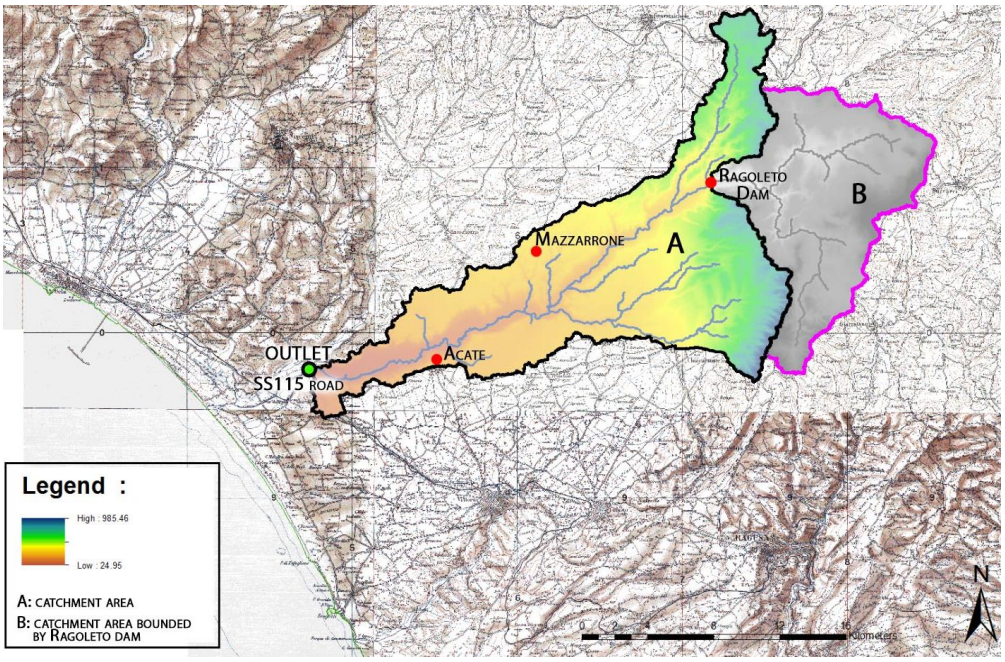

Figure 4-8: Location of Rain gauges (red points) and the catchment area:
A) Catchment area from Ragoleto dam to outlet at SS115 road;
B) Catchment area upperstream of Ragoleto dam.

In the following analyses, the downstream watershed (A) is considered. The upstream catchment area (basin B), limited by Ragoleto Dam, is considered in the analysis as it is represented by the flow releases from the dam that occurred during the flood event.

The following morphometric characteristics of the catchment area are described in Table 4-I: area (A), perimeter (P), average gradient (i_{med}); maximum altitude (H_{max}); minimum altitude (H_{min}); average altitude (H_{med}); outlet altitude (H_{sez}). With regard to the main channel, its characteristics related to the outlet are presented in Table 4-I; in particular, the length of the channel (L), the average gradient (i_{med}) and the maximum and minimum altitude (H_{max} and H_{min}) are reported.

Table 4-I: Morphometric characteristic of catchment area A [high-resolution Digital Terrain Model DTM reported by Sicily Region]

	CATCHMENT AREA					
OUTLET SS115 ROAD	A [km^2]	P [km]	i_{med} [%]	H_{max} [m a.s.l]	H_{min} [m a.s.l]	H_{med} [m a.s.l]
	230.65	138.38	17.51	903.82	24.95	505.28

	MAIN CHANNEL			
OUTLET SS115 ROAD	L [km]	i_{med} [%]	H_{max} [m a.s.l]	H_{min} [m a.s.l]
	49.98	0.96	503.82	24.95

With regard to the rainfall data, information for the 10th and 11th March 2012 is considered, for the rain gauge stations at Acate (62 m a.s.l.), Mazzarrone (303 m a.s.l.), and Ragoleto dam (331 m a.s.l.), all managed by the Water Observatory of Sicily Region. Figure 4-8 shows the location of the rain gauge stations in the catchment.

Table 4-II reports the rain data recorded at the three rain gauges, while Table 4-III gives the maximum rainfall depth for durations of 1, 3, 6, 12 and 24 hours.

Table 4-II: Rain data for March 10th and 11th 2012 collected by Acate, Mazzarrone and Ragoleto dam stations [Water Observatory of Sicily Region].

RAIN GAUGE STATION	START EVENT	END EVENT	DURATION OF THE EVENT	ACCUMULATED RAIN
ACATE	5:30 am (10/03/2012)	10:10 pm (10/03/2012)	16,67 h	36,00 mm
MAZZARRONE	00:40 am (10/03/2012)	4:40 am (11/03/2012)	28,00 h	64,40 mm
RAGOLETO DAM	00:00 am (10/03/2012)	12:00 pm (11/03/2012)	36,00 h	158,10 mm

Table 4-III: Maximum rainfall for duration of 1, 3, 7, 12 and 24 hours, collected by Acate, Mazzarrone and Ragoleto dam stations [Water Observatory of Sicily Region].

RAIN GAUGE STATION	1 hour [mm]	3 hours [mm]	6 hours [mm]	12 hours [mm]	24 hours [mm]
ACATE	5,60	12,40	18,80	26,60	36,00
MAZZARRONE	11,20	21,60	29,80	46,20	64,00
RAGOLETO DAM	14,00	32,80	59,50	101,20	155,20

Each station collects rainfall data for a different influence area and with different time resolutions. The final rainfall causing the flood event is obtained by computing the weighted average of the rainfall collected data, according to the control area of each rain station. Table 4-IV shows the extension of the control area of each rain gauge station and their percentage of influence of the total basin.

Table 4-IV: area of influence of each rain gauge station within the basin.

	RAIN GAUGE STATION	AREA OF INFLUENCE [KM^2]	PERCENTAGE [%]
OUTLET SS115 ROAD	Acate	46,22	20,05
	Mazzarrone	71,16	30,85
	Ragoleto Dam	113,26	49,10

In order to evaluate the flood hydrograph two method are used: the Soil Conservation Service Curve Number method (SCS-CN) and the rational method.

It is first necessary to determine the time of concentration. Time of concentration varies depending upon slope and character of the watershed and the flows path, and is defined as the time required for runoff to travel from the hydraulically most distant point in the watershed to the outlet. Time of concentration is generally applied only to surface runoff and it may be computed using many different methods.

In order to evaluate the time of concentration, two procedures are used: the velocity method and the empirical Giandotti's formula.

The velocity method assumes that time of concentration is the sum of travel times for segments along the hydraulically most distant flow path. Considering the flow type and the gradient, in this case the average velocity is assumed to be equal 1 m/s. The time of concentration is then computed as the ratio of flow length to flow velocity:

$$T_c = \frac{L}{v} \tag{4}$$

Using Giandotti's formula, the time of concentration is:

$$T_c = \frac{4\sqrt{A} + 1{,}5\,L}{0{,}8\sqrt{H}} \tag{5}$$

where T_c is the time of concentration (h), A the watershed area (km^2), L the length of the main channel (km), and H the difference between the mean basin elevation and the outlet elevation (m). This formula was calibrated for 12 basins with drainage areas between 170 and 70 000 km^2. It is not specified how many and which flood events were used in the calibration procedure.

Table 4-V shows the value of the time of concentration for the basin, calculated with both methods described above and as an average of those values.

Table 4-V: time of concentration for catchment area – outlet SS115 road.

OUTLET SS115 ROAD	t_c		
	GIANDOTTI'S FORMULA [hours]	VELOCITY METHOD [hours]	AVERAGE VALUE [hours]
	7,74	13,88	10,81

The time of concentration for the catchment area was approximately 11 hours. These values were used in order to evaluate the flood hydrograph of the flood event.

Soil Conservation Service Curve Number method

The SCS-CN method is an empirical relationship between rainfall (P) and runoff depth (V) as a function of ground conditions (soils, management, and antecedent moisture content). In particular, SCS-CN assumes that the ratio of actual retention (W) to potential maximum retention (S) is equal to the ratio of accumulated runoff depth (V) to potential maximum runoff (P_n):

$$\frac{W}{S} = \frac{V}{P_n} \tag{6}$$

P_n is defined as the difference between the accumulated rainfall depth (P) and the initial abstraction (I_a). After runoff has started, all additional rainfall becomes either runoff or actual retention, so:

$$W = P - I_a - V \tag{7}$$

Moreover, I_a is estimated as 20% of the potential maximum retention S.

Combining equations yields:

$$V = \frac{(P - I_a)^2}{P + 0{,}8\,S} \tag{8}$$

The potential maximum retention is evaluated as function of the Curve Number (CN):

$$S = 25{,}4\,(\frac{1000}{CN} - 10) \tag{9}$$

CN is a dimensionless parameter indicating the runoff response characteristic of a drainage basin. In the Curve Number Method, this parameter is related to land use, land treatment, hydrological condition, hydrological soil group, and antecedent soil moisture condition in the drainage basin.

With regard to the soil, the SCS method defines four hydrological groups:

A. Soils having high infiltration rates even when thoroughly wetted and a high rate of water transmission. Examples are deep, well to excessively drained sands or gravels;
B. Soils having moderate infiltration rates when thoroughly wetted and a moderate rate of water transmission. Examples are moderately deep to deep, moderately well to well drained soils with moderately fine to moderately coarse textures;
C. Soils having low infiltration rates when thoroughly wetted and a low rate of water transmission. Examples are soils with a layer that impedes the downward movement of water or soils of moderately fine-to-fine texture;
D. Soils having very low infiltration rates when thoroughly wetted and a very low rate of water transmission. Examples are clay soils with a high swelling potential, soils with a permanently high watertable, soils with a clay pan or clay layer at or near the surface, or shallow soils over nearly impervious material.

The soil moisture condition in the drainage basin before runoff occurs is another important factor influencing the final CN value. In the Curve Number Method, the soil moisture condition is classified into three Antecedent Moisture Condition (AMC) Classes: I) dray, II) average, III) saturated. These classes are based on the 5-day antecedent rainfall. Table 4-VI presents the seasonal rainfall limits for each AMC class:

Table 4-VI: Season rainfall limits for AMC classes.

AMC	Dormant season	Growing season	Average season
I	< 13 mm	< 36 mm	< 23mm
II	13 - 28 mm	36 - 53 mm	23 – 40 mm
III	> 28 mm	> 53 mm	> 40 mm

In order to evaluate the CN value of the catchment area, the soil composition is analyzed: the site is composed by limestone and sand, consequentially the hydrological soil group should be between "B" and "C". The B soil group has moderate infiltration rates, instead the C soil group has low infiltration rates. The peak runoff rate is greater if the soil is less permeable. Therefore, in the following analyses it is assumed that "C" is the hydrological soil group, to be on the conservative side.

Based on the map of land use [*Assessorato Regionale Territorio e Ambiente Regione Siciliana 2012/'13]*, each area was assigned a value of CN related to its land use and was estimated its surface area. The average value of CN for AMC II is equal to 77. Table 4-VII shows the CN value and the surface area for each land use in the catchment area.

Table 4-VII: CN value and surface area for each land use in the catchment area – outlet SS115.

Land Use	**CN**	**AREA [km^2]**
Impervious area	100	3.55
Crop planting	81	47.30
Citrus grove	78	8.86
Olive grove	73	41.73
Vineyard	78	43.04
Mixed tree and shrub crop	73	5.96
Complex cropping system	80	35.73
Mixed forest	73	9.94
Partially wood areas	73	12.97
brushwood and scrub	71	9.23
Pasture	71	10.12
uncultivated	91	1.96
Reservoirs	100	0.25

With regards to Antecedent Moisture Condition (AMC), the flood event occurred during the dormant season. The 5-day antecedent rainfall was measured at the same three rain gauges.

The measured values are 2 mm, 1 mm, and 28,4 mm. Thus, the average precipitation is equal to 14,66 mm and consequently the CN value for AMC II does not need to be modified.

To estimate the time distribution of the direct runoff at a specific location in the drainage basin, we apply the Unit Hydrograph Method. The dimensionless unit hydrograph used by the Soil Conservation Service was developed by Mockus (1957). Mockus hydrograph is relative to 1 mm depth of storm runoff and relates the ratio of general flow rate Q at general time t and the peak runoff rate Q_p at the time to peak runoff t_a.

The peak runoff rate of the unit hydrograph (m^3/s) is described by the following equation:

$$Q_p = 0.208 \frac{A}{t_a} \tag{10}$$

where A is the area of drainage basin and t_a is the accumulation time, equal to the ratio between the general time t and the time to peak runoff ($t_a=t/t_p$).

On the basis of precipitation contributions to runoff, it is possible to reconstruct the flood hydrograph of the catchment area. The estimated hydrograph is shown in Figure 4-10. The peak runoff rate Q_p is about 186 m^3/s.

Isochrone method

As mentioned above, the time of concentration is an idealized concept, defined as the time taken for a drop of water falling on the most remote point of a drainage basin to reach the outlet, where "remoteness" relates to time of travel rather than distance.

The isochrone method is generally considered an approximate deterministic model representing the flood peak that results from a given rainfall, with the rational coefficient being the ratio of the peak rate of runoff to the rainfall intensity.

First, the isochrones or lines of equal time of travel were determined. The catchment area is divided in ten isochrone areas, as shown in Figure 4-9.

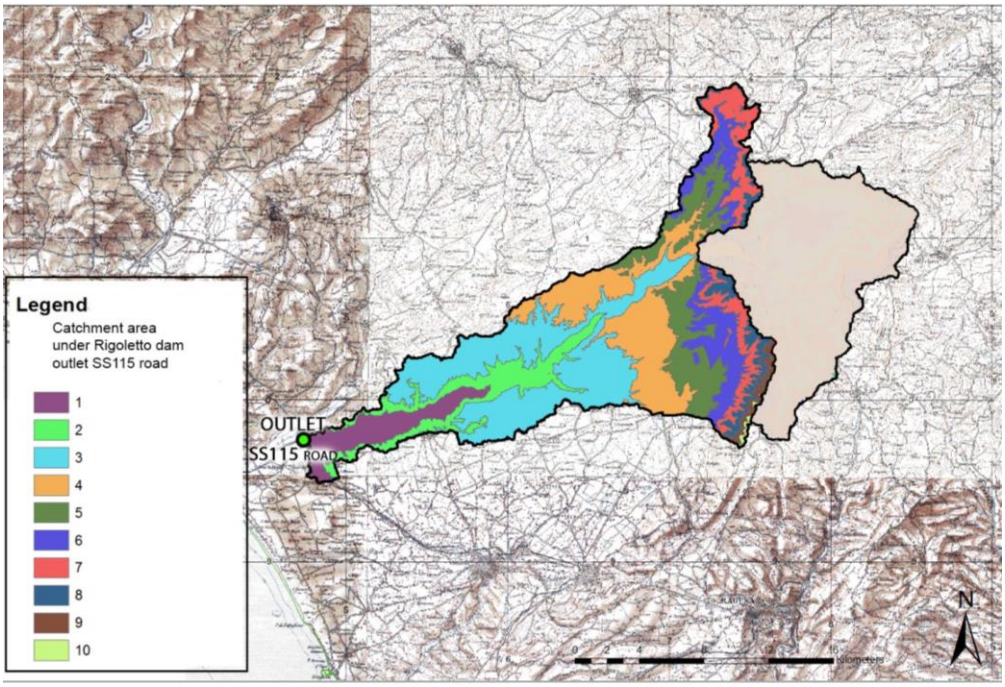

Figure 4-9: Isochrone areas for the detemination of flood hydrograph.

Defining C as the runoff coefficient that is dimensionless and loosely defined as the ratio of runoff to rainfall, the flow rate at j-th time is

$$Q_j = \begin{cases} \frac{C}{\Delta t}\left(h_j^{(1)}A_1 + h_{j-1}^{(2)}A_2 + h_{j-2}^{(3)}A_3 + \cdots + h_1^{(j)}A_j\right) & rise\ of\ the\ hydrograph \\ \frac{C}{\Delta t}\left(h_{j-1}^{(1)}A_{j-n+1} + h_{j-2}^{(2)}A_{j-n+2} + h_{j-3}^{(3)}A_{j-n+3} + \cdots + h_{j-n}^{(n)}A_j\right) & recession\ of\ the\ hydrograph \end{cases} \quad (11)$$

where Δt is the unit time as a fraction of the time of concentration ($\Delta t = t_c/n$), and $h_j^{(i)}$ is the depth of the rainfall in the i-th isochrones area.

With regards to the vegetation present on the catchment area, a Frevert's coefficient is defined for each land use. Table 4-VIII shows the values adopted for each area. The weighted average of C for the catchment area is 0,41. In order to be on the conservative side, the value adopted is 0,45.

The estimated hydrograph is shown in Figure 4-10. The peak runoff rate Q_p turned out to be about 180 m^3/s.

Table 4-VIII: Frevert's coefficient and surface area for each land use on the catchment area under Ragoleto Dam – outlet SS115.

Land Use	**C**	**AREA [km²]**
Impervious area	1	3,55
Crop planting	0,4	47,3
Citrus grove	0,45	8,86
Olive grove	0,5	41,73
Vineyard	0,4	43,04
Mixed tree and shrub crop	0,35	5,96
Complex cropping system	0,45	35,73
Mixed forest	0,3	9,94
Partially wood areas	0,25	12,97
brushwood and scrub	0,25	9,23
Pasture	0,2	10,12
uncultivated	0,16	1,96
Reservoirs	1	0,25

Flood Hydrograph

The flood hydrograph at the SS115 road outlet has to be adjusted as the hydrographs obtained by both the SCS and the rational method must be increased by the flow released from the dam, as recorded during the flood event on 10th March 2012.

The flood hydrograph is reconstructed at the SS115 section; thus, the dam outflow has to be temporally offset considering the lag time that it takes to reach the outlet.

Figure 4-10 shows five different hydrographs at the SS115 road outlet:

a) the runoff hydrograph estimated with the SCS Method;
b) the runoff hydrograph estimated with the Isochrone Method;
c) the outflow hydrograph of Ragoleto dam;
d) the flood hydrograph estimated as the sum of the runoff hydrograph obtained by the SCS method and the lagged dam outflow hydrograph;
e) the flood event hydrograph estimated as the sum of the runoff hydrograph obtained by the Isochrone method and the lagged dam outflow hydrograph.

The peak runoff rate Q_p calculated as the sum of the runoff hydrograph estimated by the SCS method and the dam outflow hydrograph is about 262 m^3/s, while that computed as the sum of the runoff hydrograph estimated by the Isochrone method and the dam outflow hydrograph is about 236 m^3/s.

The SCS method resulted in a larger value of the peak discharge. Therefore, as a precautionary measure, the combined hydrograph using the SCS method was chosen for the following analyses.

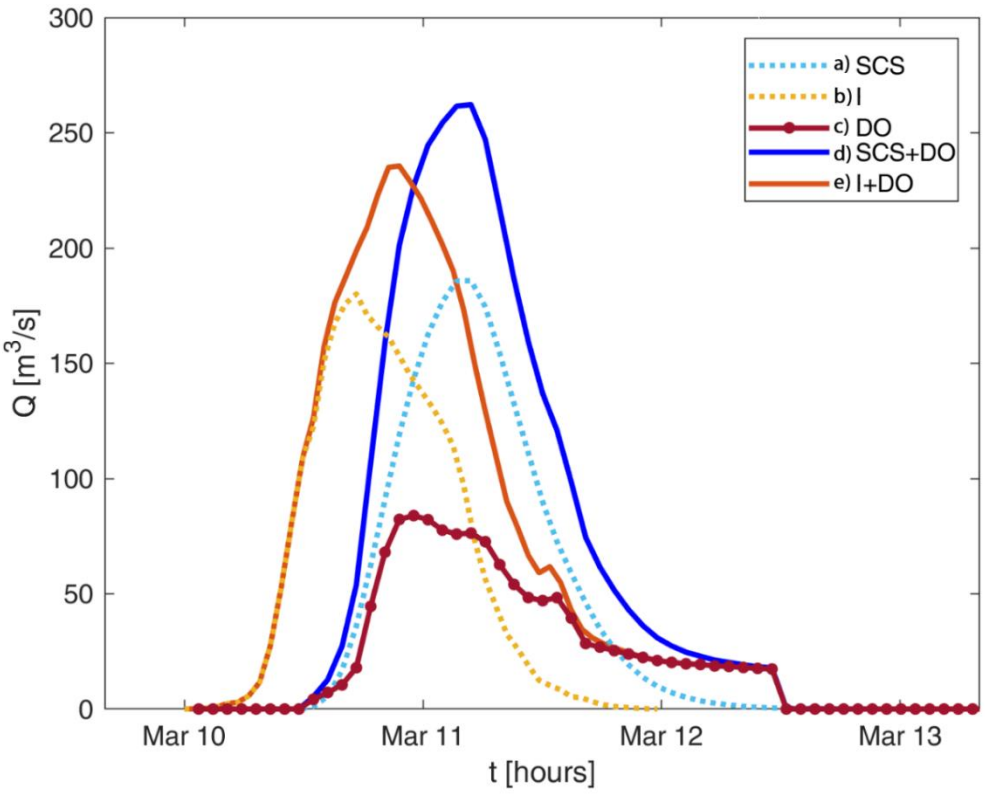

Figure 4-10: Runoff rate hydrographs of catchment area with SS115 road outlet:
a) SCS = the runoff hydrograph estimated with the SCS Method;
b) I = the runoff hydrograph estimated with the Isochrone Method;
c) DO = the outflow hydrograph of Ragoleto dam;
d) SCS + DO = Sum of the runoff hydrograph estimated with the SCS method and the dam outflow hydrograph;
e) I + DO = Sum of the runoff hydrograph estimated with the Isochrone method and the dam outflow hydrograph.

4.3.2. *Levee vulnerability: Overtopping phenomenon*

Levees can be overtopped when the river elevation exceeds the upper part of the levee.

In order to verify if levee overtopping occurred during the 2012 flood event, flow profiles are simulated using HEC-RAS, a software that performs one-dimensional free-surface profiles for steady, gradually varied flow.

HEC-RAS is a software implemented by the Hydrologic Engineering Center of the US Army Corps of Engineers and the basic computational procedure is based on the solution of the one-dimensional energy equation. Energy losses are evaluated by friction (Manning's equation) and contraction/expansion (coefficient multiplied by the change in velocity head). The momentum equation may be used in situations where the free-surface profile is rapidly varied. These situations include mixed flow regime calculations (i.e., hydraulic jumps), hydraulics of bridges, and profiles at river confluences (stream junctions).

To define the most realistic geomorphologic configuration of the river, we used the data and cartographic material available from the 2008 repair work of the control structures, performed by Ufficio of Genio Civile of Ragusa and ICARO Ecology s.r.l. of Gela. They include the most complete and up-to-date information about the configuration of Dirillo river before the flood event.

Figure 4-11 shows the configuration of the river and the position of the control cross sections used for the HEC-RAS numerical simulations. The river profile and levee elevations are shown in Figure 4-12. It is important to emphasize that the study stretch is crossed by different structures (bridges etc..) that affect the river flow, so they must be considered. The location of these structures is illustrated in Figure 4-11 and Figure 4-12 with numbers 37, 29, 22, 18 and 12.

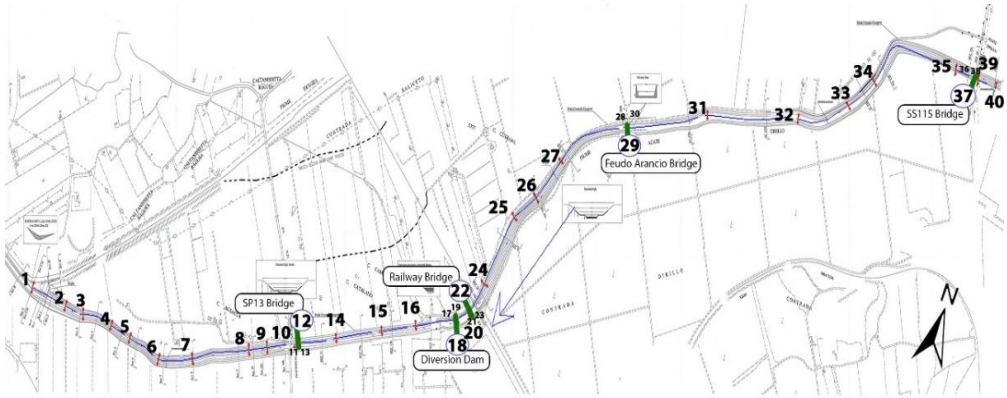

Figure 4-11: Planview of Dirillo River and location of control cross sections obtained from the project of 2008 restored works [Genio Civile of Ragusa and ICARO Ecology s.r.l. of Gela 8th May 2008].

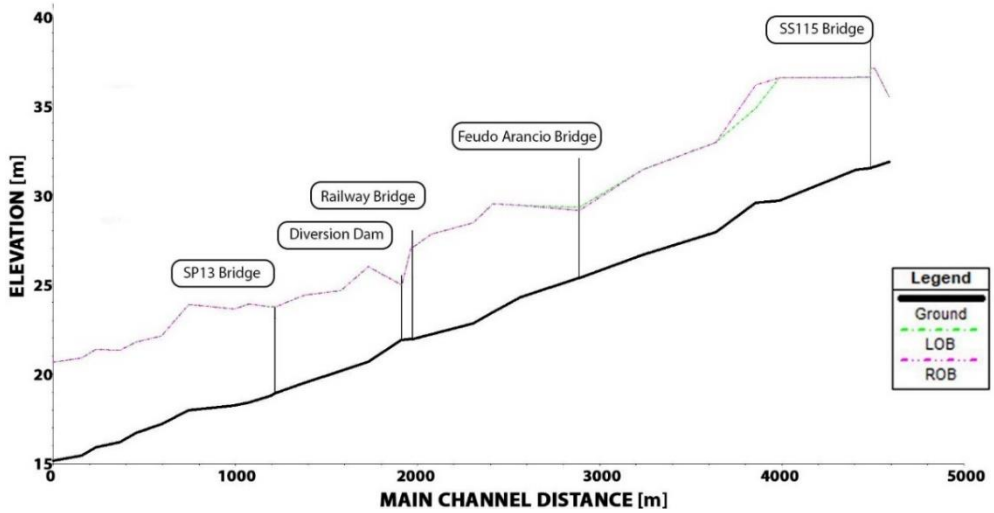

Figure 4-12: Dirillo River profile and levee level:
i) Ground= main channel;
ii) LOB= left overbank;
iii) ROB= right overbank.

Longitudinal position of elevation of cross sections investigated are presented in Table 4-IX. In order to improve the simulation, the computational grid is enhanced by a linear interpolation between each two consecutive cross sections. The maximum distance between interpolated sections is 1 meter. In the Annex, all the cross-section configurations presented in Table 4-IX are represented. As can be seen, the slope of the river is about 3‰.

Table 4-IX: Geo-morphologic characteristics of investigated cross section.

Section number	**Distance from river mouth** [m]	**Bed elevation** [m. a.s.l.]	**Notes**
40	5194,00	31,80	
39	5117,00	31,54	
38	5102,00	31,50	
37	5198,00	31,50	SS115 Bridge
36	5094,00	31,47	
35	5064,00	31,37	
34	4533,00	29,65	
33	4498,00	29,54	
32	3989,40	27,90	
31	3598,40	26,63	
30	3218,20	25,38	
29	3214,70	25,38	Feudo Acancio Bridge
28	3211,20	25,38	
27	2909,90	24,29	
26	2716,10	23,45	
25	2491,50	22,82	
24	2272,60	22,21	
23	2185,70	21,94	
22	2181,70	21,94	Railway Bridge
21	2177,70	21,94	
20	2173,70	21,94	
19	1980,30	21,91	
18	1978,10	21,91	Diversion Dam
17	1975,80	21,91	
16	1781,90	20,70	
15	1627,10	20,16	
14	1438,0	19,50	
13	1266,80	18,93	
12	1264,30	18,90	SP31 Bridge
11	1261,80	18,90	
10	1235,70	18,80	
9	1123,70	18,41	
8	1079,10	18,26	
7	1003,20	18,00	
6	778,80	17,22	
5	629,20	16,71	
4	483,90	16,20	
3	398,50	15,91	
2	266,90	15,45	
1	182,10	15,16	

Obviously, all the simulations are affected by a margin of error related to limited knowledge of real conditions. In the following analyses, the main source of error is associated to the uncertain value of roughness.

The levee repair works were made in 2008, so it is safe to assume that in 2012 the vegetation had already started to grow. Thus, since the literature suggests a Manning's coefficient between 0,10 and 0,03 $s/m^{1/3}$ for natural channels, and considering the conditions in 2012, it is appropriate to consider a Manning's coefficient equal to 0,03 $s/m^{1/3}$.

With regards to the steady flow analysis, the flow rate considered is equal to the peak runoff rate Q_p evaluated with SCS methodology at the outlet, about 262 m^3/s.

Considering the mild slope of the main channel, the distance from the river mouth and the value of flow rate, it is proper to regard the downstream flow condition as uniform flow. Moreover, the steady flow simulation models a mixed flow regimes water surface profile.

Figure 4-13 shows the water profile of the steady flow simulation. It is evident that the river levees are not always adequate to contain the water flow. In particular, the bridge structures reduce the river section and, the elevation of the levees is not enough high in correspondence at the Feudo Arancio Bridge and of the diversion dam. Consequently, close to these two structures, the water overflows the banks of the river.

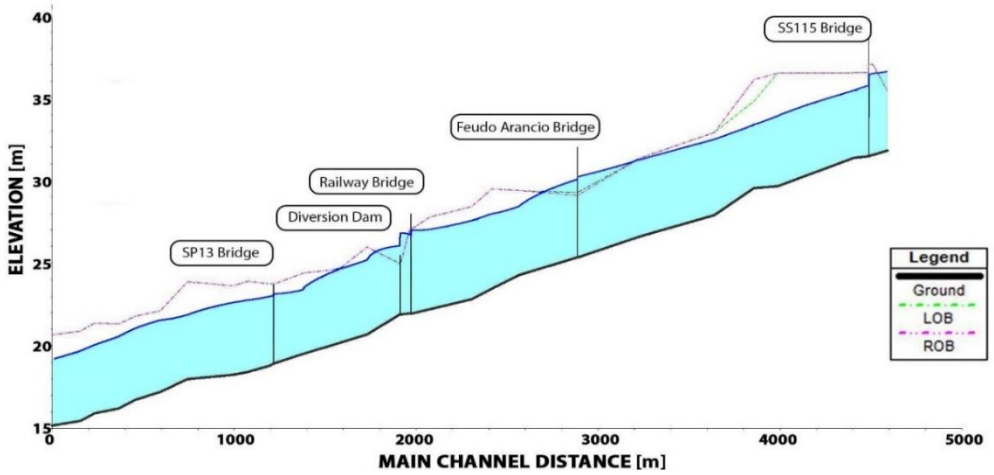

Figure 4-13: Water profile in a steady flow simulation of Dirillo River, considering a flow rate of 262 m^3/s.

With regard to the 2012 flood event, Figure 4-14 shows the locations pinpointed from the landowners' historical memory and the reports drafted by the Civil Protection Department as points with levee overtopping.

From the steady flow analysis, some overflow occurs near the crossing structures (Feudo Arancio Bridge, Railway Bridge, Division Dam). Nevertheless, during the 2012 flood event, other overflows occurred at unexpected places, such as points A, B, D and F of Figure 4-14, corresponding to sections 33, 32, 24 and 14, respectively.

In particular, the freeboards evaluated by the simulation are the following: at section 33 it is 1,42 on the left side and 2,71 m on the right side; at section 32 it is 0,42 m; at section 24 the freeboard is 0,59 m; and at section 14 the freeboard is 1 m.

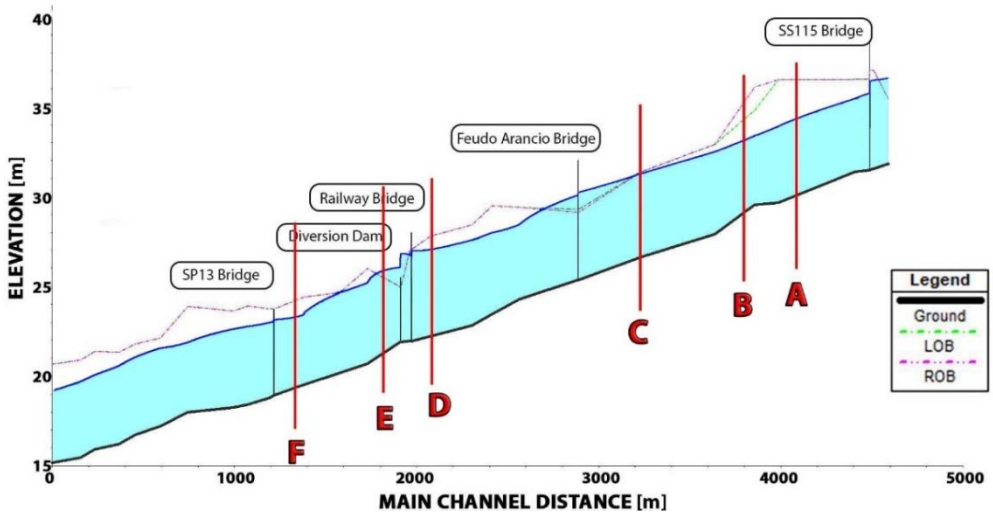

Figure 4-14: the overflow points on Dirillo levee during the 2012 flood event.

The freeboards are reported for each section, in Table 4-X. Different colors are used to facilitate reading the table; in particular, green is used for a freeboard greater than 0,50 m, orange indicates sections where overflows occurred, and yellow is used for freeboard values ranging from 0,01 to 0,50 m. As can be seen, the sections where overtopping occurred are all near bridges. Instead, at other section along river, the levees should not have been overtopped by the water profile.

Table 4-X: Freeboard evaluation through HEC-RAS stady flow simulation of the peak discharge during the 2012 flood event at each investigated cross section.

Section number	Freeboard		Notes
	Left	Right	
40	0,00		
39	0,54		
38	0,55		
37	1,04		SS115 Bridge
36	0,79		
35	1,09		
34	2,58		
33	1,42	2,71	Failure Levee A
32	0,42		Failure Levee B
31	0,11		Failure Levee C
30	0,00		
29	0,00		Feudo Acancio Bridge
28	0,00		
27	0,95		
26	1,43		
25	0,76		
24	0,59		Failure Levee D
23	0,00		
22	0,00		Railway Bridge
21	0,07		
20	0,08		
19	0,00		
18	0,00		Diversion Dam
17	0,00		Failure Levee E
16	0,80		
15	0,03		
14	1,00		Failure Levee F
13	0,59		
12	0,77		SP31 Bridge
11	0,70		
10	0,75		
9	1,16		
8	1,01		
7	2,01		
6	0,57		
5	0,75		
4	0.75		
3	1,31		
2	1,20		
1	1,47		

These discrepancies between the actual event of 2012 and the Hec-Ras simulated event could be due to other factors. Overtopping might not be the only mechanism triggering levee failures during the 2012 flood event. In the following section, seepage vulnerability is investigated.

4.3.3. *Levee vulnerability: Seepage phenomenon*

As mentioned above, during the 2012 flood event the Dirillo River levees broke at different sections shown in Figure 4-7 and Figure 4-14 with letters A, B, C, D, E and F.

In order to evaluate the seepage mechanisms that could have triggered levee failures, the cross section at location where levees failed are studied and their geometrical characteristics are shown in Figure 4-15.

For each representative cross section, the duration of flood levels in river during the flood event is assessed.

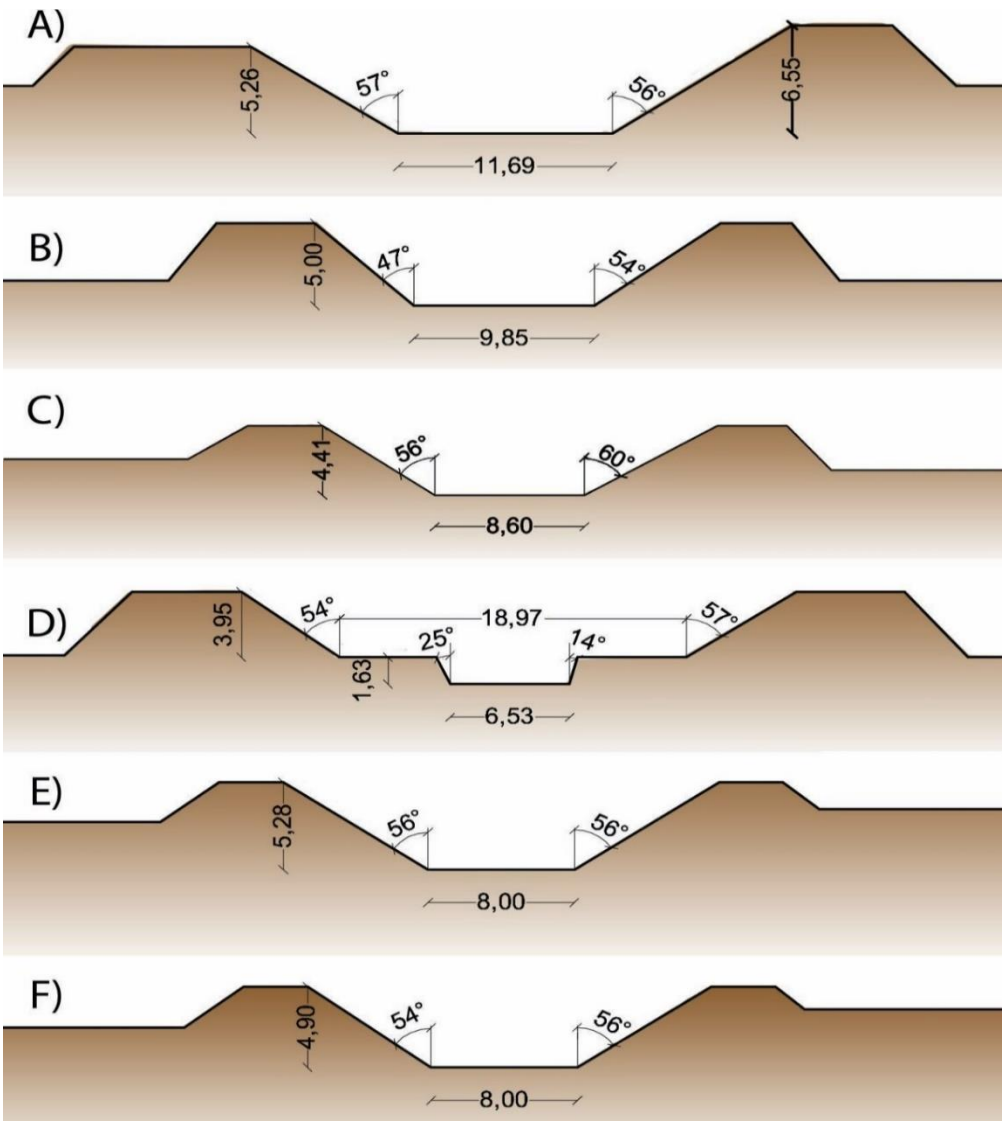

Figure 4-15: Cross sections at locations where Dirillo River levees failed.

As mentioned above, the last levee repair works before the 2012 flood event were made in 2008. It is safe to assume that in those years the vegetation (currently invasive) started to grow. Thus, since the literature suggests a Strickler value between 30 and 40 $m^{1/3}/s^{-1}$, it is considered more appropriate to pursue the following analyses by applying a Strickler value in such a range. Moreover, with the aim of evaluating

the influence of the Strickler coefficients, a sensitivity analysis to compare the flood level persistence calculated using five different Ks values between 30 and 40 $m^{1/3}/s^{-1}$ is performed. As shown in Figure 4-16, the value Ks equal to 30 $m^{1/3}s^{-1}$ is more conservative.

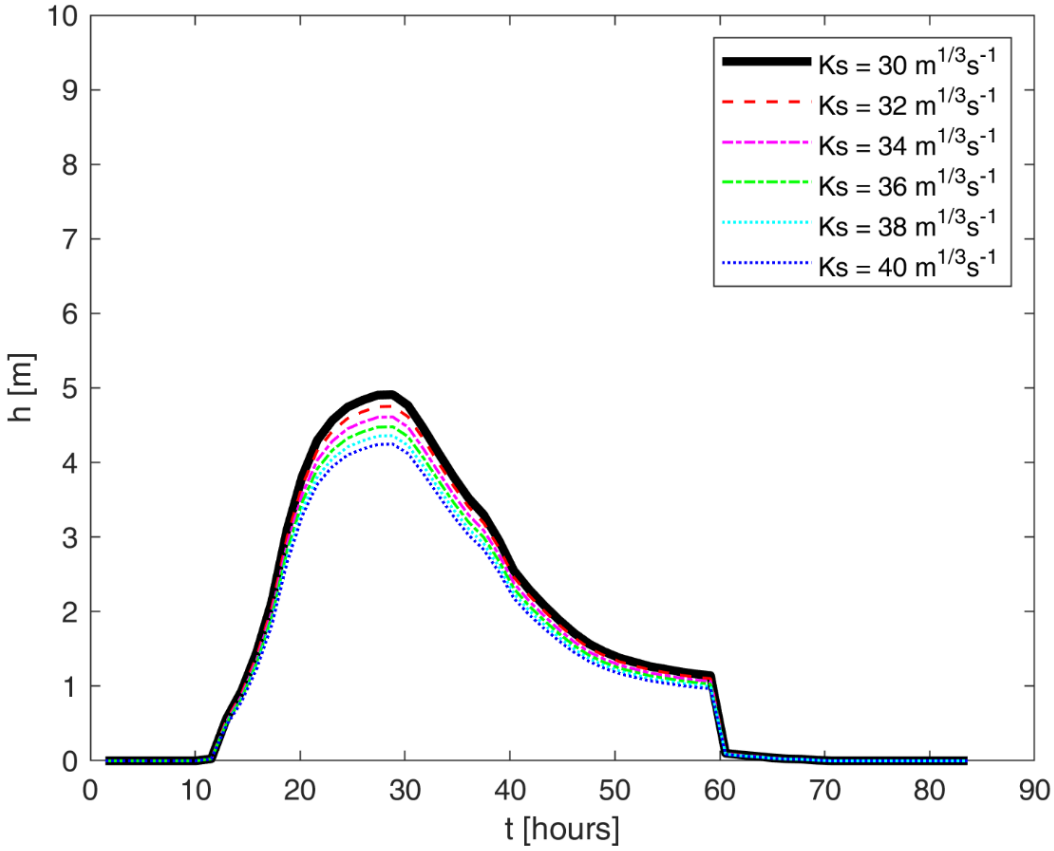

Figure 4-16: Flood level persistence of the upstream cross section (immediately under SS115 road).

A well-designed levee should contain the phreatic line within its body (Section 2.4). The condition in which the phreatic line reaches the landside is a hydraulic failure of the levee performance and represents a dangerous situation that affects the levee reliability.

In order to assess the levee vulnerability to seepage, standard methods generally compare the time scales of the seepage process and the persistence of flood levels in the river. The time scale of the through-seepage process associated with the state of the phreatic line reaching the landside surface is addressed as a typical condition that may lead to successive failures, as stated previously.

With regards to the soil characteristics, as analysed in Section 4.3.1, the soil has low infiltration rates and is composed by sand and limestone. Consequentially it is safe to assume a porosity equal to 0,4 and a hydraulic conductivity equal to 10^{-5} m/s.

Marchi's (1961) and modified Green–Ampt's (Pistocchi et al., 2004) models, mentioned in Section 2.4, are simultaneously applied on the case study. These models provide a different prediction of the phreatic line position because they are based on quite different assumptions. Specifically, Marchi's model tends to give reliable results for the seepage flow in the lower region of the levee body, whereas it underestimates the elevation of the saturation line in the region near the levee crest, where the adapted Green-Ampt's method appears to be more realistic.

Figure 4-17 to Figure 4-22 show the evolution of the phreatic line inside the levee cross sections A, B, C, D, E, and F, respectively, during the flood event. In particular, considering the flood level duration in the Dirillo river from 7:00 of the 10th March 2012 (the 1st hour in Figures) to 12:00 of the 13th March 2012 (the 84th hours in Figures), the variations of the phreatic line inside the levees are calculated.

As demonstrated, the phreatic line never reaches the landside slope of the levee cross sections, except for section D (Figure 4-20), in which the phreatic line is about to reach the landside toe.

Thus, the seepage phenomenon does not appear to be a plausible mechanism to explain the levee failures during the 2012 flood event.

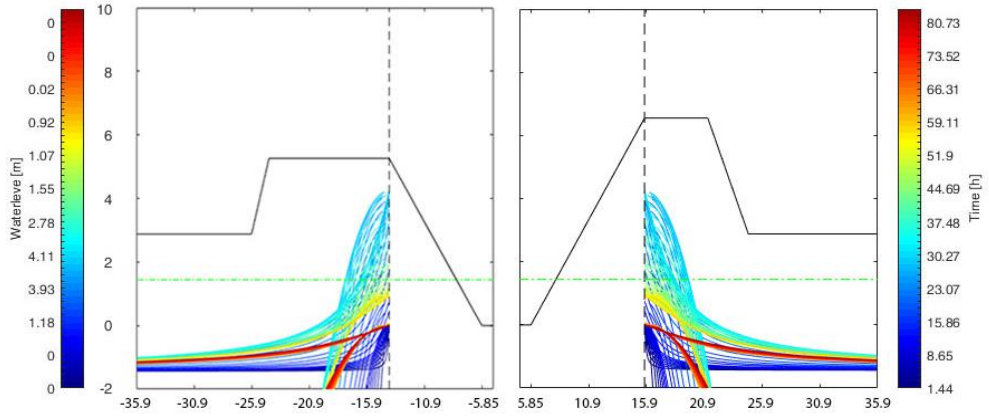

Figure 4-17: Evolution of the phreatic line inside the levee during the flood - cross section A.

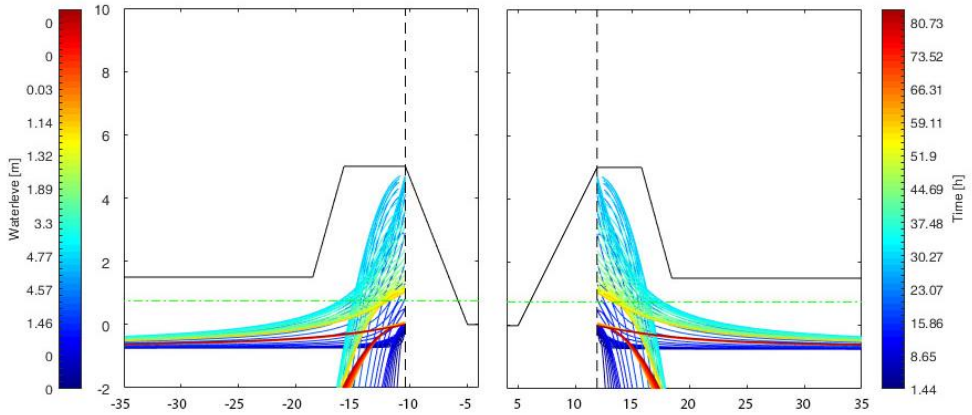

Figure 4-18: Evolution of the phreatic line inside the levee during the flood - cross section B.

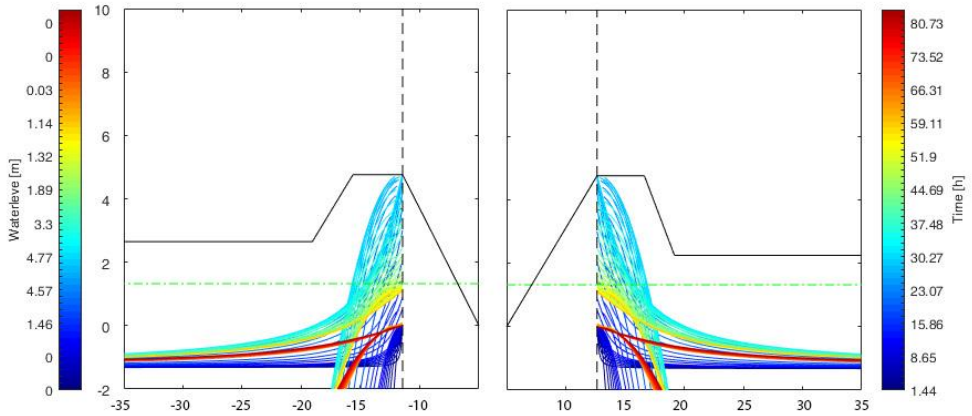

Figure 4-19: Evolution of the phreatic line inside the levee during the flood - cross section C.

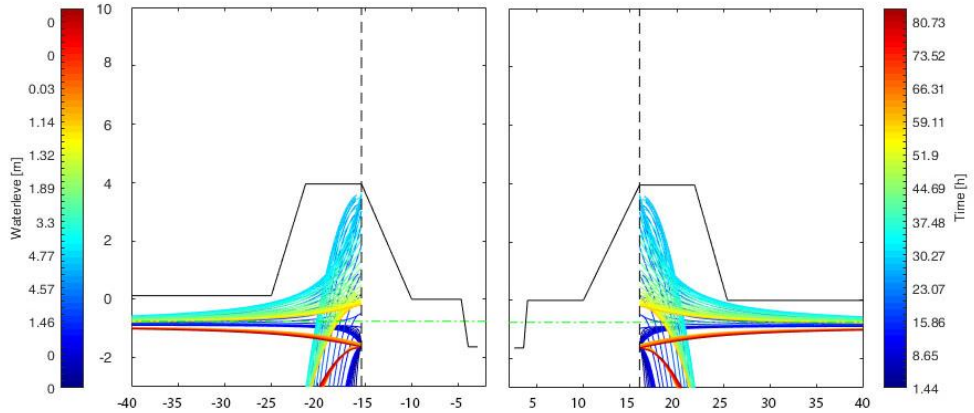

Figure 4-20: Evolution of the phreatic line inside the levee during the flood - cross section D.

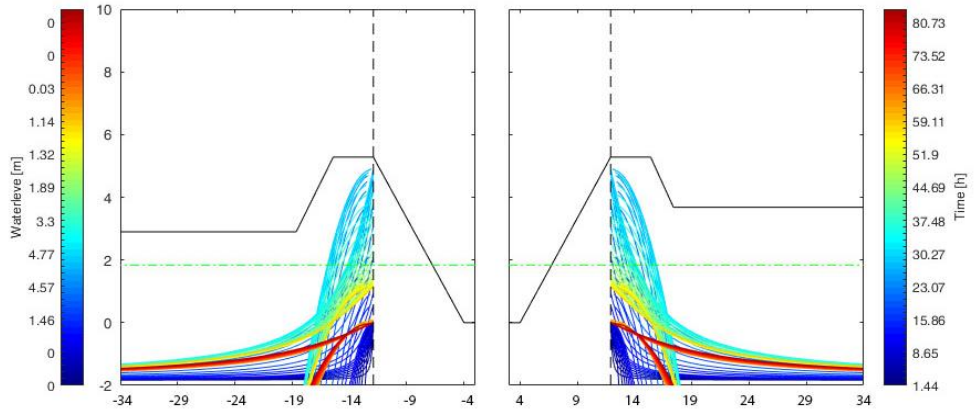

Figure 4-21: Evolution of the phreatic line inside the levee during the flood - cross section E.

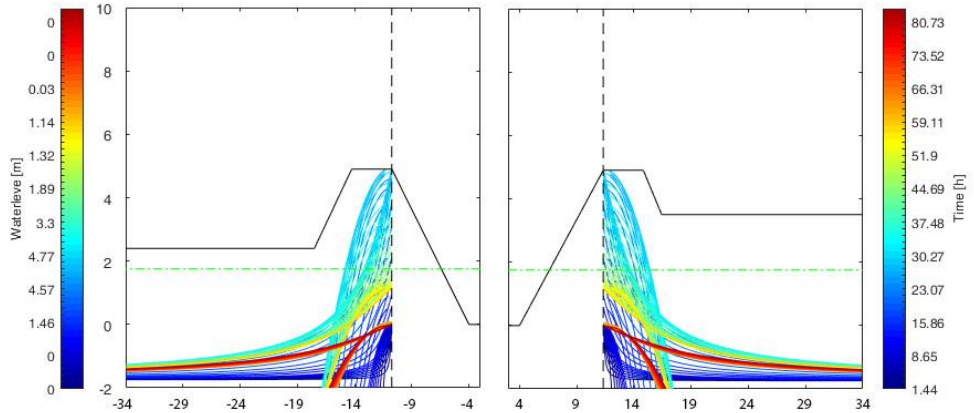

Figure 4-22: Evolution of the phreatic line inside the levee during the flood - cross section F.

4.3.4. *Discussion and conclusions about flood event analyses*

The 2012 flood event caused huge damages on the Dirillo River floodplain. Using the landowners' historical memory and consulting reports drafted by the Civil Protection Department, the locations of river levees collapses were determined, and the flooding was reconstructed. Using precipitation data and a rainfall-runoff model, the flood hydrograph at the SS115 road outlet was estimated. The peak runoff rate $Q_{p,}$ calculated as the sum of the runoff hydrograph estimated by the SCS method and the dam outflow hydrograph, was about 262 m^3/s, and it was used to assess levee failure mechanisms.

The numerical simulations carried out with Hec Ras enable to reproduce the water profile during the maximum flow rate. The results suggest that levee failure cannot always be explained through an overtopping mechanism. Moreover, application of Marchi's and a modified Green-Ampt analytic models to evaluate the position of the phreatic line suggests that, probably, the seepage phenomenon did not occur.

It may be worthwhile to mention that the hydrological and hydrological modelling outputs are subject to uncertainty resulting from different sources of errors at every step (e.g., error in input data, model structure, and model parameters). First, the number of stations, temporal scale, cell size of interpolation grid and different interpolation methods cause the uncertainty in the spatial interpolation of the rainfall data [Zhu et Jia., 2004]. Second, with regards to the time of concentration (T_c), a universally accepted working definition is currently lacking and several definitions can be found in the technical literature along with related estimation procedures [Grimaldi et al., 2012]. Moreover, the linear hypothesis that allows for considering T_c to be quasi-invariant with respect to the rainfall intensity can only be approximately verified for flood events with a high return period [Dooge, 1973]. Consequently, empirical approaches generally overestimate T_c when all the available flood events are considered in the calibration phase, irrespective of their magnitude [Grimaldi et al., 2012]. Third, the Curve Number (CN) method is an empirical rainfall-runoff

model developed in the 1950s by the USDA Soil Conservation Service (SCS), in response to the complexity of land use and the hydrological abstraction of rainfall. Several factors are integrated in the CN method, such as land cover and land use, surface condition, soil class, and antecedent runoff condition, which are combined in a single CN parameter [Oliveira et al., 2016]. However, empirical evidence shows that use of tabulated CN normally over-designs the hydrological systems [Lal et al., 2016]. Finally, the runoff coefficients can provide information on basin soil response; nevertheless, the values reported in the literature often convey less information than required to allow for catchment classification [Blume et al., 2007]. Other sources of uncertainty are related to the geometry of the investigated river reaches, the roughness coefficients as well as the presence disturbing factors during the event (e.g. partial occlusions due to debris), difficult to assess unless observations are available.

Despite the uncertainties, results seem to indicate that the main failure mechanisms were not overtopping nor seepage. Considering that the investigated area of Dirillo River is likely to be a burrowing animal site, it is reasonable to assume that some of the levee may have collapsed during the flood event because the structures were severely deteriorated by biota.

To evaluate the impact of biological activities and to gain knowledge of animal burrows, levee inspections were performed and non –destructive investigation were conducted. In the following sections, the results of in-situ inspections carried out on the 2nd July 2019 are described.

4.4. Burrows on the Dirillo river levee

Wildlife interacts with earthen levees ad if these were a natural field or forest. Thus, an important step toward fortifying a levee against the effect of nuisance wildlife damage is observing clues left by animals (FEMA 2005).

The goal of the levee inspection was to see the entire surface clearly. The Dirillo levees were inspected between the SS115 road and the SP31 road. Specifically, as shown in Figure 4-23, from SS155 road to 2 km downstream (point A), the right levee of the river was observed; from that point to SP31 road, the left levee of the river was monitored. To ensure an exhaustive field survey, the entire slope surface is observed.

Unfortunately, the presence of dense vegetation does not allow to fully investigate the riverside slope. However, as suggested by FEMA (2005), inspections are performed walking back and forth across the slope, utilizing zig-zag patterns.

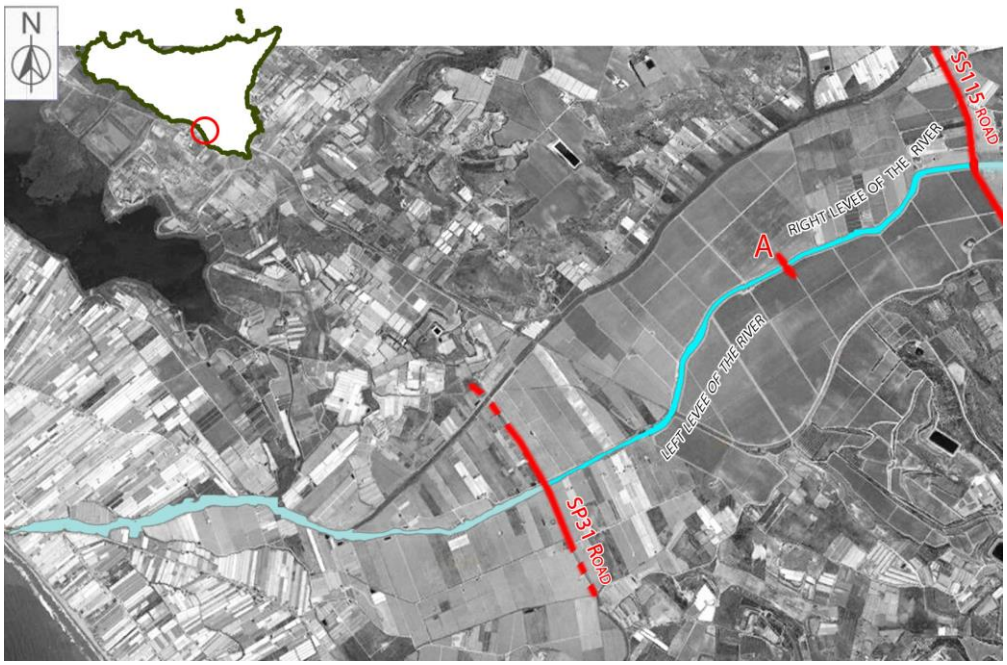

Figure 4-23: Dirillo levees ispected: right levee of the river from SS115 road to point A; left levee of the river form point A to SP31 road.

Eight interesting holes were found and inspected. Hole number 1 is located on the right levee of Dirillo River, lightly hidden under the vegetation. The "homing" of the dens and the earth put upside down demonstrate that it has been used. Another hole, number 2, on the riverside of the same levee was discovered. Its dimensions and entrance conformations suggest that the same animal species lives in all of these dens. Figure 4-24 shows the two dens and their position. The holes from number 3 to number 8, shown in Figure 4-25, are easily identifiable on the landside slope of left levee. This has been possible thanks to the good maintenance work of landowners. In fact, the landside of the levee is located on Feudo Arancio's property and the owners have committed themselves to keep the crest and the slope of the levee always tidy and clear.

Figure 4-24: Location of dens number 1 and 2 along the Dirillo river.

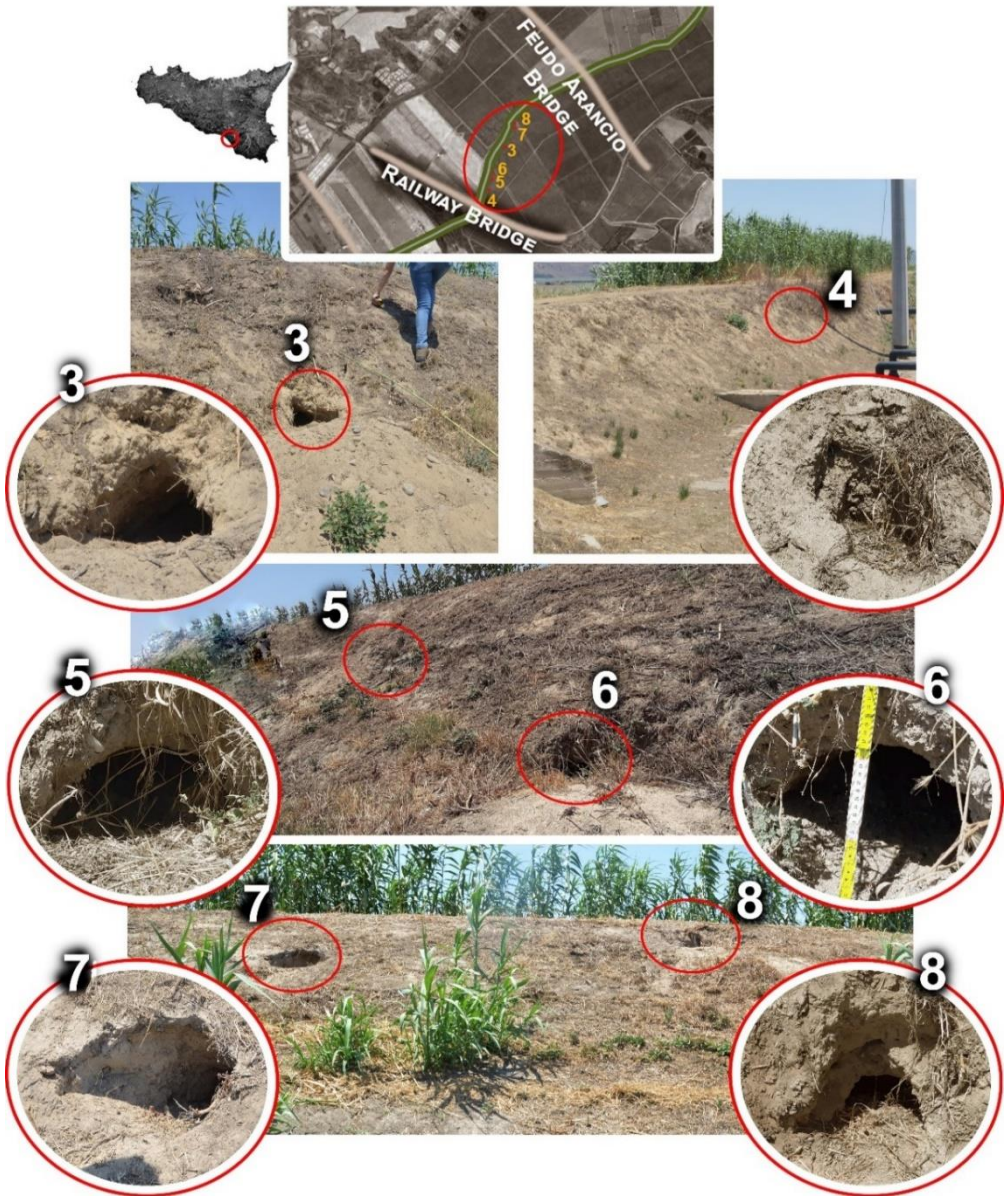

Figure 4-25: Location of dens number 3, 4, 5, 6, 7 and 8 along the Dirillo river.

The holes are located on the middle-upper part of the levee slope. Exactly, they all are near the crest of the levee, never below 2,00 m from the crest level. This suggests that the burrowers should be a terrestrial animal, because generally they

would inhabit or hunt in the crest area. On the other hand, amphibian animals like the nutria, prefer the downstream slope area.

As is the case for holes number 1 and 2, these dens are actively used by the hosts.

Moreover, even though the den entrances have different shapes, the tunnel dimensions are almost always the same: the diameter is about 0,30 meters and their depth is longer than 2 metres. Indeed, as shown in Figure 4-26, during the in-situ investigation, a 2 m-long wooden ruler was completely inserted into the holes without encountering any obstacles.

Figure 4-26: On-site investigation and burrow depth analyses.

The in-situ investigation suggests that all of the burrows belong to the same animal species. The hole dimensions and their positions on the slope levee suggest that the burrowing animal is a large mammal, most likely a terrestrial creature. Some footprints (Figure 4-27) and quills were found, suggesting that *Hystrix cristata* (a porcupine) inhabits all these dens. Their behaviour, discussed in the following section, could justify the presence of connected tunnels within the Dirillo river levee: they hide on the reeds present on the riverside slope, but go out to look for food on the landside.

For a more extensive and complete study of the burrow, a GPR survey was carried out. The underground path of the tunnel inside the levee ant the connection between the different holes is described in section 4.4.2.

Figure 4-27: Field evidence of the presence of burrowing animals: porcupine footprint and quill near hole no.6.

4.4.1. *Porcupine: the Dirillo burrowing animal*

Porcupines are terrestrial mammals covered in long spines or quills which live in family groups in their complex burrow systems [Bayoumi et al., 2011]. The term covers two families of animals: the Old World porcupines of the family Hystricidae and the New World porcupines of the family Erethizontidae. The Old World porcupine is found in the Mediterranean, including mainland Italy and the island of Sicily, Morocco, Algeria, Tunisia, Libya, and along the Egyptian coast [Camici et al., 2006]. Specifically, in Sicily, some specimens of this animal, shown in Figure 4-28, have been seen near the Dirillo River.

Figure 4-28: Portrait of a South Africa Porcupine [Bridgena Barnard - code91958341 www.gettyimages.com.au]

Their distinguishing feature is the coating of the entire body in long quills, which run along the head, nape, tail and back. The quills are modified hair, made from

keratin like human hair, but hardened. They are hollow and stiff, with a sharp, barb covered, point at the end. The quills typically lie flat until a porcupine is threatened, whom they leap to attention as a persuasive deterrent. In fact, porcupines have muscles at the base of each quill allowing them to be raised, in defence, making a crest, which gives it its common name of crested porcupine [Roze, 2009].

Two types of quill cover porcupines: sturdier quills and rattle quills [Amori et al.,1992]. The sturdier quills, which are about 35 cm (14 in) in length, run along the sides and back half of the body and are usually marked with alternated light and dark bands. If threatened, porcupines will run at speed backwards towards the threat, embedding the quills deep into them, often causing serious injury, or death through infection. Traumatic injuries caused by encounters with porcupines are relatively common in dogs and are well represented in the literature [Pilati et al., 2015]. Quills have sharp tips and overlapping scales or barbs that make them difficult to remove once they are stuck in another animal's skin. Porcupines cannot shoot them at predators as once thought, but the quills will fall out regularly just like hair [Woods, 1973]. Porcupines grow new quills to replace the ones they lose.

Rattle quills are located only at the end of the short tail instead. They are hollowed in such a way that when they are vibrated, they produce a hiss-like rattle [Amori et al.,1992]. This response is usually used when the animal is threatened or acting aggressively. The rest of the porcupine body is covered in rough dark brown bristles.

The crested porcupine is one of the largest rodents in the world, in fact, most porcupines are about 50-70 cm long and their weight is about 10-15 kg [Toschi, 1965]. The body is stocky, with short, thick legs. The fore feet have four developed and clawed digits with a regressed thumb. The hind feet have five identical digits. The paws have naked and padded soles and they have a plantigrade gait. The ears are external, and both the eyes and ears are relatively small with long vibrissae, or whiskers, on its head.

The skull is specific in many ways; first, the infraorbital foramen is greatly enlarged so portions of the masseter extend through it and attach from the frontal side surface of the snout. Second, the angular process is inflected on the lower jaw, and third, the nasal cavity is enlarged [Toschi, 1965]. Prominent pockets create enlarged areas of attachment for chewing muscles. Collarbones are very much reduced, and one incisor, one premolar and three molars are present in each quadrant. The teeth of the porcupine are specially adapted to grind down the plant material they eat, with sharp incisors, and large flat molars [Toschi, 1965]. Like all rodents, the incisor teeth grow constantly and need to be worn down. Their digestive system allows all of the undigested fibre from their food to be stored in a part of the enlarged appendix, and the large intestine, where they are then broken down further by microorganisms in the gut [Roze, 2009].

These terrestrial mammals are herbivore, feeding on leaves, herbs, twigs, roots, bark, berries, fruit, and even farmers' crops. They are also able to climbs trees to find food and they commonly chew on bones from carrion, or even dig up old bones, to sharpen their teeth and provide a source of calcium, phosphorus, and sodium. Porcupines will hoard bones and other hard items in their burrows, sometimes numbering into thousands of items.

Porcupines are not solitary. They usually live on the ground in small family groups of an adult pair and their offspring. The adult pair is monogamous, and mates for life. This family group lives in a complex tunnel system where they spend the day time. The burrow may be a hole in a cave, rock crevice, or an unused aardvark hole, but they will also dig their own burrows. Generally, the burrows are hidden in areas characterized by dense vegetation and their dens can be up to 20 meters long with a 2 meters deep living chamber. The female will move to a separate part of the tunnel system when giving birth to new young, building her own nesting chamber, where she will stay alone [Corsini et al., 1995]. However, it is common to see porcupines alone. Indeed, porcupines do forage for food alone, usually at night time when they are mostly active: they will then return to the family den for the day. These animals often

travel long distances looking for food. Sometimes, they can travel up to 15 km in a night.

The observed quills and footprints, the dimension of the holes, the characteristics of the Dirillo river area compared to those generally inhabited by porcupine, their physical features and behavioral characteristics suggest that these rodents are responsible for the presence of burrows within the investigated levees.

4.4.2. *GPR field work*

After visual inspection of the activity of burrowing animals and measuring the dimensions of the hole entrances, a Ground Penetrating Radar (GPR) survey was conducted. GPR is a geophysical technique to detect and identify structures, either natural or man-made, below the ground surface.

The application of radar in the detection of buried objects is quite an old practice; there are details of such work dating back to 1910, with the first pulsed experiments reported in 1926 when the depths of rock strata were determined by time-of-flight methods. Nowadays, GPR is applied in a wide range of engineering surveys as a non-invasive method for mapping subsoil features. However, the literature on the applicability of GPR techniques to monitoring levees and river embankments is still limited [Di Prinzio et al., 2010].

Detection and characterization of underground voids within hydraulic defence structures is one of the major issues to deal with. Determining the levee state-of-health in a non-destructive and fast way plays an important role for public safety and prevention of flooding.

GPR is a non-invasive, continuous, high speed and relatively high-resolution geophysical tool used to investigate subsurface features and near-surface soil conditions [Chlaib et al., 2014]. It works using electromagnetic waves which propagate and are reflected in the soil. The best results are obtained when the topographic cover is rather smooth and when the penetrated material is dry [Reynolds,

1997]. One of the major advantages of GPR is the capability to perform scans in a continuous way, over a wide area, in a relatively short time. In addition, GPR data can be viewed in real-time, enabling one to assess the quality of the acquired data directly in the field, and eventually adjust acquisition parameters and settings as needed [Di Prinzio et al. 2010].

The GPR used in the present investigation is an IDS GeoRadar, multi-frequency, multi-channel array systems. This innovation enables the construction of detailed 3D images of large underground areas, dramatically improving utilities detection.

The GPR system consists of the following parts:

- Two antennas: deep and shallow antennas in one compact box, 200 MHz & 600 MHz, which help the operator in locating pipes and cables by providing the proper frequency for a specific search parameter. It provides a real-time display of deep and shallow antennas on the same screen;
- An IDS multi-channel control unit: a console that allows for real-time target viewing, by means of an acquisition software for use in the field;
- A survey subsystem: four wheels.

For its operations, the GPR system relies on the transmission of electro-magnetic energy, usually in the form of a pulse, and on the detection of the small amount of energy that is reflected from the target. The round-trip transits time of the pulse and its reflection provides a range information on the target. Using an image analyses, a reconstruction of the soil vertical section is possible, and the discontinuity and inhomogeneity trends of the investigated site may be detected.

In this work, the depth of penetration was from the crest level (0 meters) to 4 meters using the 200 MHz antenna, and from the crest level to 2 meters, using the 600 MHz antenna. Generally, the penetration depth may vary depending on soil conditions.

The levee sections were chosen considering the presence of nearby holes. Thus, the sections analysed were in correspondence of holes 1 - 2 , located on left levee as

and shown in Figure 4-24, and holes 5 – 6, located on left levee as shown in Figure 4-25.

Before starting the survey, in order to define the instrumental configuration that guarantees the required depth survey and optimizes the signal quality, the GPR was calibrated and the electromagnetic characteristics of the soil were verified. As it is recommended to carry out the calibration phase on a planar surface to obtain a better response, it was performed on the SS115 road, as shown later.

A time window, which represents the penetration depth, was selected; the chosen value was a function of the antenna's central frequency and soil conditions. For example, the time window of the low-frequency antenna is long while the high-frequency time window is short. Keeping in mind that the purpose of the investigation is to identify burrows up to a depth of about 4,00 m (the height of the levee), a time windows of 150 ns was set, allowing for a 6,00 m deep survey.

The levee section was 3,50 m large. The survey area was 3,00 m long over the crest. In order to survey the site (3,50 m x 3,00 m), an imaginary 1,00 x 1,00 m grid was considered on the crest. The GPR surveys collected for this study consisted of 16 profiles in grid configurations: 8 for each analysed site.

Using an imaginary grid, the GPR survey was performed along longitudinal and transverse line over the entire crest surface. When a discontinuity was detected, its position was marked with red spray paint. Identifying a sufficient number of discontinuity points allowed for reconstructing the burrow path inside the levee. Figure 4-29 shows the main phases of the GPR survey and the final reconstruction of the animal's den path inside the levee.

From the calibration test, the values of wave propagation velocity and permittivity were obtained. The reflection time was converted into depth by knowing the propagation velocity. The time-slice distance was in meters.

Figure 4-29: GPR survey for holes 1-2 and 5-6:
A) GPR position on the levee crest;
B) GPR scans;
C) Record soil discontinuity;
D) Recontruction of burrow path inside the levee.

In order to evaluate the vertical position and dimensions of the burrow, the GPR data were analysed. Figure 4-30 shows an example of the surveyed soil as obtained by the GPR using different antennas. The analysed section was a longitudinal section of the crest levee where holes number 1 and 2 were identified. The two antennas provide two different resolution of the same vertical cross section. This example of a GPR scan presents clearly visible hyperboles, highlighted by the arrows.

Figure 4-30 shows that the burrows are not a single straight tunnel but are forked ("ψ" shaped). A few tens of cm beyond the main entrance, the main burrow splits into smaller branches, which is typical of porcupine burrows.

These burrows are located about 1 meter under the crest surface. The tunnel dimensions are variable but are almost never less than 0,35 m in diameter.

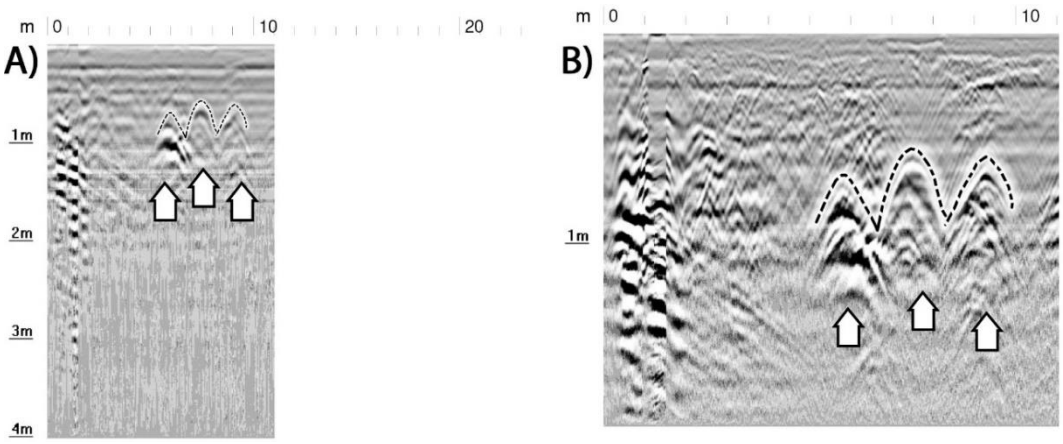

Figure 4-30: GPR Scan: graphic visualization of animal burrow with A) 200 MHz antenna analysis, and B) 600 MHz antenna analysis; the hyperboles indicated by the dashed line are the reflections from the den tunnels.

4.4.3. *Discussion and conclusions on field survey*

The Dirillo river levees were inspected and eight holes were identified. It seems that the burrowing animals creating these burrows are porcupines.

Crested porcupines are strictly nocturnal animals. Daylight hours are spent in a den dug out by themselves or made by other animals, while during the night they emerge from the dens to hunt for food on cultivated ground. Moreover, dens are usually burrowed in sloping ground, covered with thick vegetation. Thus, the cane located on the riverside slope of the Dirillo river levee, which is an area of very difficult access, and the presence of agricultural neighbouring land areas are suitable habitats for this animal species. This hypothesis was confirmed when porcupine quills and footprints were found.

Having identified the existence of porcupine dens by visual inspection, the position and paths of the burrow tunnels inside the levee were reconstructed by means of a GPR survey. All the burrow data measured are reported in Table 4-XI.

Table 4-XI: Measure of Holes.

BURROW	LOCATION	LEVEE HEIGHT [m]	VERTICAL POSITION [m]	ENTRANCE LENGTH [m]	ENTRANCE HEIGHT [m]	TUNNEL DIAMETER [m]	HYPOTHETICAL BURROWING ANIMAL	CONNECTED WITH ANOTHER HOLE
1	LANDSIDE	3,00	2,50	0,35	0,35	0,30	PORCUPINE OR RABBIT	YES, HOLE 2
2	RIVERSIDE	3,00	2,50	0,35	0,30	0,30	PORCUPINE OR RABBIT	YES, HOLE 1
3	LANDSIDE	4,00	3,50	0,35	0,30	0,27	PORCUPINE	PROBABLY NOT
4	LANDSIDE	4,00,	2,50	0,50	0,35	0,31	PORCUPINE OR RABBIT	PROBABLY NOT
5	LANDSIDE	4,00	3,50	0,60	0,55	0,33	PORCUPINE	YES, HOLE 6
6	LANDSIDE	4,00	3,00	0,50	0,45	0,32	PORCUPINE	YES, HOLE 5
7	LANDSIDE	4,00	3,50	0,35	0,35	0,32	PORCUPINE	YES, HOLE 8
8	LANDSIDE	4,00	3,80	0,60	0,35	0,30	PORCUPINE	YES, HOLE 7

The tunnel investigated by GPR survey corresponds to the holes number 1, 2, 5 and 6. The riverside entrance was not found during the visual inspection, because the cane field is inaccessible.

Through the survey, hole number 1 was found to be related to another hole located on the riverside (number 2). The tunnel that connects both holes is shaped like an “s” and is located 45 cm below the levee’s crest level. Moreover, its path inside the levee is aligned along the flow direction of the river.

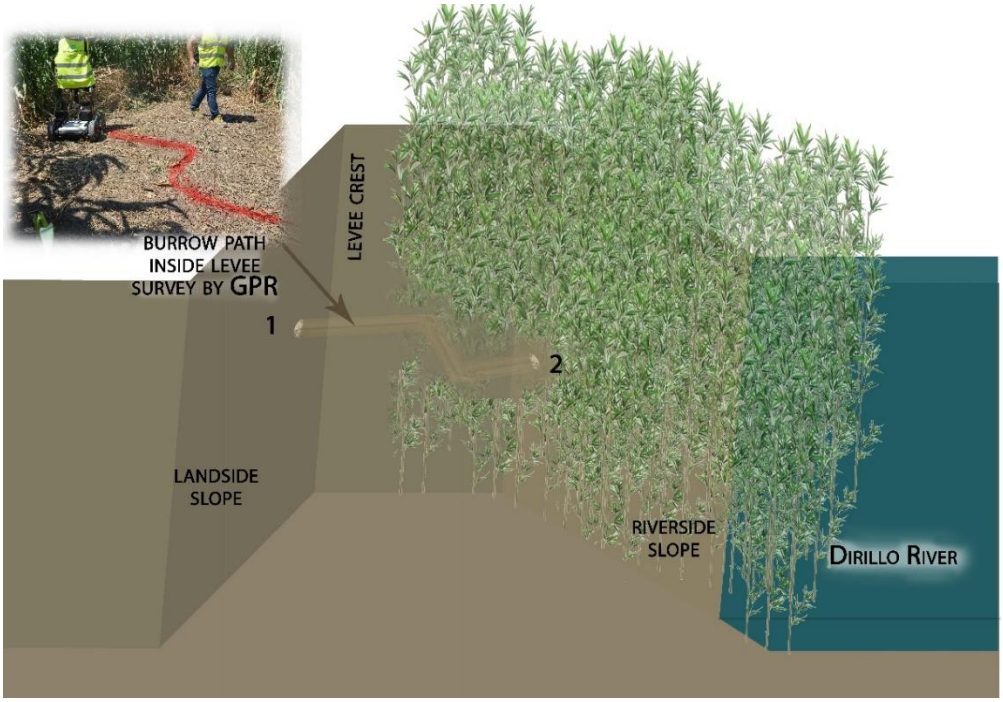

Figure 4-31: Reconstruction of burrow path inside the levee. Investigated holes 1 and 2.

Holes 5 and 6 are also connected together by a tunnel. Moreover, the tunnel connects these two burrows with a third entrance located on the riverside. This burrow is also located on the high part of the levee, approximately 50 cm from the crest level. In this case, it is not a single straight tunnel, but is rather shaped like a "y": two entrances on the landside slope and one on the riverside slope. Its development inside the levee is inclined in the opposite direction of the river flow. Figure 4-32 displays the reconstructed burrows inside the Dirillo river levee.

The GPR survey allowed evaluating the hole dimension: it is 30 cm wide. Moreover, the presence of tunnel forks inside the levee have been revealed.

Considering the burrow dimensions and their path shapes inside the levee, the survey also suggests that these dens are populated by porcupines.

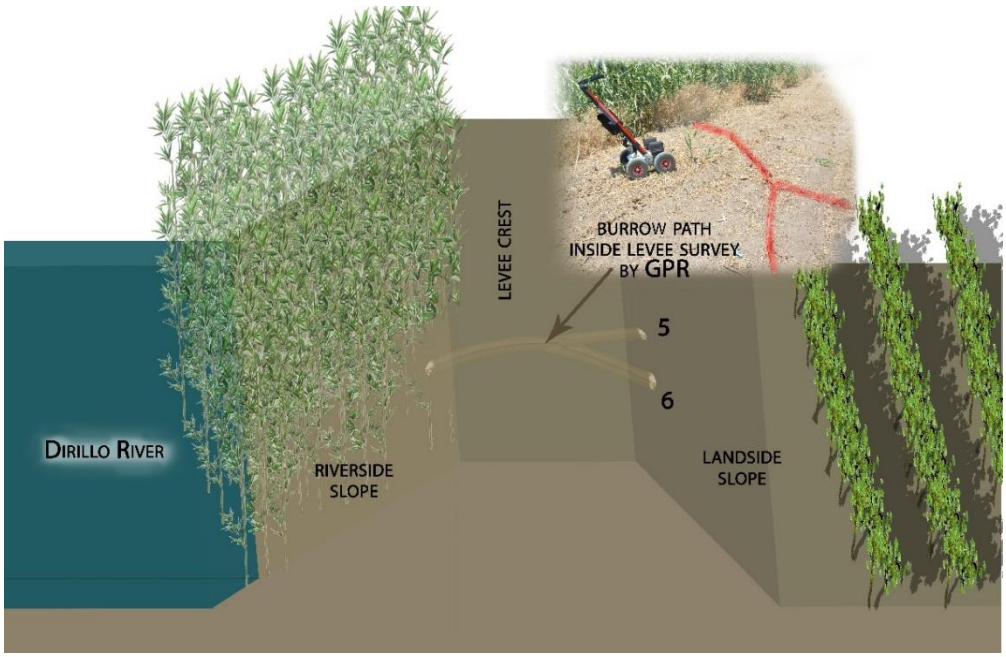

Figure 4-32: Reconstruction of burrow path inside the levee. Investigated holes 5 and 6.

4.5. Results and Discussion

In recent years, numerous levee failures have occurred that cannot be justified only on the ground of hydraulic and/or geotechnical failure mechanisms. A potential failure mechanism could be due to animals digging their burrows inside earth structures which can have a negative impact on levee stability.

Within this framework, the 2012 flood event in the Dirillo River, which caused huge damages consequent to levee failures, was investigated in order to identify failure mechanisms. A reconstruction of the event was carried out, the levee breach points were identified, and overtopping and seepage phenomena were hypothesized as main levee failure mechanisms.

Such analysis showed that the reconstructed 2012 flood profiles appear to be insufficient, in terms of peak river stage and duration of high river stages, to trigger the overflow phenomenon. Furthermore, the river stages were such that no seepage

phenomenon may have occurred and that the evaluated peak value of flow rate overcome levees only at a few river sections. Therefore, other causes of the levee failure should be considered by contemplating other factors that could induce a decrease in levee stability.

In order to assess factors that could have a negative impact on levee stability, field surveys were carried out. These clearly indicated that there are dense burrow systems inside the Dirillo levees and that crested porcupines dug these dens. Non-destructive investigations provided information on burrow structure inside the levees. With the aim of inspecting entire levees, a GPR survey was conducted. The analyses showed that tunnels connect the holes facing both slopes of the levee.

In order to support the evidence of overtopping, as reported by local landowners and by the reports from the Civil Protection Department, it is conceivable that river levee sections collapsed before the overtopping phenomenon occurred. In particular, it is reasonable to assume that levees were deteriorated severely by animal burrows, and that this, along with the surface erosion phenomenon, triggered the collapse of the levees.

In Chapter 5, experimental analyses are carried out with the aim of estimating the impact of biota on levee stability. Specifically, erosion times of undisturbed levees are compared to the case of levees deteriorated by the presence of burrow. The information collected about burrows during the field investigation is used to set up the experimental analysis parameters.

5. PHYSICALLY-BASED ANALOGUE MODEL OF BIOTA IMPACTS ON LEVEE EROSION

5.1. Overview

In general, the most erosive flow occurs at the toe of the slope, where the velocity is higher and where the break in slope makes it easier to dislodge particles and move them away. On levees that are overtopped by floods, severe erosion is often observed. The erosion proceeds to attack the soil directly until a “headcut” is initiated. Erosion generally continues in the form of "headcutting," where an upstream progression of deep eroded channel(s) eventually leads to levee failure.

The present experimental investigation aims at contributing to the flood risk mitigation in river with levees through the development of methodologies that confider the interactions between biological activities and levee stability. Understanding the failure mechanisms of damaged earth structures is pivotal for sound post-failure analysis, and for adequate design of earth structures.

The experimental activities described here were performed at the Laboratory of Geography, Geology and Environment, University of Hull (UK), where researchers specialize in the analysis of eco-hydraulic systems. The experimental set-up is designed in order to represent real burrow configurations.

Experimental modelling is conducted in a physically-based analogue model, to study the failure mechanisms of modified bio-levees. Taking into account the results of the field survey described in Section 4.4 and trying to expand from it, the experiments investigate the effects of burrow density, length, vertical position, and angle relative to the flow direction, by comparing the results with an undisturbed levee. In particular, the erosion times of modelled levees, weakened by different burrow configurations, are compared with the performance of an undisturbed levee.

A description of the physical model, summary of the methodology used to analyse images, and description of investigated experimental parameters are presented

in this chapter. Laboratory results for an intact levee model are compared with those measured for different cases of deteriorated levees.

5.2. The importance of setting an analogue model

As mentioned in Chapter 2, earth levee failures have not been explicitly connected with the presence of animal burrows and these mechanisms were not sufficiently investigated in the past. The present lack of data prevents to have a complete and comprehensive knowledge of the phenomenon and therefore there are no laws regulating it.

In order to discover the hydromorphodynamics parameters that regulate the complex functioning of the phenomenon, we must have a clear understanding of the phenomenon itself first. An experimental approach at the laboratory scale is an interesting method for obtaining physical information on eroded levees where burrows are present.

The use of analogy has long been recognized as a powerful tool both in the reasoning process and in throwing a new light on reality [Chorley, 1964]. Reasoning by analogy involve the assumption of a resemble relations or attributes between some phenomenon or aspect of the real world in which one is interested and an analogue model. In fact, “two analogues are more likely to have further properties in common than if no resemblance existed at all, and the additional knowledge concerning one consequently provides some basis for prediction of the existence of similar properties in the other” [Black, 1962].

Analogue models allow to integrate conceptual models of levee failure in concrete terms, but necessarily simplify some parameters, such as rheological and/or geometrical parameters, that exert a potential control on levee behavior.

The aim of the present experimental research is therefore to obtain physical data on the parameters controlling the instability of a levee deteriorated by biota, determining which burrow configurations speed up the erosion phenomenon. In order

to achieve this goal, a physically-based analogue model is utilized, and the results are analysed to highlight the main control parameters of increased erosional process in the presence of dens.

5.3. Experimental set up

The physical model is designed in order to highlight the interaction between the levee structure and the biological activities, and thus determine the influence of the latter on the levee failure mechanisms. In particular, the aim of the physical model is to investigate the impact that different burrow configurations have on an earth levee.

The experimental apparatus consists of a single channel delimited on the right side by an earth levee, as sketched in Figure 5-1:

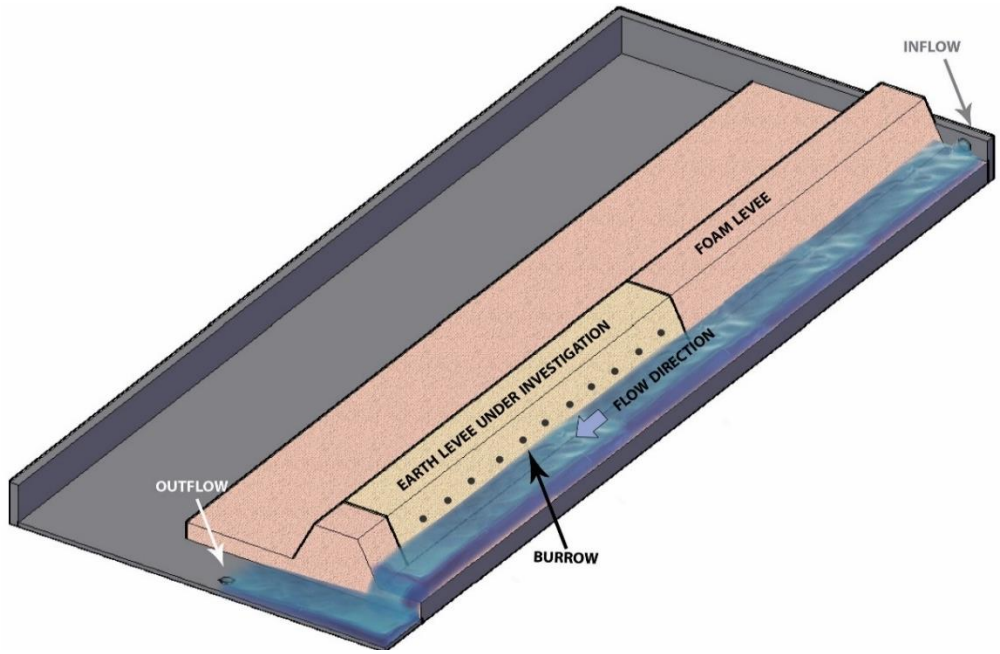

Figure 5-1: Three-dimensional sketch of the model system used in the experimental investigation.

The channel is 2,00 m long and its base is 0,10 m wide. The channel longitudinal slope is 1%. A recirculating system constantly pumps 8 l/min into the channel. The flow velocity and water depth are maintained almost unchanged. In order to control and regulate the inflow, a control area consisting of gravel placed under the inflow tube allows to reduce, flow turbulence. The water falling down from the output section is collected in a container and recirculated by the pump.

In order to define an optimized model, Rocscience (2003) conducted a series of simplified two-dimensional limit equilibrium analyses with SLIDE software. The study, described in section 3.4, considered different levee geometries, side slopes, and water levels. The stability for the intact levee was investigated using Spencer's method for different side slopes: 1H : 1V, 1.5H : 1V and 2.5H : 1V [Sagheea et al., 2016]. Based on numerical simulations, an optimized levee section with equal side slope is proposed for the purposes of this investigation. The 1H:1V side slope is found to provide an acceptable balance between stability of the intact levee and a reasonable vulnerability to failure of the deteriorated levee [Sagheea et al., 2016].

Although the chosen geometric configuration may not replicate an existing earth levee, it allows for the occurrence of accelerated failure under a short-term rise in upstream water level. Other researchers have used a similar approach [Bayoumi et al., 2011; Hori et al., 2011] to investigate the failure of embankment dams subject to seepage conditions [Sagheea et al., 2016].

Foam was used to create the levee shape, as only part of the levee is built with soil: levee sections upstream and downstream of the test section levee are built using foam. The test levee was realized compacting and pressing layer by layer the soil and then the extra soil was removed. With the aim of reducing the difference of the levee roughness and foam roughness, all foam surfaces were coated with sand.

The scaled-down earth levee is 5 cm high with a 10 cm wide crest and the selected 1H:1V side slope. Figure 5-2 and Figure 5-3 show the cross section and the top view of the experimental apparatus along with all the dimensions, respectively.

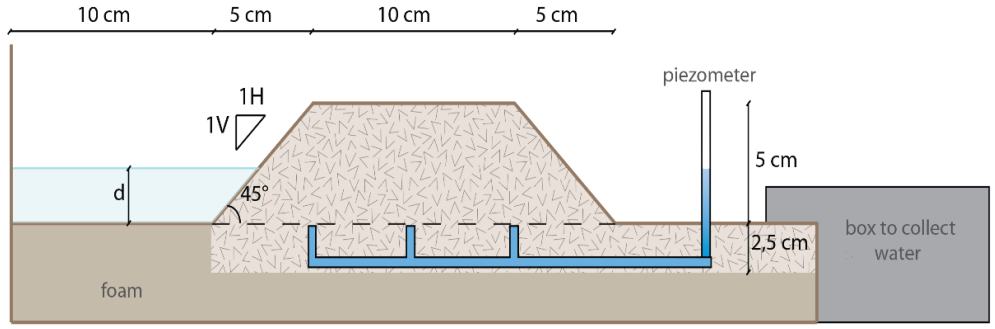

Figure 5-2: Levee modelling set up --- Cross-section view.

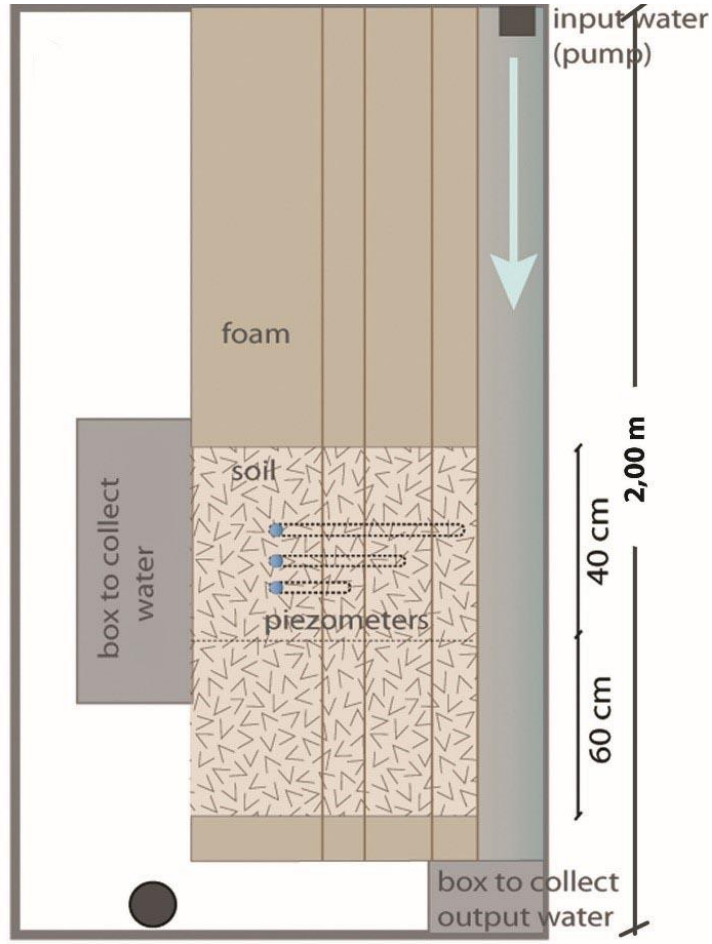

Figure 5-3: Levee set up modelling --- Top view.

Two different levee lengths were tested: 40 cm and 100 cm.

Hydraulic and geometric parameters for each experiment run, are reported in Table 5-I

Table 5-I: Hydraulic and geometrical characteristics adopted for experiments.

Hydraulic parameters				Levee geometry		
d *Water Depth*	v *Flow velocity*	Fr *Froude number*	Re *Reynolds number*	H_L *Levee Height*	L_C *Crest Length*	α *Slope inclination*
[cm]	[m/s]	[-]	[-]	[cm]	[cm]	[°]
2,30	0,48 ±0,03	1,07 ±0,065	$1{,}10 \times 10^4$	5,00	10,00	45°

As demonstrated by Saghaee et al. 2017 experiments (Section 3.4), the levee deterioration for the waterside burrow model result in higher settlements than the landside burrow model. For this reason, only waterside burrows were considered in the following experiments.

In order to simulate animal burrows on the waterside, horizontal cylindrical burrows were introduced within the levee section using a glass rod 6 mm in diameter. This geometrical configuration was selected by considering an analogue with those reported in the literature and with the measures gathered during the non-destructive investigation described in Section 4.4.

5.4. Measuring equipment

With the purpose of analysing the development of levee surface erosion, the progression of geometrical changes on the levee crest was measured as a proxy of the overall surface erosion process (see Section 5.7). Specifically, the images of crest erosion were captured using a GoPro Camera (digital photography) fixed on the ceiling and taking snapshot of the levee crest every 5 seconds.

A miniature current meter, and several rules located along the channel were used to monitor flow velocity and water level, respectively.

In order to measure the behaviour of the piezometric line inside the levee, three piezometers were used, measuring water level in the core of the levee, and at the two slope breaks between the crest and both the landside and waterside slope.

Figure 5-4 shows the miniature propeller and the piezometers that were used.

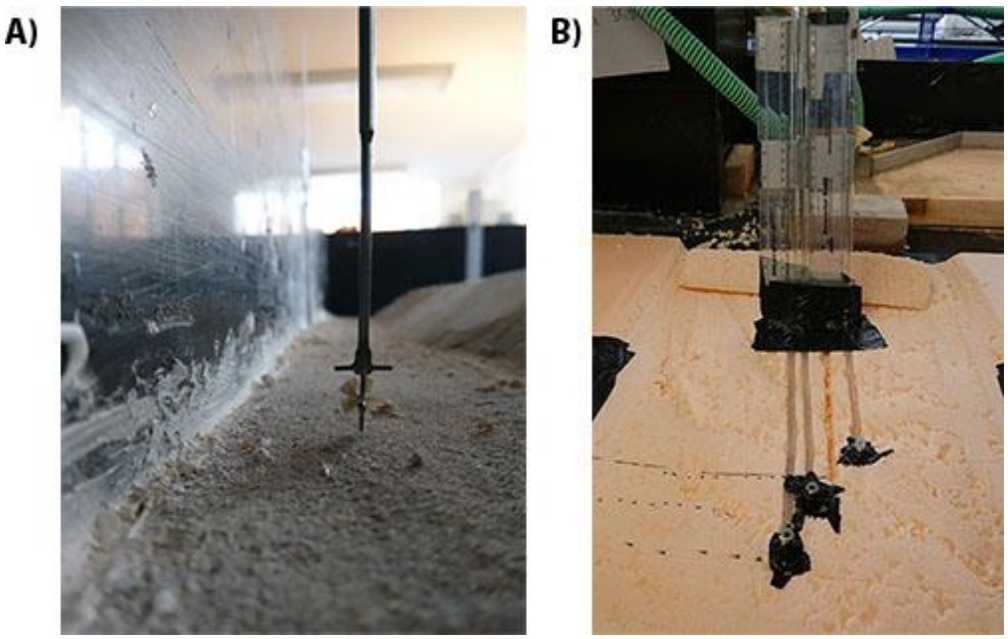

Figure 5-4: A) Miniature current meter; B) Piezometers.

5.5. Test procedure

The experimental procedure for the laboratory tests included the different steps described on the flow chart in Figure 5-5. For every experiment, the first step is to build the earth levee. The soil is positioned between the two foam levees, and is compacted always in the same way, layer by layer, using a trowel. Then the extra soil is removed, and edge are perfected. At this step, the levee geometry is defined.

The second step is to build the burrows on the levee. By simple using some rules, it establishes the exact point where the burrows are scheduled to be make. Then a clinometer is used to define the burrows inclination and, using a glass rod, the tunnels are drilled.

The most important step, which should not be taken lightly, is the control of the camera, as its position on the ceiling should not be modified. Thanks to a mobile app it is possible to verify the position of the camera without moving it. After turning on the camera, the experiment can start. The chronometer and the pump are switched on simultaneously. In order to evaluate the flow velocity, the miniature current meter is switched on.

Each experiment lasted for 60 minutes.

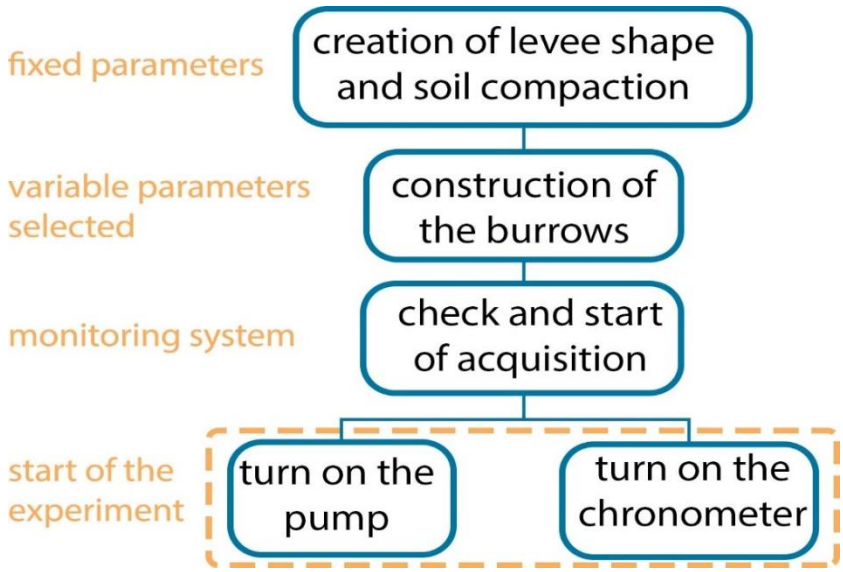

Figure 5-5: Flow chart of experimental procedure.

5.6. Preliminary test: Testing material

The experimental design involves building a scaled-down levee model, and introducing idealized animals burrows into it. Previous studies suggest that burrowing animals, such as porcupine or nutrias, tend to dig into soft substrata, displacing grains, and altering material structure around the burrow, e.g. through compaction. To define an optimal soil composition, which allows a proper trade-off between the mean time of erosion and burrow stability, preliminary tests were performed on the levee material. Five mixed soil compositions are analyzed:

a) Medium sand (D_{50} = 0,40 mm);
b) 95% medium sand (D_{50} = 0,40 mm) + 5% clay (D_{50} = 0,0035 mm);
c) 50% medium sand (D_{50} = 0,40 mm) + 48,75% fine sand (D_{50} = 0,12 mm) + 1,25% clay (D_{50} = 0,0035 mm);
d) 50% medium sand (D_{50} = 0,40 mm) + 50% fine sand (D_{50} = 0,12 mm);
e) Fine sand (D_{50} = 0,12 mm).

The time duration of these preliminary experiments was 1h.

The first experiments using medium sand showed the effects of a lack of cohesion between material granules. Indeed, after 1 hour the slope erosion and the complete soil saturation trigger the liquefaction phenomenon resulting in the slow collapse of the whole levee.

In order to increase the material cohesion, a mixed soil with 95% medium sand (D_{50} = 0,40 mm) and 5% clay (D_{50} = 0,0035 mm) was created. The excessive difference in particle sizes did not permit an optimized mixture; thus, during the experiment the sand and clay start to divide themselves: the former slides off with the flow, while the latter creates compacted and increasingly cohesive agglomerates.

With the aim of optimizing the material mix, fine sand (D_{50} = 0,12 mm) was added. The material mix for this new experiment was composed of the following proportions: 50% of medium sand, 48,75% of fine sand and 1,25% of clay, resulting a cohesive soil mix. A third experiment with four burrows was conducted with the same mix soil, where the burrows did not collapse too quickly. Unfortunately, after 5 hours of experiment, no relevant surface erosion or levee failure had been triggered. Thus, we decided to perform further experiments with a combination fine and medium sand, and with only fine sand.

Using fine sand only allowed for an optimized balance between time experiment and the effects of the flow on the levee, due to some soil cohesion. For this reason, it was decided to continue the analyses using only fine sand (D_{50}=0,125 mm). The particle size analysis is shown in Figure 5-6. The porosity of this fine sand is estimated to be 0,43, and its hydraulic conductivity is assessed to be about 10^{-3} m/s.

Production site : Chelford **Grade :** CH30 DRY

Size (microns)	Limits	% Retained Cumulative
1180	-	0.2
1000	<1.0	0.5
710	<5.0	2.8
600	-	5.8
500	-	19.5
425	-	44.1
355	-	73.5
300	-	89.4
250	>96.0	97.3
180	>98.5	99.9
125	-	100.0
-125	-	100.0

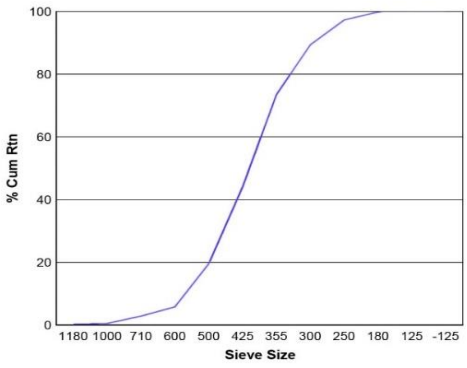

Figure 5-6: Particle size analysis of fine sand used in experiments.

To gain a more exhaustive view of the problem, some experiments were performed with fine sand and clay. The particle size analysis of this clay is shown in Figure 5-7. Nevertheless, no interesting results in term of surface erosion were obtained considering this last soil mixture.

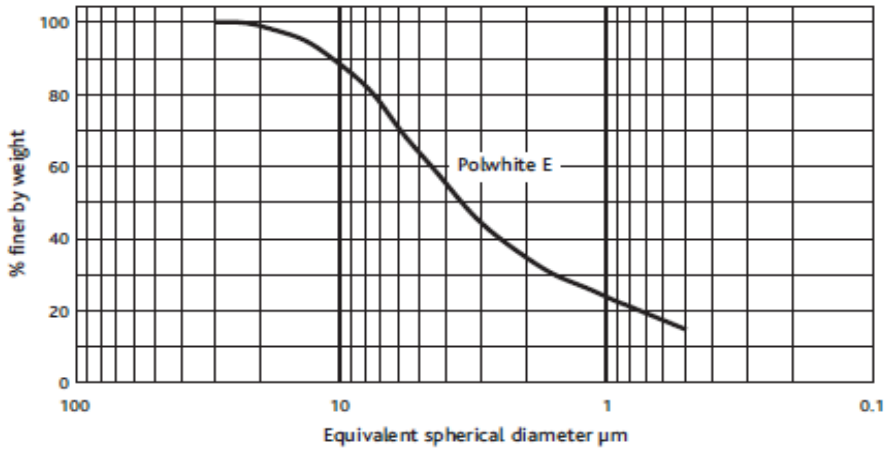

Figure 5-7: Particle size analysis of clay.

5.7. Development of procedure for the image analysis

The analyses carried out in the lab start from the images taken with the GoPro camera positioned on top of the channel. With image analysis, we were able to investigate the progression of geometrical changes on the levee crest as a proxy of the overall surface erosion process. Figure 5-8 shows an example of how the eroded area is measured in a 3D sketch of the experimental model.

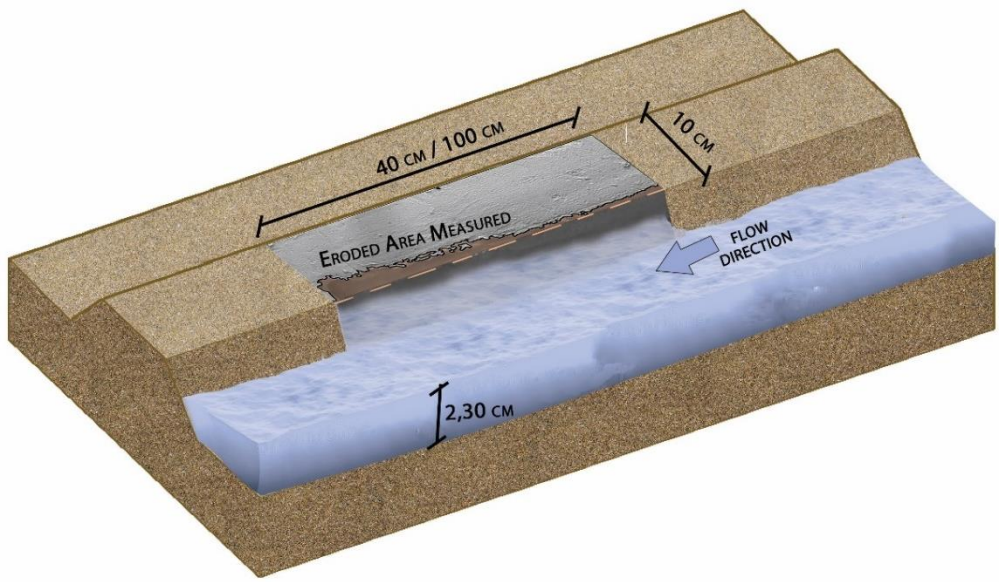

Figure 5-8: Eroded area measured on a 3D sketch.

Unfortunately, GoPro images have a distinctive fisheye look due to a very strong distortion. Straight lines become bent and the centre of the frame becomes oversized in relation to its margins, giving it a bulging look. Thus, the images needed to be rectified. For this reason, a checkerboard of known dimensions was used to calibrate the photographs. Different photos were taken changing the inclination of checkerboard, as shown in Figure 5-9. The dimensions of each square of the checkerboard are 1x1 cm.

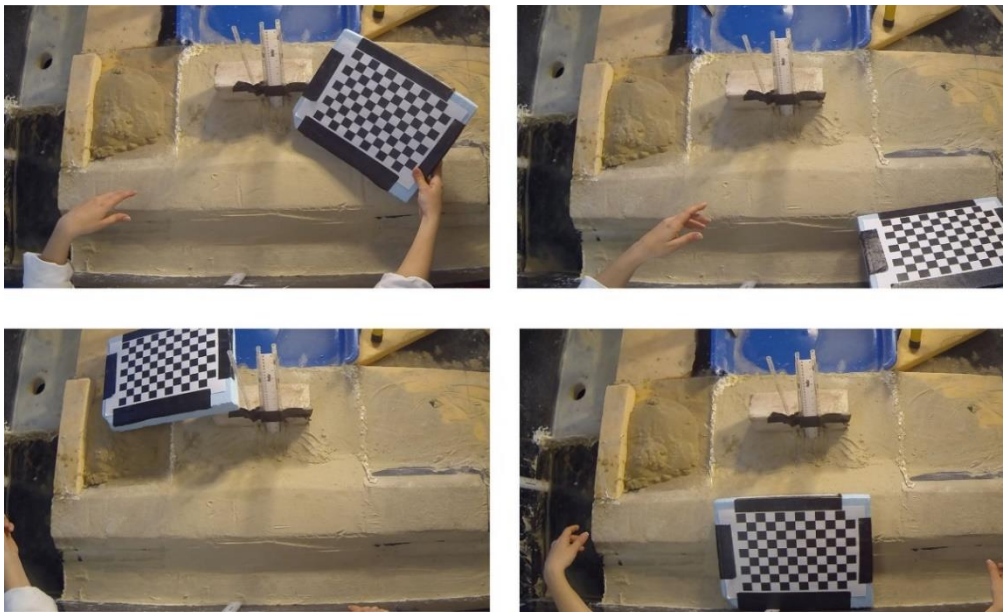

Figure 5-9: Images of the checkerboard used for the calibration of Gopro camera in the Lab.

Thanks to a MATLAB script, just knowing the actual dimensions of the checkerboard, it was possible to obtain a rectified picture in which every pixel corresponded to a fixed measure, following the conceptual strategy described in Figure 5-10.

With these operations, we were able to obtain the conversion parameters, and applying these to all frames of each experiment, we rectified all of our images.

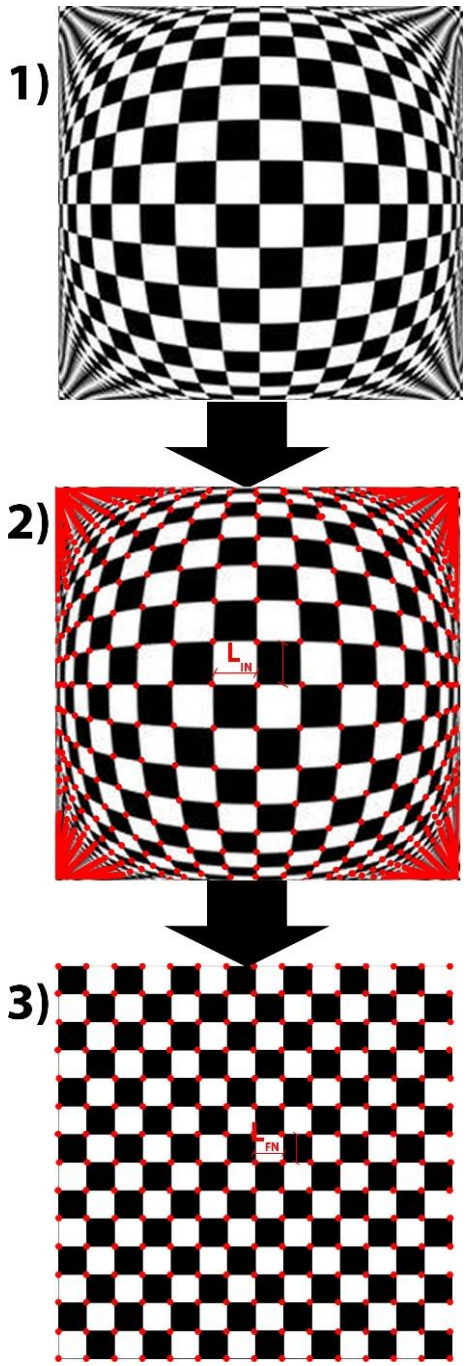

Figure 5-10: 1) Photograph of the checkerboard;
2) Determination of square limits;
3) Changing and homologation of square dimensions, after rectifying the photos.

First, all the experiment frames were trimmed and rotated (Figure 5-11-B) in order to focus attention only on the crest of the earth levee. Then, the images were modified into grayscale and were converted to binary images by applying a threshold (Figure 5-11-C). Thresholding is a methodology that separates a region of an image corresponding to objects in which we are interested, from the background of the figure. Thresholding often provides an easy and convenient way to perform a segmentation on the basis of the different intensities in the foreground and background regions of an image. The black pixels correspond to the background and the white pixels correspond to the foreground (or vice versa). Image thresholding is most effective for images with high levels of contrast.

The eroded area was determined using a single parameter known as the intensity threshold. When the intensity threshold is applied, each pixel in the image is compared with this value. If the pixel's intensity is higher than the threshold, the pixel is set to, say, white in the output. If it is less than the threshold, it is set to black.

After applying the threshold value and obtaining a black and white image (Figure 5-11-D), a post-processing was performed to remove small imperfections. The resolution was improved through a series of operations that allow eliminating disturbances in the image (Figure 5-11-E): removing small-unconnected white pixels; dilating picture by adding a rank of 1's to all sides of each white pixel; filling every hole (black pixel) if it cannot be reached by white pixels from the edge (consider connectivity). Then the black and white were switched (Figure 5-11-F) and the contour of eroded area (white pixel) was determined (Figure 5-11-G).

In order to quantify the eroded area, the number of pixels under the contour was multiplied by the dimension of a single pixel as defined during the rectification procedure.

After all these operations, the boundary of the earth levee crest is determined and so that it is possible to identify the eroded area. All these phases of image analysis are graphically described in Figure 5-11.

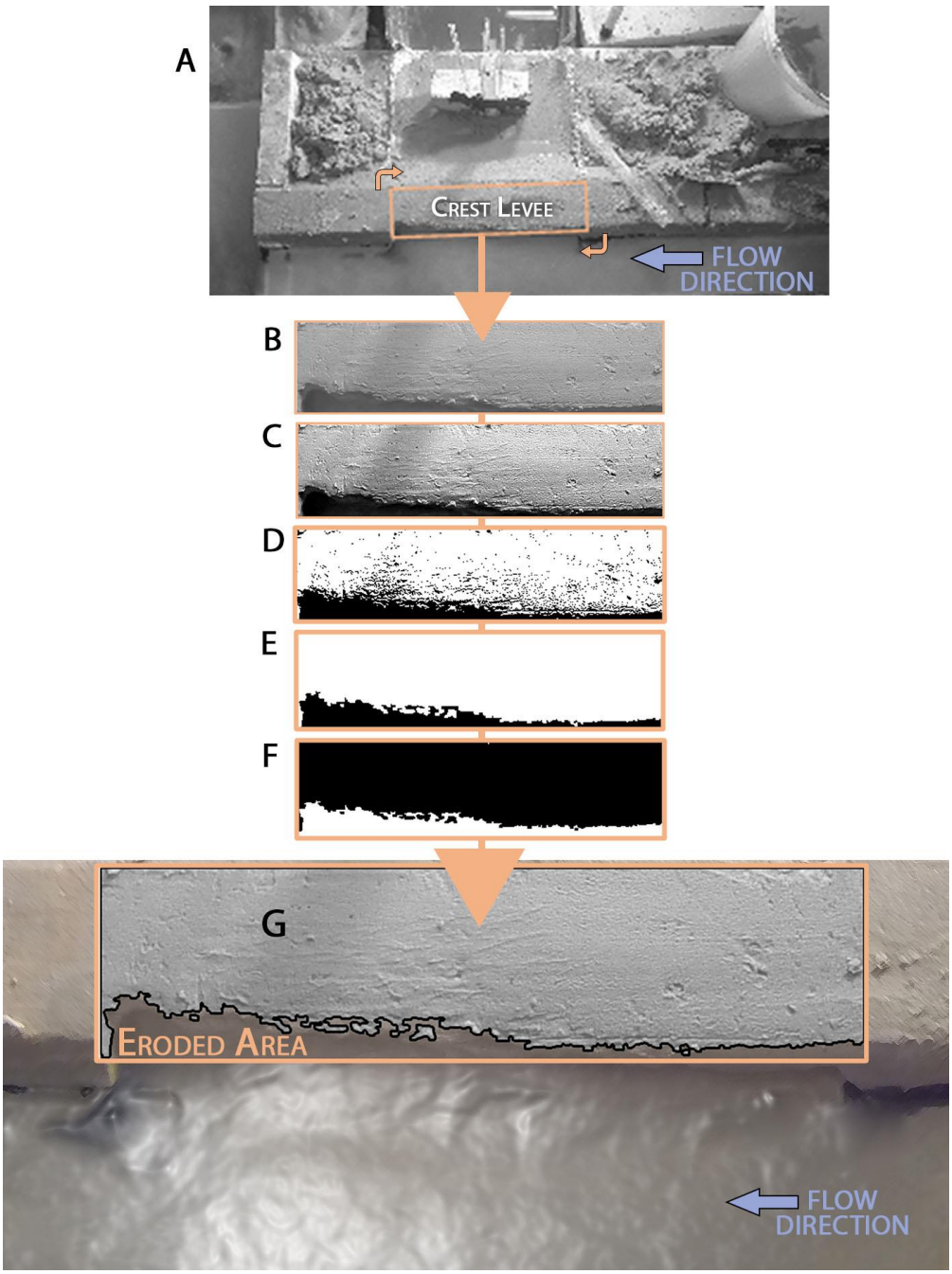

Figure 5-11: Intermediate products of image processing from greyscale image to boundary line of the eroded area.
A) Rectified image; B) Rotation, definition of analysed area and converting to a greyscale images; C) Image definition and sharpen edges; D) applying threshold; E) noise reduction; F) reverse black and white; G) define the contouring of eroded area.

5.8. Preliminary image test: Threshold investigation

In order to define the correct boundary of the eroded area measured, the choice of the threshold is very important. In fact, a small change of the threshold value can substantially affect the binary images, as shown in the threshold analyses for the same experiment frame reported on Figure 5-12.

For each experiment, 720 frames were collected, and for each frame of the experiment the eroded area was evaluated changing the threshold value between 0,1 and 0,5, with a pic of 0,01.

Analyses demonstrated that the optimal value was between 0,2 and 0,35: indeed, those are the best threshold values that allow to define the contour of the eroded ground in an appropriate way.

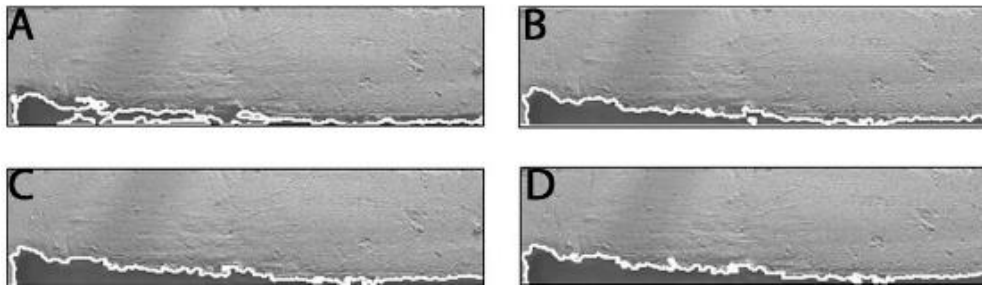

Figure 5-12: The eroded area conturing of the same frame evaluated appliying different threshold values: A=0,10; B=0,20; C=0,30; D=0,40.

Figure 5-13 shows the analyses made for first, intermediate and last frame of the same experiment. On the left, a graph shows all the measures of the eroded area by varying the threshold values. On the right, the contouring of the measured eroded area is graphically shown.

For the first frame, the threshold value that describe better the eroded area is very low, as 0,2 (Figure 5-13-1). For the middle, it is better to use a threshold value like 0,25 or 0,30 (Figure 5-13-2). Indeed, for the last frame a threshold value equal to 0,35 is the better choice (Figure 5-13-3). Therefore, for the same experiments a fixed

threshold value is not suitable to describe the evolution of eroded area. This is because between the first and the last frame the light intensity can change. Indeed, when the levee crest is intact (beginning of the experiment), a very low threshold should be used to describe the situation in order to perceive very small light variation. As the experiment goes on, the eroded area increases. The eroded area becomes more evident and it is necessary that the small light variation is no longer identified. Thus, the threshold should change between the first to the last frame.

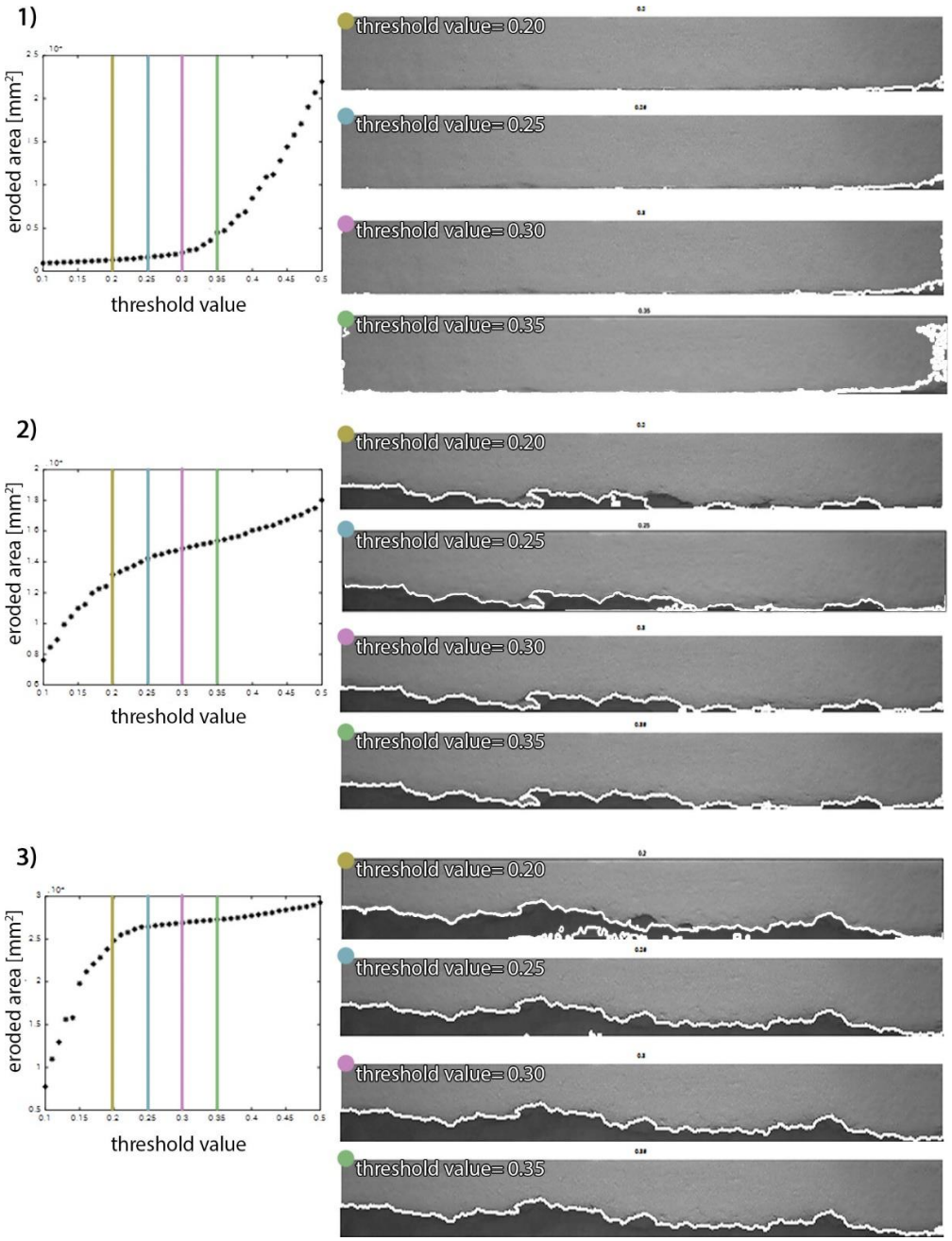

Figure 5-13: Threshold analyses for different frames of the same experiment to define the optimal threshold value: 1) first experimental frame; 2) intermidiate experimental frame; 3) last experimental frame.
On the left the measures of the eroded area by varying the threshold values; on the right, the graphical display of eroded area contour evaluated with four different thresold values.

In order to find a correct threshold, several analyses with all frames of all experiments were carried out. The best solution was to relate the threshold variation with the increase in eroded area. On the first frame a threshold equal to 0,1 is applied. Then, for each increase of 1000 mm^2 of the measured eroded area, the threshold value changes step by 0,01, until the maximum value 0,45, which is applied on the last frame.

Figure 5-14 shows an example of measurement of eroded area gauged by increasing the threshold value as a function of the increasing of eroded area.

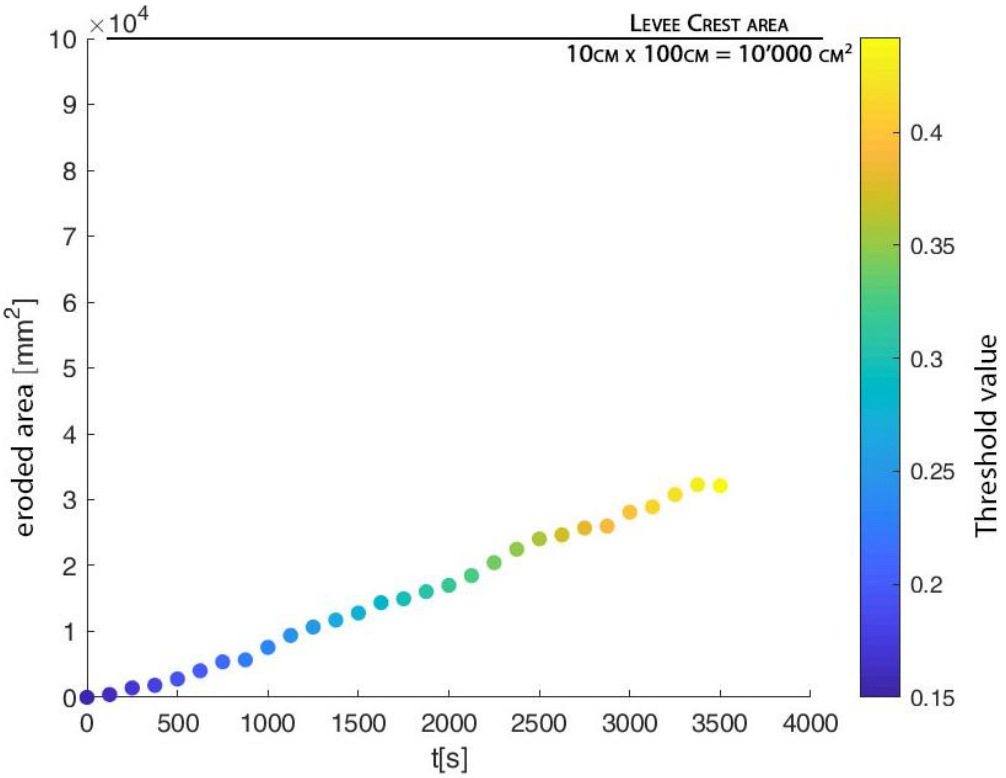

Figure 5-14: Measurement of eroded area for all the frames of a single experiment gauged by increasing the threshold value with the increase of eroded area.
The threshold value applied on a frame is indicated by the colorbar on the right. The threshold value range is from 0.15 to 0.45.

5.9. Experimental programme

The experimental programme was carried out at the Laboratory of Physical Geography of the University of Hull (UK), using the experimental apparatus described in Section 5.3. First, analyses were made on a 40 cm long earth levee. Then a 100 cm long earth levee was used. The experimental campaign is composed of 110 experiments.

The first tests were conducted on an undisturbed levee, for both the 40 cm long and 100 cm long cases. The results for the undisturbed levee were used as a reference for an objective comparison with the cases of levees deteriorated by biota, where different burrow configurations were tested.

The parameters analysed are four: vertical position of the burrows along the levee slope, length of the burrows inside the levee, burrow density, and angle inclination with respect to the flow direction. The geometrical parameters of the burrow experimental model are shown in Figure 5-15.

Two vertical positions of the burrows were tested: above and under the water depth, which is 2,30 cm. Considering the 0,6 cm diameter of the holes, the two vertical positions evaluated were: H_{H1} = 1,80 cm and H_{H2} = 2,80 cm.

The length of the burrows studied in these experiments depended on their vertical positions; for each vertical position, two different burrow lengths were analyzed: 50% and 75% of the levee width. The width of the levee at 1,80 cm height was 16,40 cm. It means that burrows at this height had L_{H1a}= 8,20 cm and L_{H1b}= 12,30 cm. Instead, the length of the levee at 2,80 cm was 14,40 cm, thus the burrows lengths in this case were L_{H2a}= 7,20 cm and L_{H2a}= 10,80 cm.

The other controlled parameters were the density of holes, which is related to the distance of the burrow δ. For the 40 cm long levee, two configurations were analyzed: holes 8 cm and 4 cm apart, meaning that configurations had 5 and 10 burrows, respectively. For the 100 cm long levee, 10 cm, 5 cm and 2,5 cm distance are studied: it means that 10, 20 and 40 burrows are built in this case, respectively.

The last, parameter considered is β, the angle between flow direction and burrow. Three possible angles were studied: 45°, 90° and 135°.

In order to evaluate the replicability of the experiments, tests were repeated two times.

Table 5-II shows the experimental design.

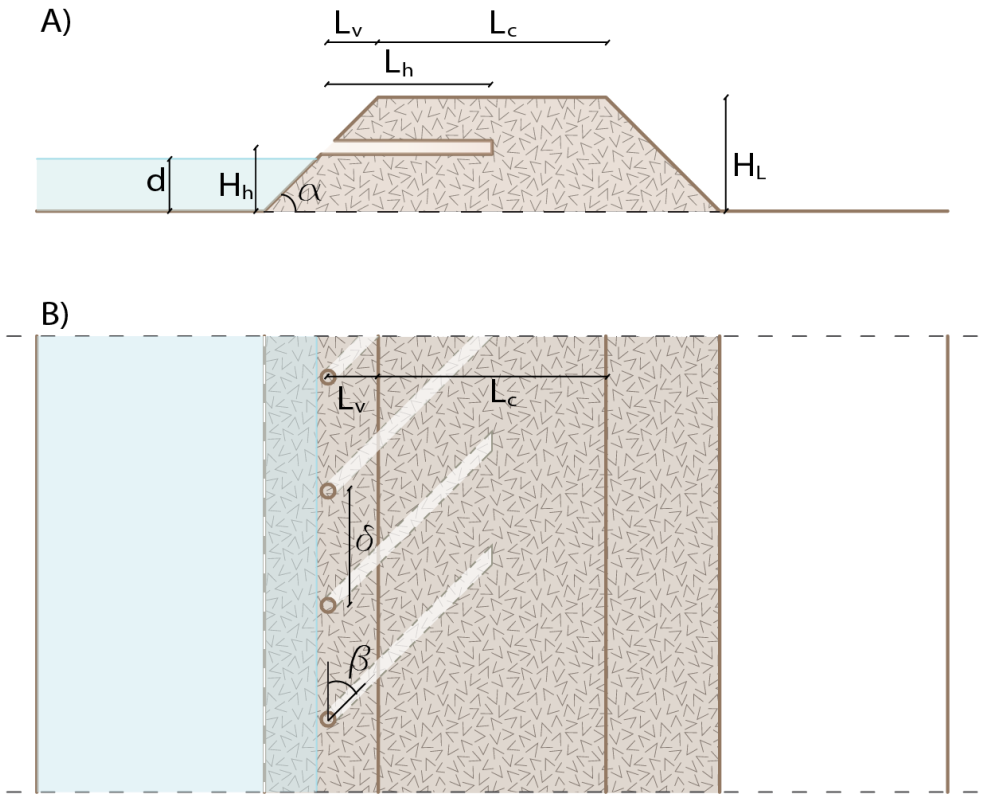

Figure 5-15: A) Sketch of the cross section of the levee with the experimental parameters; B) Sketch of top view of the levee with the experimental parameters.

Table 5-II: Experimental programs.

Levee material	Levee length	Experiment number		Hole vertical positions H_H	Hole depth L_H	Angle between flow and hole direction β	Horizontal distance between holes δ
Fine sand	40 cm	from 1 to 50	1 (x 2)	UNDISTURBED LEVEE			
			2, 3 (x 2)	1,80 cm	8,20 cm	90 °	8 cm ÷ 4 cm
			4, 5 (x 2)			45°	8 cm ÷ 4 cm
			6, 7 (x 2)			135°	8 cm ÷ 4 cm
			8, 9 (x 2)		12,30 cm	90 °	8 cm ÷ 4 cm
			10, 11 (x 2)			45°	8 cm ÷ 4 cm
			12, 13 (x 2)			135°	8 cm ÷ 4 cm
			14, 15 (x 2)	2,80 cm	7,20 cm	90 °	8 cm ÷ 4 cm
			16, 17 (x 2)			45°	8 cm ÷ 4 cm
			18, 19 (x 2)			135°	8 cm ÷ 4 cm
			20, 21 (x 2)		10,80 cm	90 °	8 cm ÷ 4 cm
			22, 23 (x 2)			45°	8 cm ÷ 4 cm
			24, 25 (x 2)			135°	8 cm ÷ 4 cm
	100 cm	from 51 to 89	51	UNDISTURBED LEVEE, ROUNDED EDGE			
			52 (x 2)	UNDISTURBED LEVEE, SHARPED EDGE			
			53, 54, 55, (x 2)	1,80	8,20 cm	90°	10 cm ÷ 5 cm ÷ 2,5 cm
			56, 57, 58 (x2)			45°	10 cm ÷ 5 cm ÷ 2,5 cm
			59, 60, 61 (x2)			135°	10 cm ÷ 5 cm ÷ 2,5 cm
			62, 63, 64 (x 2)	2,80 cm	7,20 cm	90°	10 cm ÷ 5 cm ÷ 2,5 cm
			65, 66, 67 (x 2)			45°	10 cm ÷ 5 cm ÷ 2,5 cm
			68, 69, 70 (x2)			135°	10 cm ÷ 5 cm ÷ 2,5 cm
Sand and clay	100 cm	from 90 to 110	90 (x3)	UNDISTURBED LEVEE, SATURATED SOIL			
			93, 94, 95	1,80	8,20 cm	90°	10 cm ÷ 5 cm ÷ 2,5 cm
			96, 97, 98			45°	10 cm ÷ 5 cm ÷ 2,5 cm
			99, 100, 101			135°	10 cm ÷ 5 cm ÷ 2,5 cm
			102, 103, 104	2,80 cm	7,20 cm	90°	10 cm ÷ 5 cm ÷ 2,5 cm
			105, 106, 107			45°	10 cm ÷ 5 cm ÷ 2,5 cm
			108, 109, 110			135°	10 cm ÷ 5 cm ÷ 2,5 cm

6. ANALYSES OF EXPERIMENTAL DATA

6.1. Overview

The experimental data are presented and elaborated below in order to evaluate the impact of the following burrow parameters on erosion surface: vertical position related to water depth, hole depth related to vertical position, burrow inclination angle related to water flow, and horizontal distance between the holes. In particular, the study investigates the impact of the burrow configurations on the performance of the modeled levee, comparing it with the case of erosion of undisturbed levee.

The analyses of the experimental evidence are carried out considering the image analysis procedure described in section 5.7. First of all, the problems of the assessing surface erosion on a 40 cm long levee are enlightened. Then, in order to have a benchmark, the analyses of the undisturbed levee are presented. The next assessments gather experiments into two main groups: tests on 40 cm long levees and tests on 100 cm long levees. Initially, the 40 cm long levee experimental analysis are briefly described. Then, the subsequent observations allow to explain the failure mechanism and to diversify two main types of burrow configurations: burrows above water level and burrows under water level. The other burrow parameters are separately discussed.

As regards to the experiments with levees made of sand and clay, the erosion mechanism is too slow so that after one hour the levee crest has not eroded enough. Thus, considering the used image analysis procedure, the impact of burrow presence on this type of levee material was not taken into account in the present study.

6.2. The challenges of studying the superficial erosion process on a 40 cm long levee

The actual experimental activities started with an earth levee that was long 40 cm. This part of the experimental campaign includes 50 tests. The tested levee material was composed by fine sand.

The experiments made with a 40 cm long levee present critical issues due to a problem with material discontinuity downstream at the point of contact between the earth levee and the foam levee. After eroding the first layer of soil, the water flow impacted the foam edge triggering recirculation. Levee erosion occurred due to the formations of this cove. Figure 6-1 is a simplified sketch of this material discontinuity during the levee erosion development.

The experiments lasted 60 minutes, but the analyses were only done for the first 20 minutes, after which the discontinuity effect seemed to become too pronounced, altering the results.

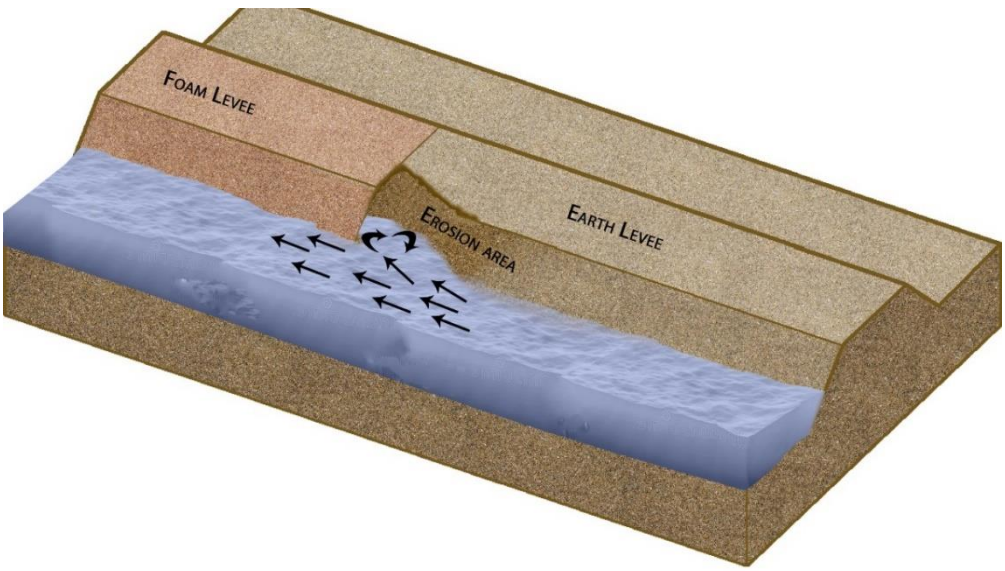

Figure 6-1: three-dimensional sketch of erosion mechanisms that is triggered by the material discontinuity on a 40 cm long levee.

6.3. The process of surficial erosion on undisturbed levee: 100 cm long

The experimental programme aims at evaluating the impact of biota on earth levee stability. With this purpose, the first step is to evaluate the erosion surface phenomenon on an undisturbed earth levee. The levee is 100 cm long and made with fine sand. In order to validate the repeatability, different intact levee experiments were done.

The surface erosion of an intact levee after one hour involves the loss of $1{,}7 \times 10^4$ mm^2 of levee crest surface, 17% of the levee crest area. This value will be used as comparison parameter to evaluate the evolution of erosion in all other experiments.

Moreover, the experiments on an intact levee highlight the correlation between the surface erosion and the levee edge definition. In fact, repeating the test on 100 cm long undisturbed levee made with fine sand, it was demonstrated that a rounded edge between the crest and the slope reduces the total erosion, as shown Figure 6-2. Thus, the way the earth levee is built has fundamental effects on the total erosion.

However, the repetitions of the same undisturbed levee show the same evolution of the eroded area measured.

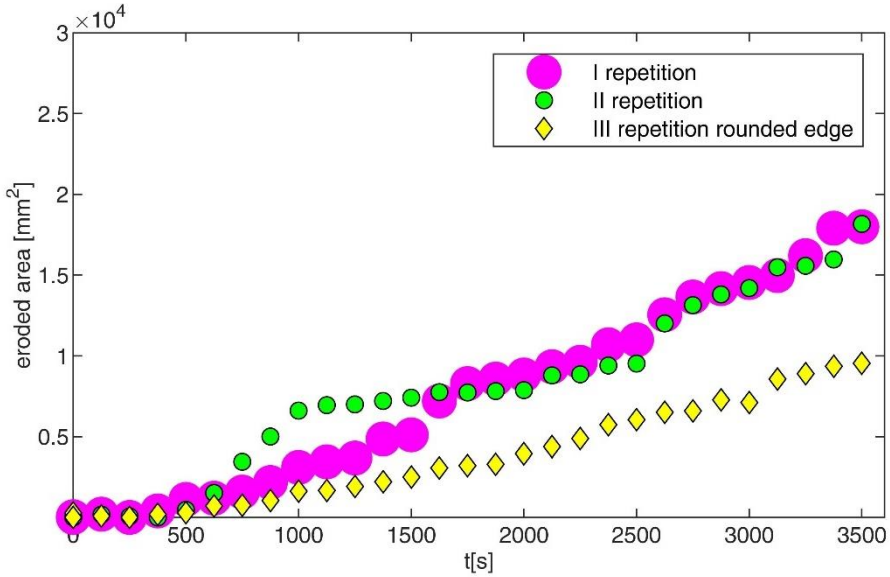

Figure 6-2: Repetition of experiments considering an intact levee long 100cm.

6.4. The process of surficial erosion on undisturbed levee: 40 cm long

The average eroded area of the 40 cm long undisturbed levee after 20 minutes (1200 sec) is approximatively 1200 mm^2, as shown in Figure 6-3. The total crest area is 40000 mm^2.

Considering the experiments made for the 100 cm long levee, the eroded area after 20 minutes is approximatively 4'100 mm^2, as show in Figure 6-2. But the total crest area is 100'000 mm^2. It means that the erosion percentages for 100 cm long levee and 40 cm long levee are 4% and 3%, respectively. Thus, the erosion surface experiment develops almost in the same way for the first 20 minutes.

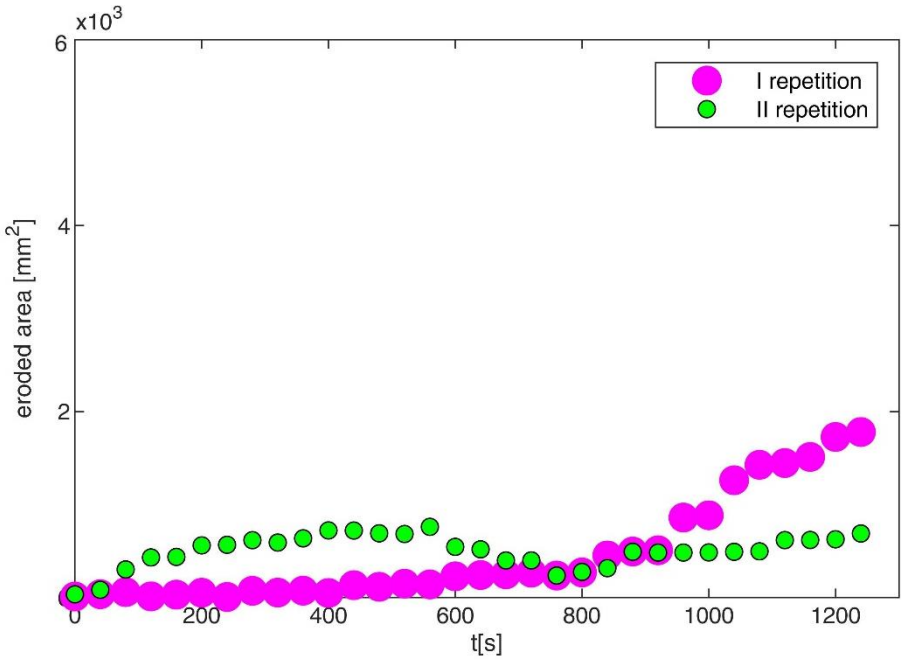

Figure 6-3: Repetition of experiments considering an intact levee long 40cm.

Consequently, it is possible to come up with some conclusion about parameters investigated considering only the first 20 minutes of experiments. The results are presented in the next section (Section 6.5).

6.5. Impact of burrows on surface erosion for the 40 cm long levee

As a result of the problem of material discontinuity, only the analysis of the first 20 minutes of each experiment was carried out (see Section 6.4). These analyses are not exhaustive, but they provide a first overview of a complex phenomenon.

Considering the inclination of the holes, it is possible to determine different behaviors. Specifically, burrows orthogonal to the water flow (90° inclination) seem not to cause a significant additional erosion phenomenon as shown in Figure 6-4. Otherwise, the holes angled at 45° and 135° to the flow direction trigger a greater impact on the surface erosion compared to the intact levee.

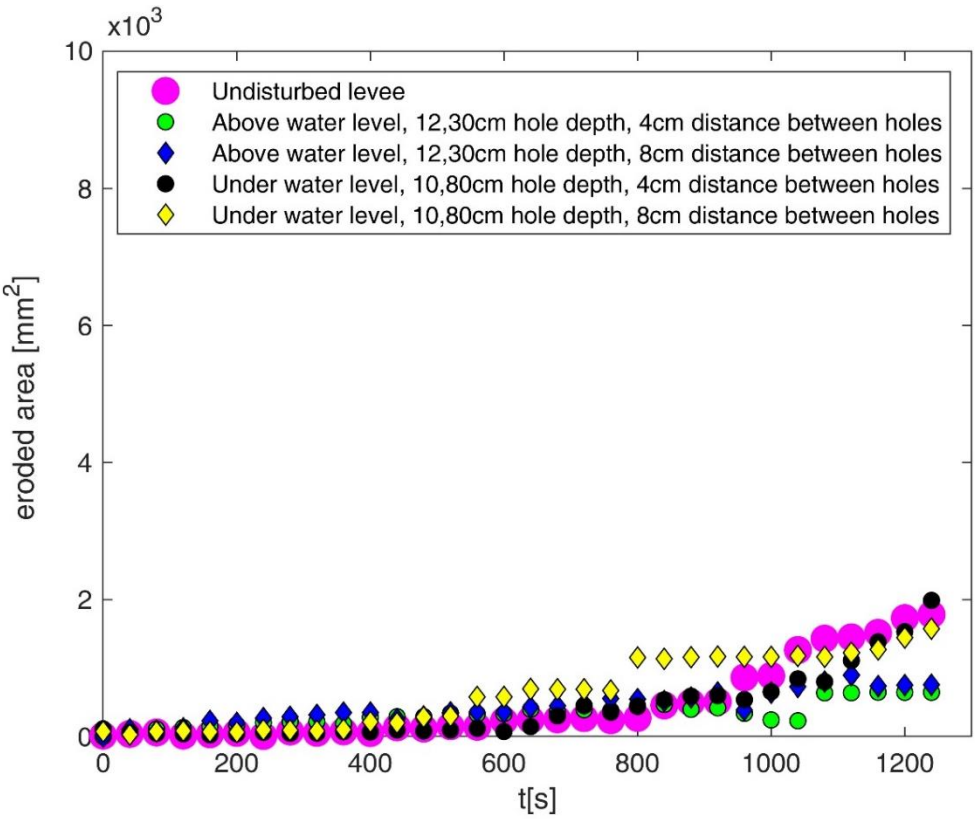

Figure 6-4: Experimental test of 90° inclination holes referred to the water flow.

Actually, in the presence of burrows angled at 45° to the flow direction, the eroded area is on average equal to the 5,80 % of the crest area (Figure 6-5). Thus, it is almost 100 % increase compared to the undisturbed levee.

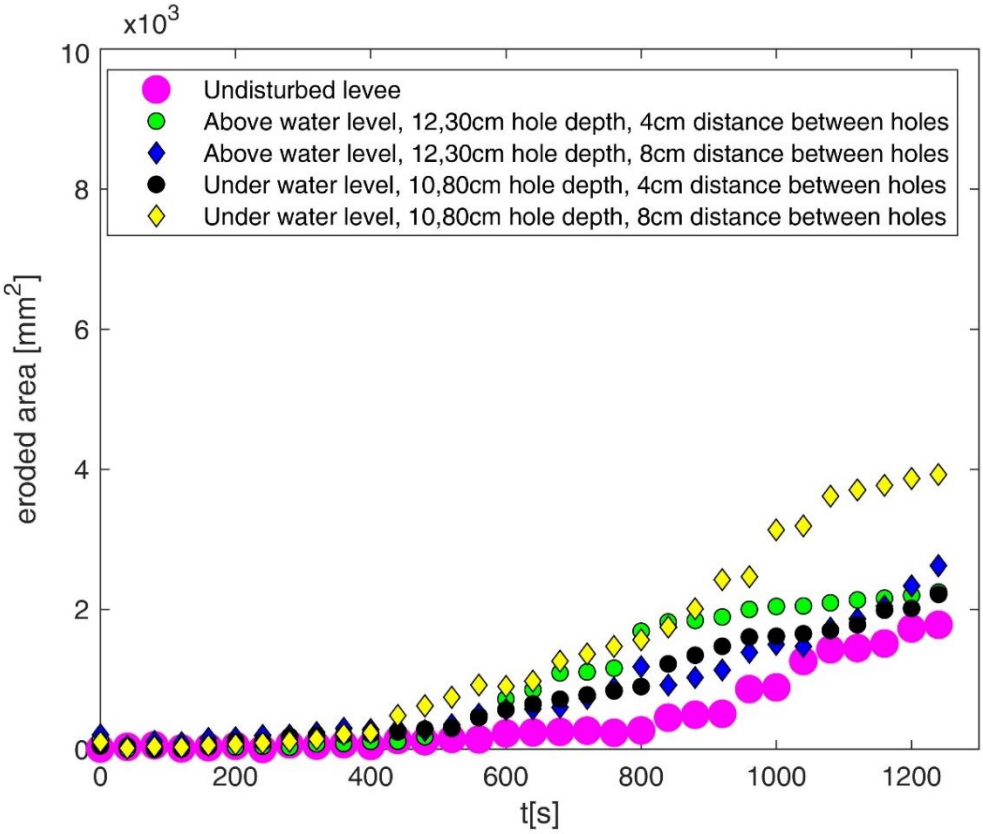

Figure 6-5: Experimental test of 45° inclination holes referred to the water flow.

Otherwise, in the presence of burrows with 135° inclination to the water flow, the eroded area is on average equal to the 4,20 % of the crest area (Figure 6-6). Thus, it is a 40 % increase compared to the undisturbed levee.

Contrary to what one might suppose, the erosion is not greater if there are four burrows at 8 cm distance rather than eight burrows at 4 cm distance. In fact, the eroded

area seems to be the same or, at the most, increase inversely with the number of burrows.

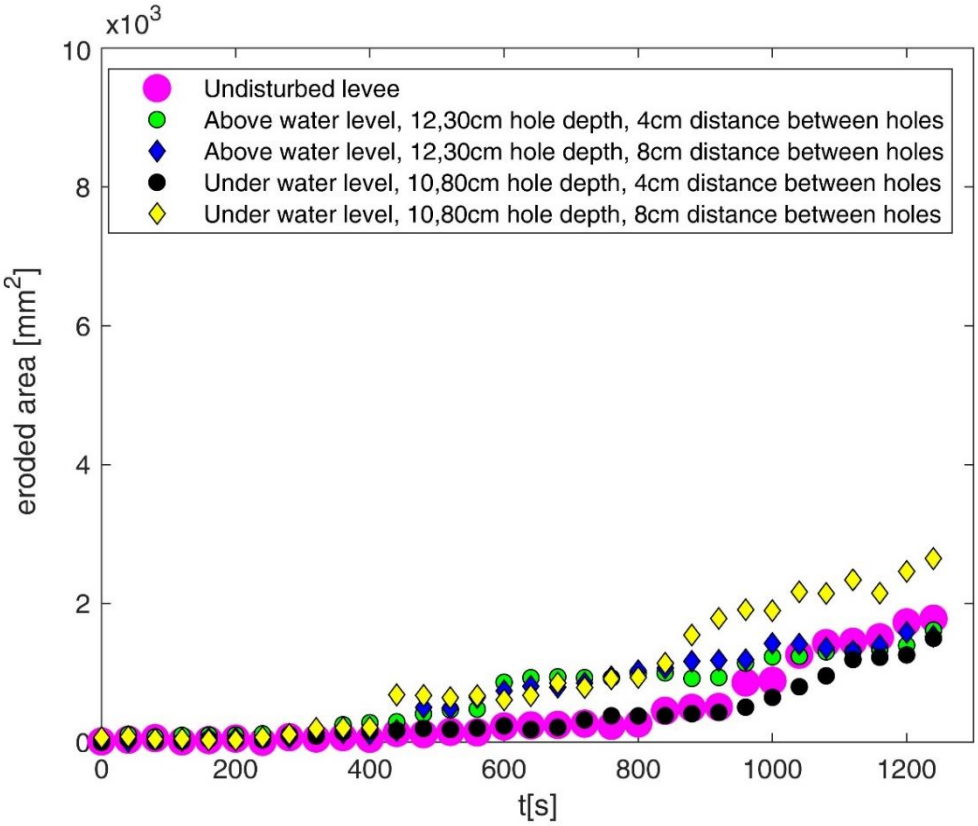

Figure 6-6: Experimental test of 135° inclination holes referred to the water flow.

With regard to the different depth of the burrows, the trend of levee erosion does not seem to involve any significant variation. It is considered that these experiments are not suitable to evaluate the impact of the burrow depth on the surface erosion. Thus, the 100 cm long levee experiments are conducted always considering the same burrow depth: 8,20 cm, for burrows under water level, and 7,20 cm, for burrows above water level.

6.6. Impact of burrows on surface erosion for the 100 cm long levee

There are 39 experiments involving 100 cm long levees. In the following sections, the burrow parameters described in Section 5.9 are separately investigated. In particular, the first section explains how the failure mechanism changes related to the vertical position of the burrow. Then the other parameters are independently investigated, differentiating them from their position associated to the water level.

The eroded area for the undisturbed levee after 60 minutes is 17% of the levee crest area. Thus, it is the benchmark for the following analyses.

6.6.1. *Analyses of burrow parameters: Vertical position*

The water flow starts to erode the levee slope. The sediment is transported downstream and they are deposited on the riverbed. As the time goes by, slope erosion grows towards the crest.

During the experiments an interesting tendency of the eroded area development was noted. Observing the erosion progress of levees with burrows, a substantial difference related to the vertical position of the burrows was found. In fact, after one hour of experiment, levees with burrows above water level were more eroded than those with burrows under the water level. Specifically, if the burrows were located above the water level, the total erosion increases between 35 % and 106 % compared with the eroded area of an intact levee. While, if the burrows are located under water level, the erosion area is between 3% and 26% of the total levee crest area. It means that in some cases the burrow presence under the water level decreases the surface erosion phenomenon to 82% compared with an intact levee erosion.

The analysis shows in Figure 6-7 that burrows above water level are always more dangerous than burrow configurations under water level. By analyzing images, it was possible to understand the two different mechanisms of erosion.

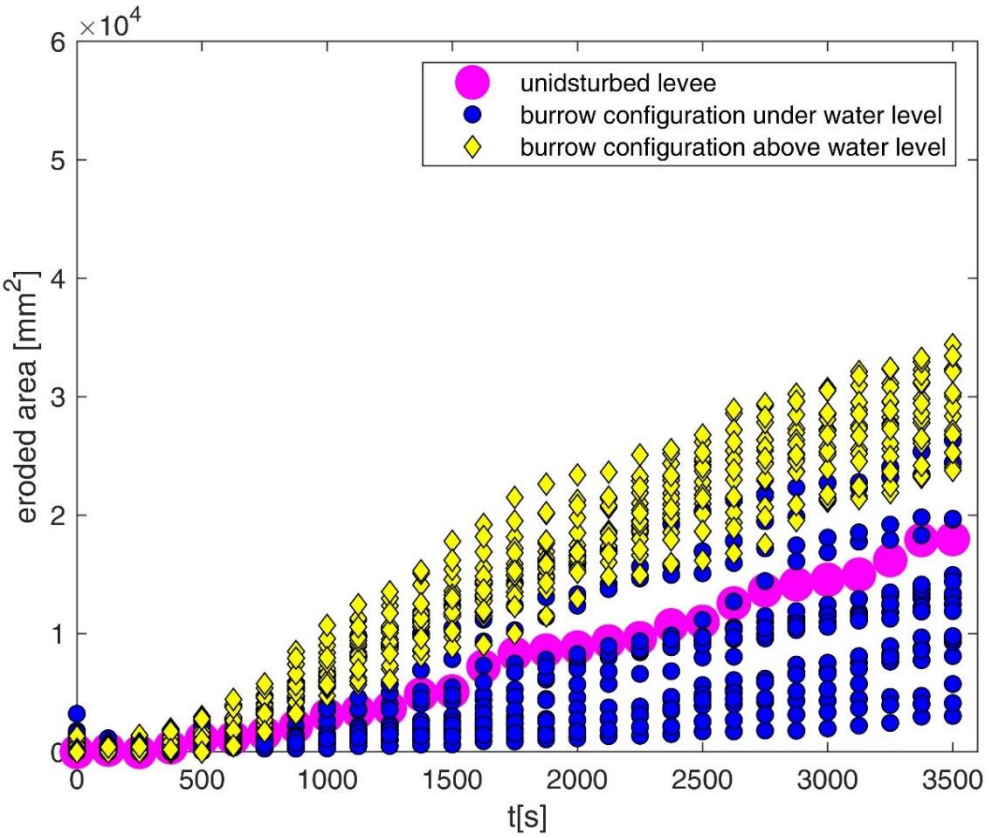

Figure 6-7: Comparison between all the configuration above (yellow) and under water level (blue) and the undisturbed levee benchmark.

If the burrows are located above the water level, the erosion of the levee slope allows the water to reach the burrow entrances. Then, the water flow erodes the hole edges, increasing their diameter, and starts to flow into the burrows. The water entering inside the burrow triggers erosion also in the burrow's interior, the soil that covers the burrow collapses and the total erosion increases towards the crest of the levee, as shown in Figure 6-8.

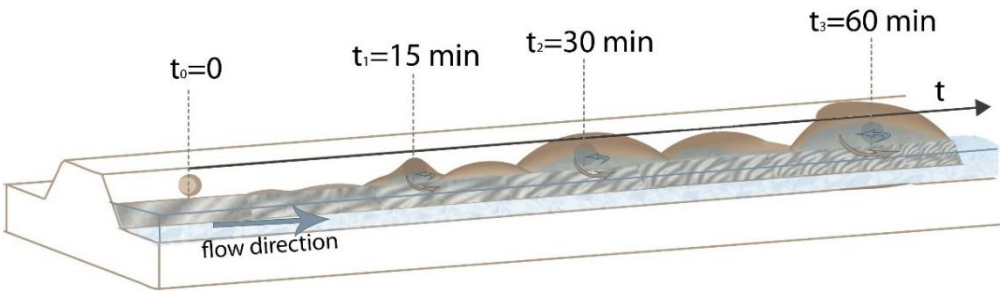

Figure 6-8: Erosion mechanism on deteriorated levee in the presence of burrows above water level.

If the burrows are located under the water level, the sediment transported by the water clogs up the burrow entrances. Probably, the presence of burrow entrances under the water level creates more grip, reducing the rate of sediment transport, and delaying the total erosion. Figure 6-9 tries to explain this mechanism.

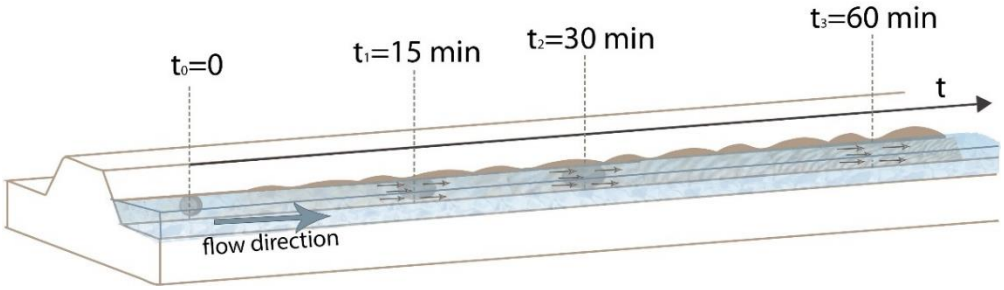

Figure 6-9: Erosion mechanism on deteriorated levee in the presence of burrows under water level.

Considering these different erosion mechanisms, comparison between eroded area for burrows above and under water level are made. Analyzing burrow configurations with the same burrow inclination angle, the different mechanism becomes evident.

6.6.2. *Analyses of burrow parameters: Angle with respect to the flow*

In order to understand the impact of the burrow inclination with respect to the flow direction, the burrow configurations are grouped according to density. In particular, to estimate the most dangerous configuration, experiments made with the same number of burrows are presented together, as shown in Figure 6-10.

As explained above, burrow configurations above and under water level are separately analyzed.

Considering all the burrow configurations above water level, the evaluation of the effects of burrow inclination is carried out. All the analyzed configurations increase the eroded area compared to that of the intact levee. However, as discussed for the 40 cm long levee experiments (Section 6.5), the 90° inclination burrow configurations seem to be the less dangerous. Indeed, the erosion surface is increased by 82%, 41% and 59%, respectively for 10, 20 and 40 burrows, compared with the benchmark. Otherwise, considering the 45° inclination, the erosion surface is always increased by about 88%, compare with the undisturbed levee. Moreover, the 135° inclined configurations are often the most dangerous. Actually, the erosion surface is increased of 100%, 76% and 106%, respectively for 10, 20 and 40 burrows, compared with the benchmark. Generally, as can be seen, in the configurations with the smaller number of burrows, 10 burrows at 10 cm distance, and those with the greater number of burrows, 40 burrows at 2,5 cm distance, the 135° inclination burrow configuration appears to be the most perilous. For configurations with a medium number of burrows, 20, the 45° seems to cause greater erosion.

Considering the burrow configurations under water level, only the 135° inclination burrow configurations seems to increase the surface erosion process. In particular, the eroded area is increased by 53%, 41%, and 18% respectively for 10, 20 and 40 burrows, compared with the benchmark eroded area. The 90° inclination burrow configurations seem to reduce the eroded area. Otherwise, in the 45° inclination burrow configurations, the eroded area is not relevant compared with the intact levee.

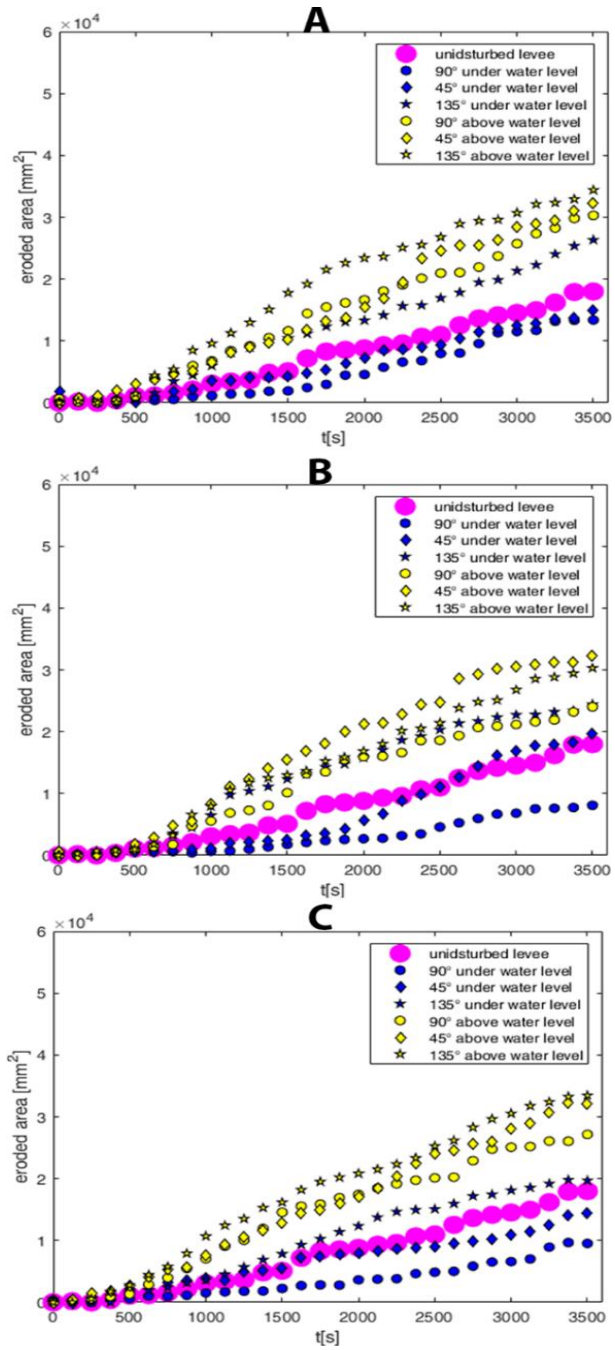

Figure 6-10: comparison between burrow configurations with the same number of burrows:
A) 10 burrow at 10 cm distance;
B) 20 burrows at 5 cm distance;
C) 40 burrows at 2,5 cm distance.
Configuration above water level are yellow, those under water level are blue.

6.6.3. *Analyses of burrow parameters: Density of burrows*

In order to evaluate the effect of burrow density, comparisons between burrow configurations above and under water level with the same inclination angle are carried out as shown in Figure 6-11.

With regards to configurations above water level, there is a similar trend of the erosion curve. Specifically, configurations with the smallest and the greatest number of burrows have the same evolution time, while the average density configuration has some variation in its trend, but it is not significant. Indeed, considering 10 burrows above water level, the erosion area compared to the benchmark is increased of about 76%, 88%, and 100%, for burrow configurations angled at 90°, 45° and 135°, respectively. The greatest density (40 burrows) increases the erosion area of about 59%, 88%, and 100%, for burrow configurations angled at 90°, 45° and 135°, respectively. While the erosion area of medium density burrow configuration (20 burrows) is increased of about 41%, 88% and 76%, for burrow configurations angled at 90°, 45° and 135°, respectively. Thus, although the above water level configurations always increase the total erosion compared to the benchmark, those results suggest that the burrow density variation does not affect the surface erosion too much.

Taking into consideration the configurations under water level, the greatest burrow density (40) has an erosion of 9%, 14% and 20% of the total crest area, for configurations angled at 90°, 45° and 135°, respectively. It means that only for burrows inclined at 135° the total erosion is increased by 18% compared to the intact levee. The average configuration with 20 burrows has an erosion of 6%, 15% and 24% of the total crest area; so, the total erosion of the configuration angled at 135° is increased by 41% compared to the benchmark. The erosions of a levee with the smallest density burrows (10) are 13%, 15%, and 26% of the total crest area, thus for 135° angled configuration the total erosion is increased by 53%. It is interesting to note that, for configurations positioned under water level, reducing the numbers of burrow, increases total erosion. Indeed, the total erosions of levee with burrows angled at 90°, are 9%, 6%, 13% of the total crest, for configurations of 40, 20 and 10 burrows,

respectively. Considering 45° inclined burrows, the surface erosions are almost the same for all the considered density. While for burrow configurations angled at 135°, the levee total erosions are 20%, 24%, 26% of the crest for configuration with 40, 20 and 10 burrows, respectively.

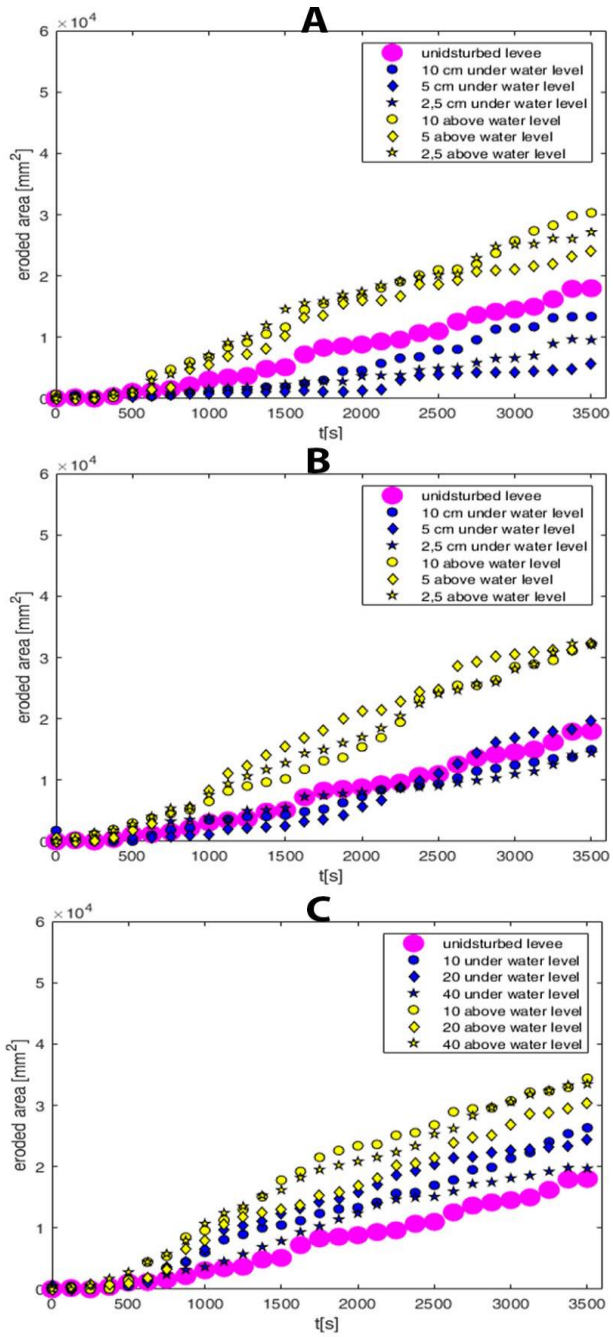

Figure 6-11: comparison between burrow configurations with the same angle inclination:
A) 90° inclination burrows;
B) 45° inclination burrows;
C) 135° inclination burrows.
Configuration above water level are yellow, those under water level are blue.

6.7. Results and Discussion

In order to understanding the impact of animal burrow on the levee stability, an experimental activity in a physically-based analogue model was carried out at the Laboratory of Geography, Geology and Environment, University of Hull (UK), where researchers specialize in the analysis of eco-hydraulic systems. Specifically, implementing an image analysis procedure, the progression of geometrical changes on the levee crest as a proxy of the overall surface erosion process are measured.

Preliminary experiments were made on 40 cm long earth levee, but after 20 minutes the downstream material discontinuity alters the results. Thus, a 100 cm long earth levee was investigated, instead. The parameters examined are four: vertical position of the burrows along the levee slope, length of the burrows inside the levee, burrow density and angle inclination with respect to the flow direction.

The surface erosion of an intact levee after one hour involves the loss of 17% of the levee crest area. This value is used as a comparison parameter to evaluate the erosion evolution for all other experiments.

The analyses demonstrate that failure mechanisms should be divided related to two main types of burrow configurations: above water level and under water level. Indeed, the erosion mechanism changes as a function of the vertical position of the burrows. The burrows above water level trigger an erosion that is 23% and 35% of the levee crest area; it means that the erosion is increased between 35% and 106% compared to an intact levee. While, if the burrows are located under the water level, the erosion area is between the 3% and 26% of the levee crest area.

With regards to the angle inclination of the burrow with respect to the flow direction, considering the configurations above the water level, the analyses demonstrate that burrows angled at 135° are the most dangerous configurations: the eroded area is between the 30% and the 35% of the levee crest area, thus, the increase is between 76% and 106% of the benchmark. While burrows orthogonal to the flow direction have the less impact on the levee instability, between the 24% and the 31%

of the levee crest surface, increased between 41% and 82% compared with the intact levee. For burrows angled at 45°, the eroded area is always the 31% of the levee crest surface, 82% increase. Considering burrows under the water level, only the burrow configurations inclined at 135° seem to increase the surface erosion process as compared with undisturbed levees. Otherwise, the erosion development of levee with 45° inclined burrow configurations under water level seems to have the same trend of an undisturbed levee. Additionally, the burrow configurations angled at 90° seems to reduce the eroded area.

Concerning the burrow density investigation, unexpected results are obtained. For the under-water level configurations, reducing the numbers of burrow, increases total erosion. For the above water level configuration, a mean density of burrows generates the smallest erosion area. However, there is a similar trend of the erosion curve for all the densities.

The experiments are focused on the geometrical parameters of the burrows. Nevertheless, the flow characteristics may have affected the results. Thus, future research should be concentrated on the development of the erosion process in the presence of burrows changing the flow parameters, and more importantly, changing flow rates to simulate a flood.

Moreover, in light of these results, we believe that analyses on the seepage phenomenon cannot be separated from surface erosion effects. For instance, the numerical analyses performed by Taccari et Van Der Meij (2016 - A) suggest that burrows placed above the water level do not influence levee safety. Nevertheless, our experiments refute their argument. The experimental activities highlighted the different development times of erosion and seepage phenomenon: when the water starts to flow on the landside, the levee is already quite eroded. Maybe, the conjunction of these two mechanisms can completely alter the outcome of results. Future numerical analyses should be focused on a three-dimensional levee to investigate simultaneously erosion and seepage mechanisms in the presence of burrows.

7. PROPOSED RISK MITIGATION MEASURES – TREVI INTERNSHIP

7.1. Overview

Because of repeated episodes of levee failures, the consequent floods cause massive flood damage every year in worldwide. Consequently, it is essential to design river levees that conform to principles of safety and reliability, and that have a structure able to holds dangerous water flows. As mentioned above, the most common failure mechanisms of earth structures related to animal activities are overtopping, seepage, internal erosion, and surface erosion.

The solution to the levee degradation problem, resulting from the combination of different of several factors, such as river flow, rainfall, erosion process, and biological activities, requires the adoption of a technology, which is quickly executable, long lasting, adaptable to various surface situations and at the same time environmentally sustainable. In order to achieve this aim, a successful "restoration" project should be designed after gaining a complete know-how of the principal soil consolidation techniques and with regard for ecosystem-wide processes and overall biodiversity.

Thanks to the internship at TREVI spa, different technologies of soil improvements (i.e. consolidation, improvement of permeability, increased strength, etc...) were studied and analyzed.

Trevi S.p.A. is a company specialised in the field of special foundation and soil consolidation works and it is a worldwide leader in underground engineering and in the design and manufacturing of specialised rigs and equipment for this industry. In particular, this company is the technological point-of-reference partner in the field of engineering projects for underground works and for research and development of water and energy resources and it is specialized in the field of underground engineering, executing special foundations and soil consolidation works for major infrastructural interventions and environmental protection. Moreover, since 1995,

Trevi has obtained the certifications that officially state the conformity of the Quality, Safety and Environmental System with the strict European standards UNI-EN ISO 9001, 14001 and OHSAS 18001. The Quality, Safety and Environmental culture has always been a Trevi's distinctive feature, the "business card" of the Company on the national and international markets.

Furthermore, this company has been involved in the repair of existing dams and levees presenting seepage problems, thus tackling major engineering, geological and geotechnical issues requiring special attention, especially with respect to water-tightness of the dam body and foundations. They designed, tested and used special technologies and systems in order to reduce drastically seepage.

In the following sections, the most successful technologies studied in situ throughout the internship are presented. These techniques aim at consolidating different types of terrains and to reduce soil permeability. Furthermore, in order to find the most suitable technology with the least environmental impact and with a good cost-effectiveness ratio, a geotextile material is introduced that is generally used for reducing surface erosion: Trevimat.

7.2. Successful techniques of soil consolidation: Cased Secant Piles (CSP)

Cased Secant Piles (CPS) is a technology that offers organizational advantages for the site as well as lower costs due to reduction of material to be dumped compared to the traditional excavation techniques. This technology is suitable for consolidating any type of soil, limiting the soil deformation and without vibrations or impulses typical of percussion systems.

The first step of CSP construction is the hole drilling of primary piles by mean of a continuous flight auger coaxial to an external casing. In particular, the auger and casing are operated by two independent rotary tables, which mutually counter-rotate and travel along the mast of the drilling ring. Then the auger filled with soil is

extracted, and at the same time concrete is pumped through the central hollow stem to fill the gap left by the drilled soil up to the work level. Having fully withdrawn the auger and the casing, the secondary piles can be drilled. While drilling the latter, the adjacent primary piles are partially destroyed. After having pumped concrete also in the secondary pile and having withdrawn the auger and the casing, a reinforcement cage is installed inside secondary pile through the freshly pumped concrete. Figure 7-1 shows the sequence used for CSP construction. To ensure the fast position of the cage into fresh concrete, the latter should have the following features: aggregates with a diameter of max 18 mm and S5 or SCC slump classes shall be used. Using S5 concrete with slump higher than 220mm, the max cage positioning depth is usually 12-15 m, whereas using SCC it is possible to apply reinforcement cages to longer piles.

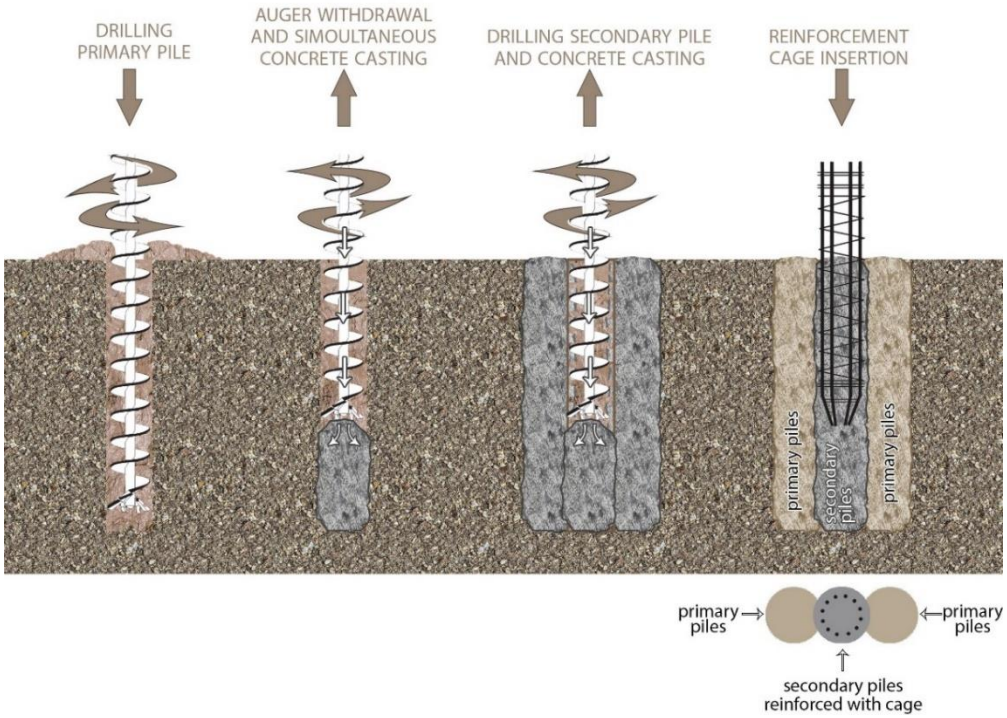

Figure 7-1: Sketch of the operating sequence to realize CSP.

The diameter of drill piles is between 600 to 1200 mm. The max depth achievable by the casing is 21 m, whereas the max depth technically admitted by the auger is roughly 30 m (depending on drilling diameter and tool). Modifying the pile diameters and the distance between them, it is possible to obtain the best compromise between the real final thickness of the wall (pile cross-section) and the concrete to be cut while constructing secondary piles.

The rotary tables travel along the mast independently: as a result, it is possible to penetrate the auger and casing to different depths, depending on soil type. In case of cohesive or fine non-cohesive soils, the auger bit and casing shoe are maintained at the same level. Instead, in the event of coarse non-cohesive materials, the auger penetrates more deeply than shoe in order to lighten the soil and to enhance movement into casing. In case of rocky soil, the casing advances like a core barrel, whereas the auger bit fitted with suitable teeth for rocks breaks up the "core" created by the casing. Both the auger bit and casing shoe could be fitted with teeth, depending on the type of material to be drilled.

The secant pile diaphragms can be reinforced with different techniques and methods. The primary pile is not usually reinforced; however, if needed, it can be strengthened by a reinforcement with a shape that allows the partial demolition of the concreate primary elements while the secondary pile is excavated. The primary and the secondary piles can be constructed using different concrete types. For instance, it is possible to use a plastic mixture for primary piles, so that they have a hydraulic retaining function only, whereas reinforced secondary piles assure the structural function of the diaphragm wall.

This technology is applied to consolidate the soil surrounding the new Palermo's railway ring, specifically the central area near the Politeama Theatre, as shown in Figure 7-2.

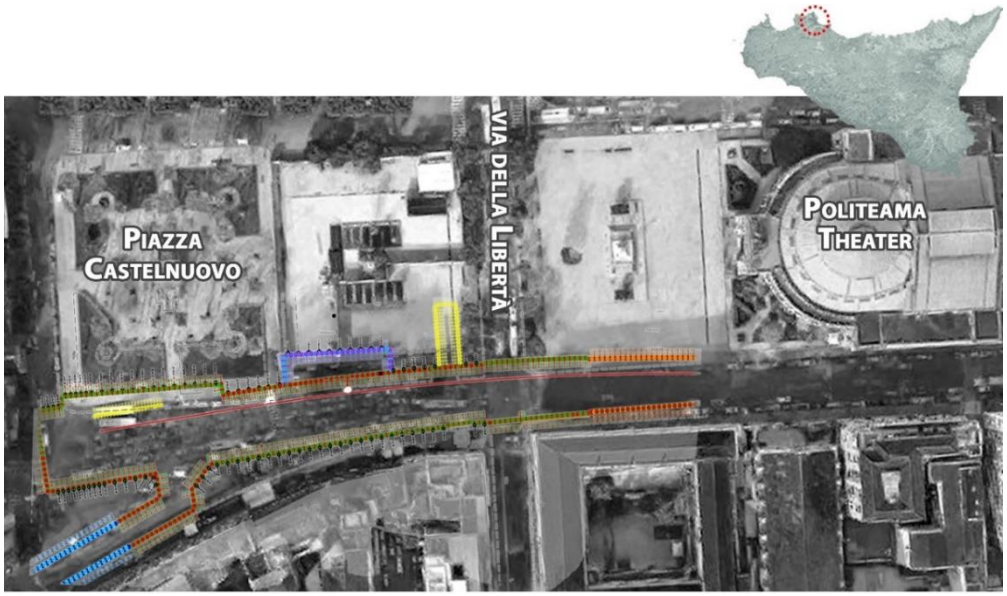

Figure 7-2: Cased Secant Piles for the new Palermo's railway ring (Top view of the area).

As a result of an executive problem, a reinforcement did not reach the project quote. In order to resolve this situation of non-conformity, to consolidate the soil, and to reduce the soil permeability, a Jet grouting technique was proposed around that portion of pile without strengthening. The proposed solution is shown in Figure 7-3.

The characteristics, performance, and execution techniques of jet grouting are described in the following section.

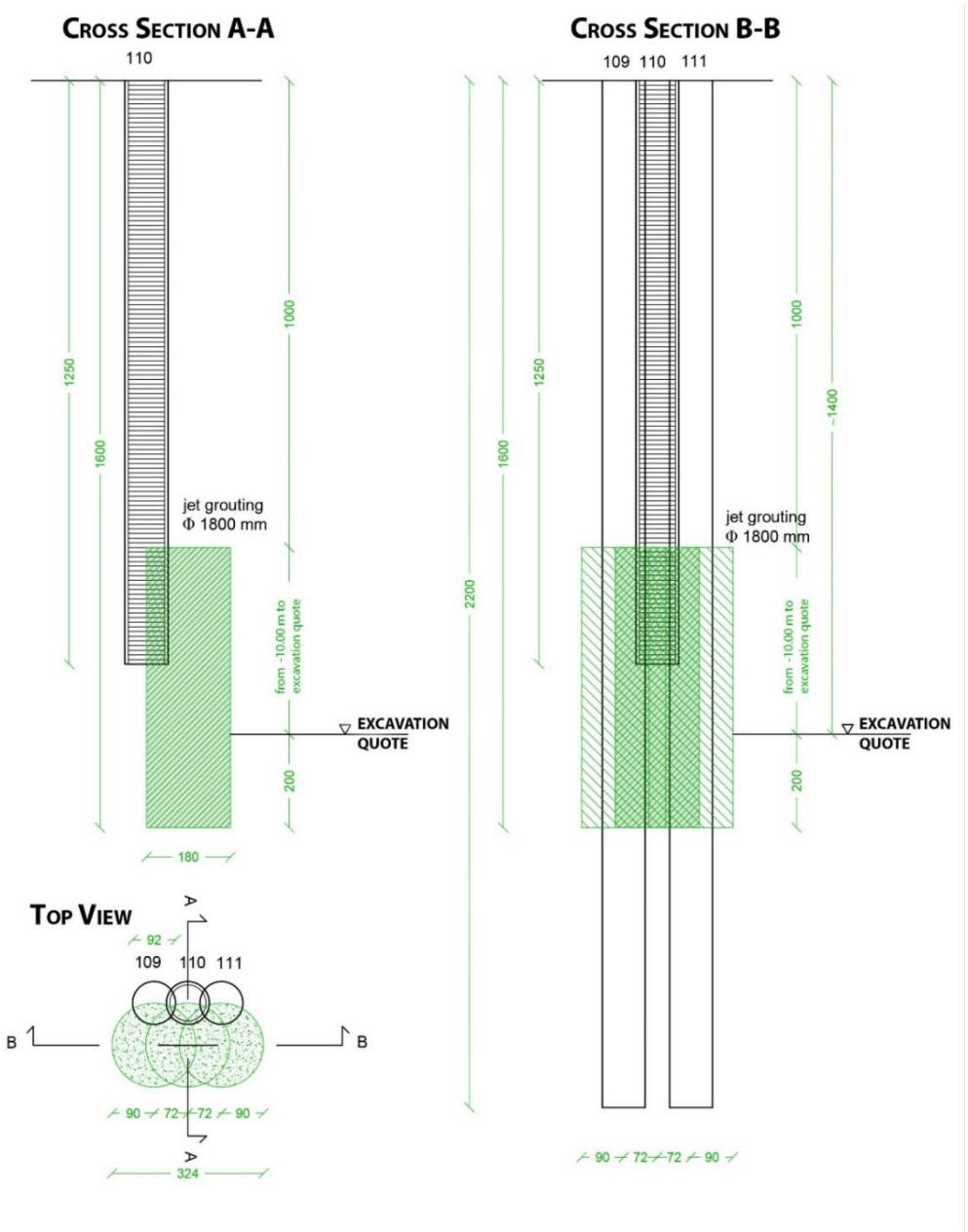

Figure 7-3: Non-Conformity resolution project for a secondary pile of Palermo's railway ring.

7.3. Successful techniques of soil consolidation: Jet grouting

Jet Grouting is the process of dis-aggregating the soil and at the same time injecting and mixing it with cement admixtures using high-pressure jets. It improves the mechanical properties of a wide range of soil types, reduces the permeability properties of the ground, and is the most profitable technique in the presence of obstacles to cross, in confined spaces, in high-depth treatment with crossing of voids, and in difficult logistic conditions. Indeed, it allows to realize consolidated soil elements with different diameter using high-speed jets of water/cement mixtures injection treatment and overcoming underground obstacles.

Although the diameters of drilling range from only 90 to 140 mm, columns of consolidated soil with diameters ranging from 600 to 2000 mm can be obtained by the Jet Grouting technology. Main applications are generally for underpinning, diaphragm wall gaps, tunnel consolidations, bottom plugs, slope consolidation, impervious cut-offs, and break-in or break-out for the TBM.

Figure 7-4 shows the operative sequence used for the Jet grouting implementation. After a preliminary phase of perforation, the drill is extracted and simultaneously a fluid at a high pressure is injected. There are three main executive techniques depending on the number of fluids uses: mono-fluid (water/cement mixture); bi-fluid (water/cement mixture and air); triple fluid with (water/air and water/cement).

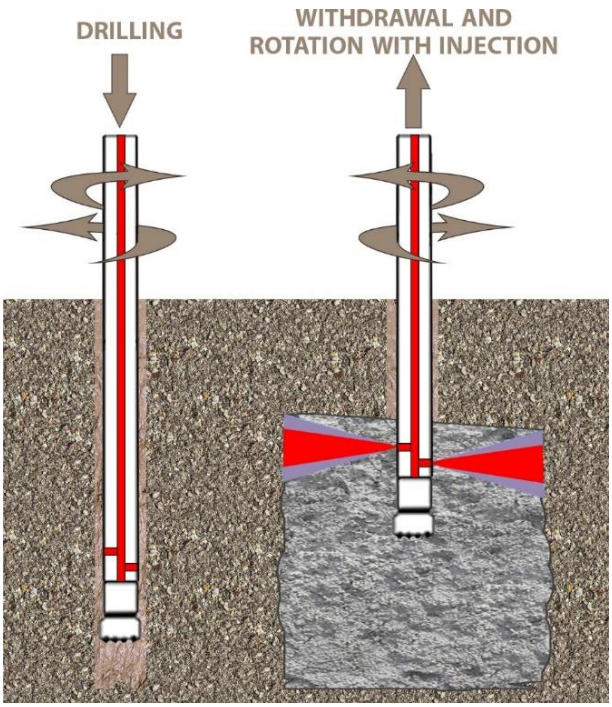

Figure 7-4: Operative phases of Jet grouting.

The common treatment of jet grouting is a cylindrical column obtained by keeping a constant speed of rotation and ascent, without variation during the return way. However, in order to achieve other shapes of consolidate structure, it only requires modifying the rotation speed. For instance, it might be obtained a pseudo-elliptical column. It involves changing the rotation speed in a planned way, as shown in Figure 7-5, and thus allows to maximize the use of jet grouting. This type of consolidation shape is used, for example, for treatment aimed at the constructing of curtain walls, guaranteeing significant savings in terms of times, materials, and therefore costs.

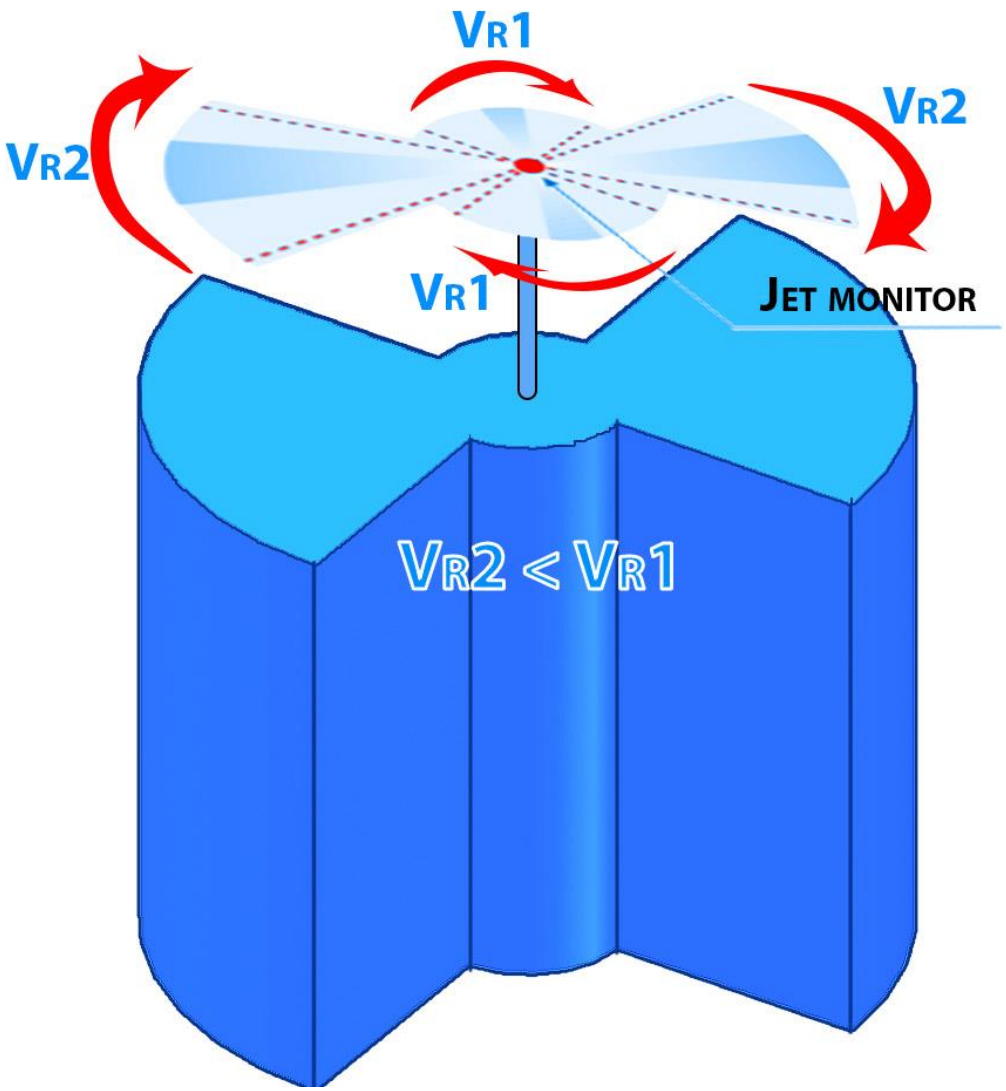

Figure 7-5: Pseudo-elliptical column created by jet grouting.

7.4. Successful techniques of soil consolidation: Micropiles

One of the most interesting techniques available to achieve an improvement of the soil features in situ is the micropile. Micropiles are small cylindrical structural elements in lengths varying usually from 10 to 40 m and in diameters ranging from 100 to 350 mm. These can be used in varied and diverse applications, such as supports and structural foundations of roadway ramps, steel towers of transmission lines, industrial plants, tunnel roofs and old or existing structures that require preservation, strengthening, augmentation, or rehabilitation. Their main advantages are the high bearing capacity compared to the borehole diameters, and the capability to overcome obstacles or pre-existing foundations. As the plant and equipment do not demand big or wide working areas, micropiles can be constructed even in limited and narrow spaces.

The micropiles can be installed by using self-drilling pipes or con be built in three operative phases, as illustrated in Figure 7-6. First, the soil is drilled, and a fluid is injected into the hole to support it and to clean it from debris and excavated soil. Among the drilling techniques, the most used are rotation and roto-percussion, with or without the aid of casing. Another suitable method for micropiles installation is auger and coring. Once the hole is ready, a reinforcement is inserted into it; generally, it is a tubular steel reinforcement. Finally, the hole has to be cemented by injecting a cement mortar under pressure from the bottom up.

Micropiles can be used as single load bearing elements, or in groups. Whether built in group, micropiles can be used to build support structures (as a wall, for example).

During the 2019, the micropiles technology was applied by Trevi S.p.A. in the yard of Taranto. In Section 7.5 the construction site is described.

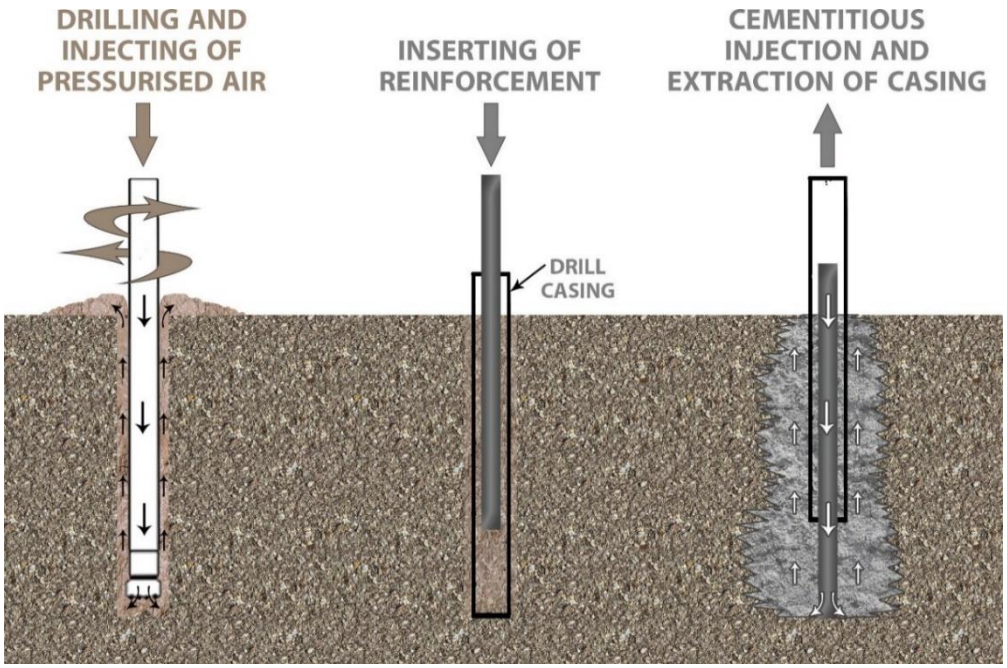

Figure 7-6: Operative phases to built Micropiles.

7.5. Micropiles Case study: Italcave (Taranto)

Italcave is one of the most important operators for limestone aggregate mining located in the south of Italy, precisely in the Province of Taranto. The mining district extends over 350 hectares of land, as shown in Figure 7-7. Moreover, the extracted limestones have a higher degree of purity than the 98% and, for this reason, it lends itself to use very versatile. Specifically, it is used in the building industry and in the production of premixed products, in the agro-food sector for producing animal feed, in the paper industry, in the sugar industry and, at last, in thermoelectric industry for flue gas desulphurisation, refining of metals, production of glass, glass fibres and optical fibres.

Figure 7-7:The Italcave extention, the limestone aggregate mining in the province of Taranto, and its divided areas.

The high performance of the machines used in the crushing and grinding plants allow to produce over 1.200.000.000 tons of product per year in several particle size compositions.

In 2014, the project to create another dumping ground area was authorized. This area is an extension of Italcave mining and in Figure 7-7 it is mentioned as III plot.

Before the starting of the work, the buildings rise in the area called "*Ex campo contumaciale"* were demolished and in their place a service area was built. The service area consisted of a new office building, cells of waste storage, warehouses of wastes selection and inertization, leachate treatment plant, biogas extraction and upgrading plant, meteorological water collection and treatment network. Figure 7-8 shows the area as it was a few years ago and the project of the area as it is now.

Figure 7-8: On the left the III plot as it was when it is called "Ex campo contumaciale"; on the right the project of the new area.

In order to increase the third plot of the mine to be used for the landfill, approximately 1.650.000 cubic meters of soil had to be removed. Figure 7-9 shows the limits of the project area and the demarcated area where soil should be removed. In particular, the area numbers suggested the time sequence of the work.

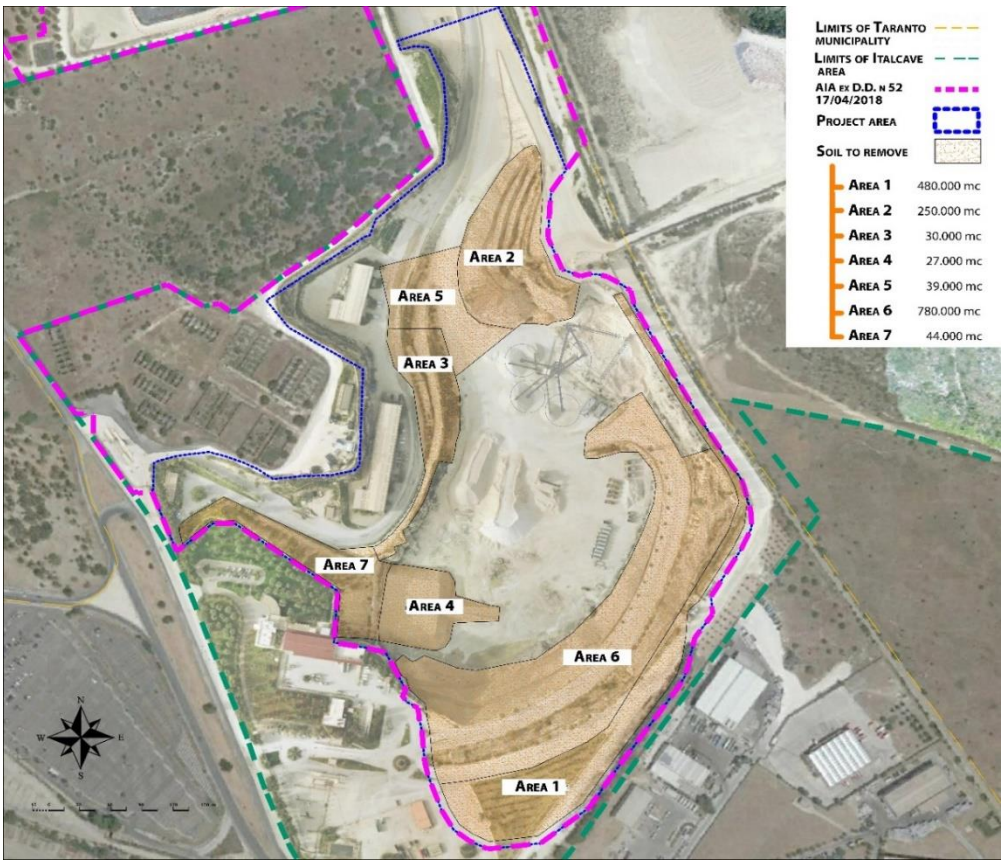

Figure 7-9: Soil that needs to be removed in order to increase the III plot area.

On AREA 2 a bulkhead was fitted. In order to guarantee the safety of the fronts during the excavation and stability over time of landfill, and to achieve the structural connection between the other banks, was studied and dimensioned a bulkhead design solution. It stretched 200 meters and was high about 40 meters. The work was carried out step-by-step, for levels and for alternating fronts, and according to the strong time constraints of consolidation and excavation works. Figure 7-10 shows the area before the project implementation and a section where the old and new profile are compared.

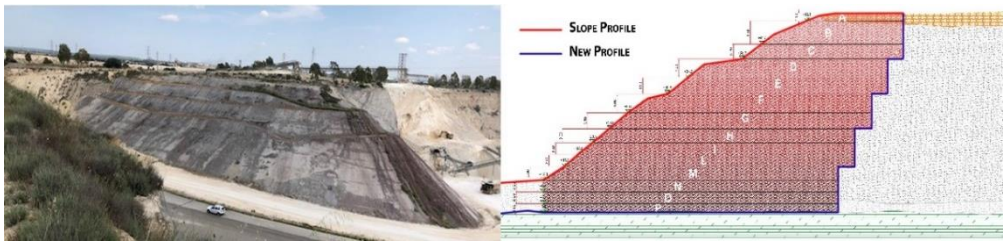

Figure 7-10: a front view of AREA 2 and a section of design solution: current slope profile and future bulkhead.

The bulkhead was created on five level of micropiles with an axle spread of 0.4 meters. On the first two level, micropiles of 200 mm diameter were used and the reinforcement was a tubular steel of Ø139.7≠8.0 mm. On the third and the fourth level, the micropiles diameter was 250 mm, the reinforcement Ø159≠8.0 mm. On the last level, the drilling holes were 300 mm wide and the tubular steel was Ø193.7≠12.5.0 mm. Figure 7-11 shows the first level of micropiles.

Figure 7-11: The first level of micropiles built in the AREA 2.

The holes were excavated by both rotation and thrust and were carried out according to an alternating execution sequence, as explained in Figure 7-12.

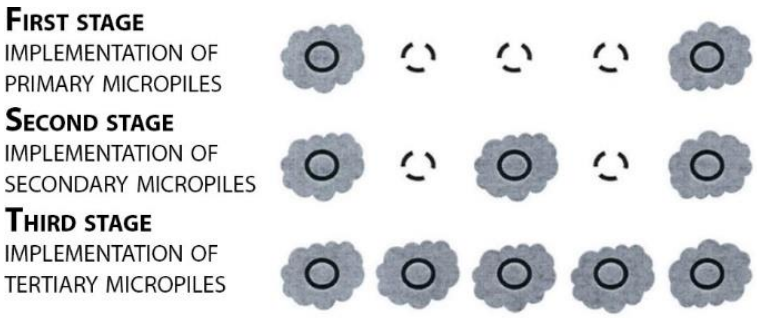

Figure 7-12: Execution sequence of micropiles.

The micropiles were connected each other with reinforced concrete beams. Between each micropiles, a tie rod was built. The tie rods are structural elements undergoing traction and suitable for conveying loads to soil depths.

After carrying out the structural works, the first level could be excavated, as suggest in Figure 7-13 - B. Repeating the process (Figure 7-13 C - D), the bulkhead was realized.

During the excavation activities, the soil removed was sifted, sorted by type and, then, it was recovered or disposed of without harming the environment.

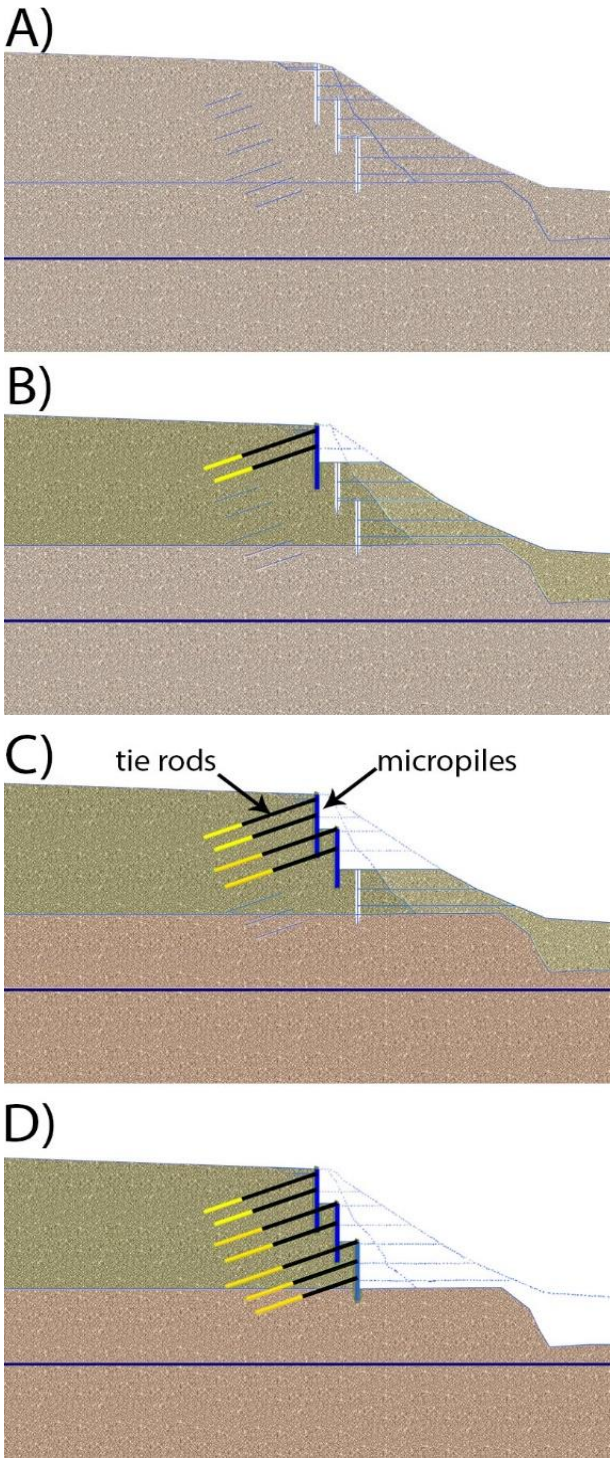

Figure 7-13: sketch of work phases to built a bulkhead.

7.6. Successful techniques to reduce the soil permeability: Cement and Chemical Grouting

The process of injecting a substance into the ground is the oldest method of civil engineering construction in order to improve or modify the mechanical and permeability properties of different types of subsurface. The technique relies on mechanical means to create in-situ mixtures of soil, cement and chemical grout. The cement and chemical injections could be used both for temporary intervention, to make excavation possible in unstable soil or under water table, as permanent intervention, to consolidate foundation soils, to create watertight structures, or to structurally renovate brick or concrete works. Moreover, this technique is effective on both loose and rocky soil. Depending on soil type, the grouting system and the injection mixture change.

The successful filling depends in the first place on the size of the solid particles of the injected grout compared to the dimensions of the gaps or rock fissures to be injected.

For rock formations or loose coarse-grained soils, cement-based grouts are recommended. Cement grouts can be stabilized by means of pre-hydrated bentonite, whereas they are made less cohesive and more fluid by adding special formulations and deflocculating-fluidifying additives (MISTRA grouts).

For rock fissures and finer-grained soils, fine cement or micro-cement grouts are suggested. In these cases, it is possible to use Silicate-Mineral based grouts (SILACSOL), which ensure good results in terms of both consolidation and waterproofing, or “soft” Silicagel for waterproofing only.

For even finer soils, the use of colloidal silica can be envisaged (nano-silica). It is a nano-silica based grout in colloidal aqueous solution with no addition of mineral agents or insoluble salts (ROSIL grouts). It is injected in one single phase, by adjusting the setting time through the dosage of inorganic salt. Once injected, Rosil grouts harden and create a stable product free of syneresis.

For soils characterized by high porosity, expanding cement grouts can be used. It is a standard stable cement-based mixture in which an agent is added to generate micro-bubbles that remain entrapped within the mix and expand it. At the beginning, the mixture is easy to pump, then it expands and turns into a rigid foam. Expanding grouts can be usefully exploited in several applications: filling large natural or artificial cavities, filling and re-compressing soils hit by landslides, contact grouting of tunnel, etc...

From an operational point of view, there are three different grouting systems depending on the soil type. In bedrock, the injection is executed directly into the open borehole through two different methods: upstage and downstage methods. With the first one method, also known as "ascending stage", the borehole is drilled at the project depth; then selective upstage grouting by areas is carried out using a specific single packer that breaks up the borehole in several lengths. Due to the aforesaid procedure, this method is suitable for grouting in boreholes that remain stable throughout significant lengths and it is described in Figure 7-14.

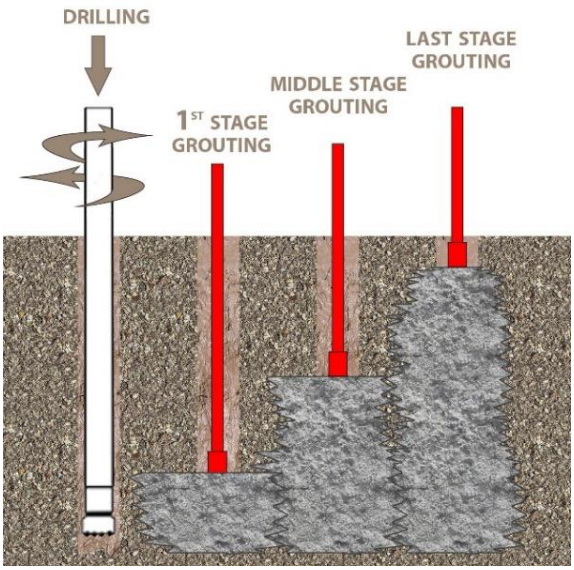

Figure 7-14: Upstage grouting with packer in rock formation (ascending or up-stage)

Other way around, the downstage method, also known as “descending stage”, is chosen for unstable boreholes. The injection is carried out step-by-step: a stretch of borehole is drilled and grouted. After waiting for the time required to harden of the mixture, a length of borehole is drilled, then the tool is raised for a few meters and grouting is performed. In both cases, borehole inclination must be defined depending on the position of soil layers and the direction of discontinuities, so as to affect the highest number of joints or fissures. It is described in Figure 7-15.

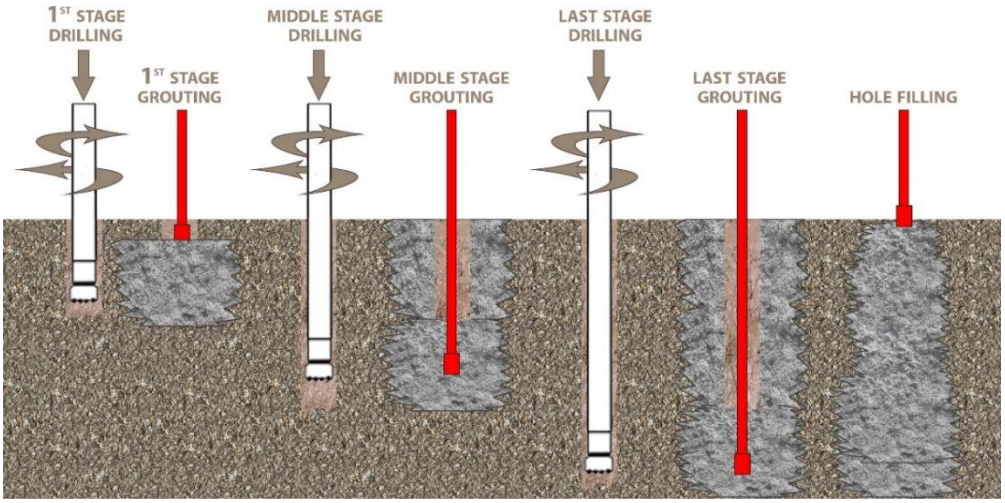

Figure 7-15: Downstage grouting with paker in rock formation(descending or down-stage).

In the case of soil characterised by fine-grained, TMG (Trevi Multi Grouting) system is recommended. This method is to insert into the borehole a group of small-diameter tubes with different lengths and fitted with one single valve, as shown in Figure 7-16. Every tube is directly connected to the grout delivery line, without the need for sliding the packer down into the hole. Thus, the injection occurs at different levels of the same borehole simultaneously, and in a selective way (with different pre-set parameters). The tubes, with high burst strength and length identified by the colour, are simultaneously connected to special plants with tens of low flow rate pumps and to a device controlling and recording the parameters of grouting.

Depending on the type of soil to be treated (level of fissures/porosity) and intervention requested (consolidation and/or waterproofing), a specific project is prepared to define the distance between the holes, the most suitable grout, and the grouting parameters to use.

The grouting parameters (volumes, pressures, flow rate) are constantly controlled and recorded during every grouting stage. The outcomes are processed and analysed in order to assess the effectiveness of treatment carried out so far and manage the following stages in the best way possible.

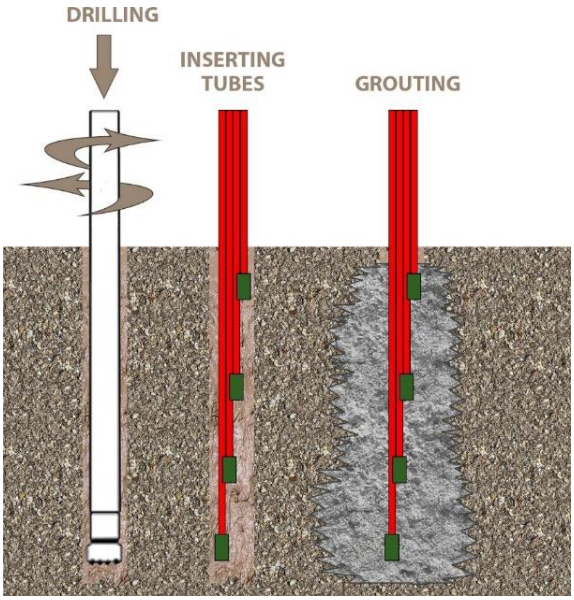

Figure 7-16: TMG system.

TAM and MPSP method are advisable in weathered rocks or loose soil. The TAM method, known as “manchette tube” and described in Figure 7-17 A, seals the tube to the soil by means of sheath grout for loose soil permeation. The valves are located every meter. The MPSP method is a multi-packer sleeve pipe and is designed and developed to treat weathered rocks. As shown in Figure 7-17 B, this technology

consists of dividing the boreholes into several section with shutter bags, which are fitted every meter of tube length.

These technologies were applied in the Dry Dock Project of Palermo Industrial Port, which is described in the Section 7.7.

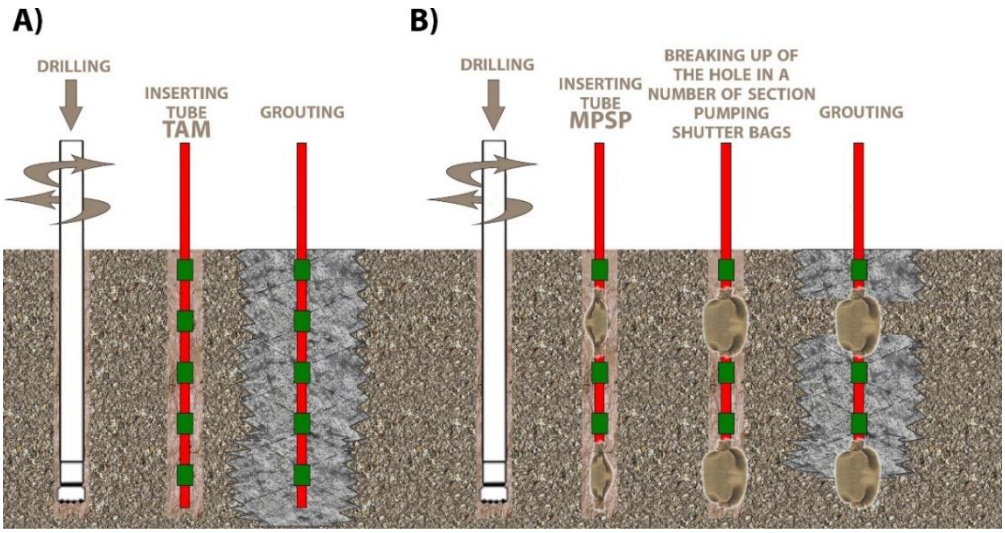

Figure 7-17: A) TAM method; B) MPSP method.

7.7. Grouting case study: Dry Dock Project (Palermo)

The dry dock is a structured area wherein are performed the construction, repairs, and maintenance of merchant vessels and boats. In the 80s, Palermo Port Authority started the construction of the 150.000 DWT Dry Dock, shown in Figure 7-18, within Palermo Industrial Port. However, due to a dispute arisen with the subcontractors, the work was delayed.

Figure 7-18: Top view of the Dry Dock subject to intervention within the Palermo Industrial Port.

Before the beginning of 2000s, after remediation with removal of seabed deposits, the subcontractors performed the construction of the foundation bench and installation of cellular caissons with the exception of the basic gate-caisson. Moreover, they implemented a diaphragm wall on the caissons' external perimeter to extend the seepage paths during the construction phases up to realization of the foundation slab, and performed a completion of grouting, in order to improve

imperviousness of the diaphragm wall single panels' joints. Finally, they completed the installation of the foundation piles of the dock's slab, with insertion of tie rods to be stressed later.

Afterwards, the subcontractors changed and Trevi S.p.A. took over the dry dock work. In order to assess the state of works already carried out, it was necessary to perform consolidation and static safety works before emptying the dock basin. Works specified in the Contract included dredging of approximately 76.000 m^3 of sediments and waste, for a total of about 117.000 tons of mainly sandy material, contaminated by hydro-carbons C>12, heavy metals and mixed waste, mostly conveyed by 2 sewage pipes (about 500.000 AE) which, until 2014, were discharging next to the Dock. A Sediment washing treatment was proposed. The objective of the Sediment Washing treatment was the recycling of materials and subsequent reduction of waste to be disposed of.

At the beginning of 2019, an alternative project provided a work of soil permeability reduction lengthening of seepage paths. Then, the Dry dock of Palermo would have been ready to be emptied in order to evaluate the characteristics of the substrate, and, if necessary, improve its quality.

In order to reducing values of gradient in the sedimentary soils lengthening the paths of the seepage, two type of works were provided: a cement and chemical grouting treatment and a system of wells drainage around the dry dock.

The injection treatment was done on the discontinuity point of the dry dock perimeter, specifically on the diaphragm previously made. As shown in Figure 7-19, for each diaphragm an injection trio was made: one was carried out on the diaphragm wall, the other two inside the caisson, composed of earth.

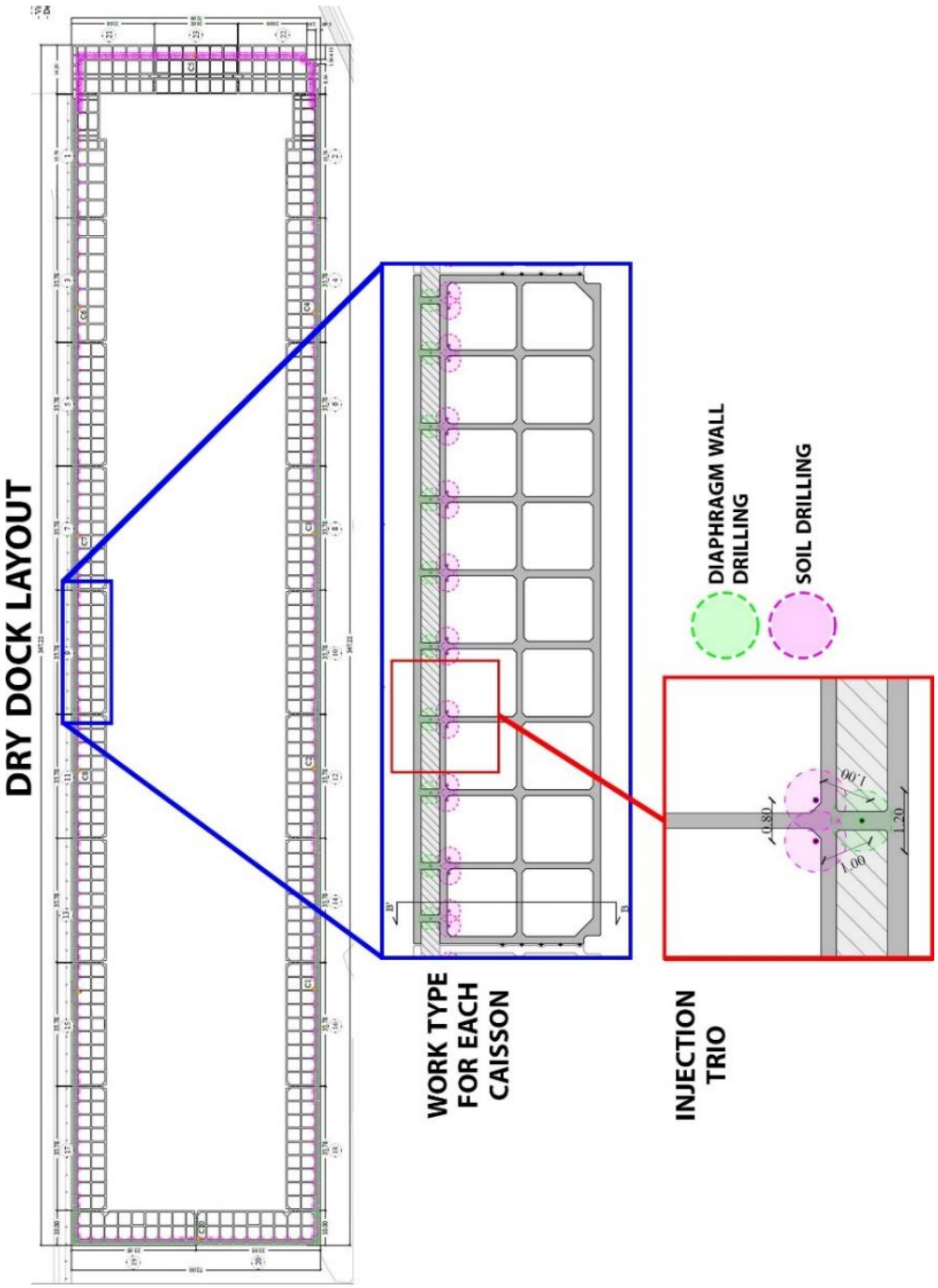

Figure 7-19: top view of cement and chemical grouting project on dry dock.

The perforations were drilled down to the depth of 33 m and they were 15 cm wide. In order to realize about 800 perforation, six micro-drilling, as those shown in Figure 7-20, worked simultaneously.

Figure 7-20: Some of the microdrilling used in the building site of Palermo.

In order to verify the hole alignment, SAAScan was used, as shown in Figure 7-21. SAAScan contains MEMS sensors in every segment that measure acceleration, tilt, and temperature inside the hole. If it is installed near vertical, it measures the magnitude and direction of lateral deformation to display a 3D shape. The measured maximum inclination of holes was about the 0.06%.

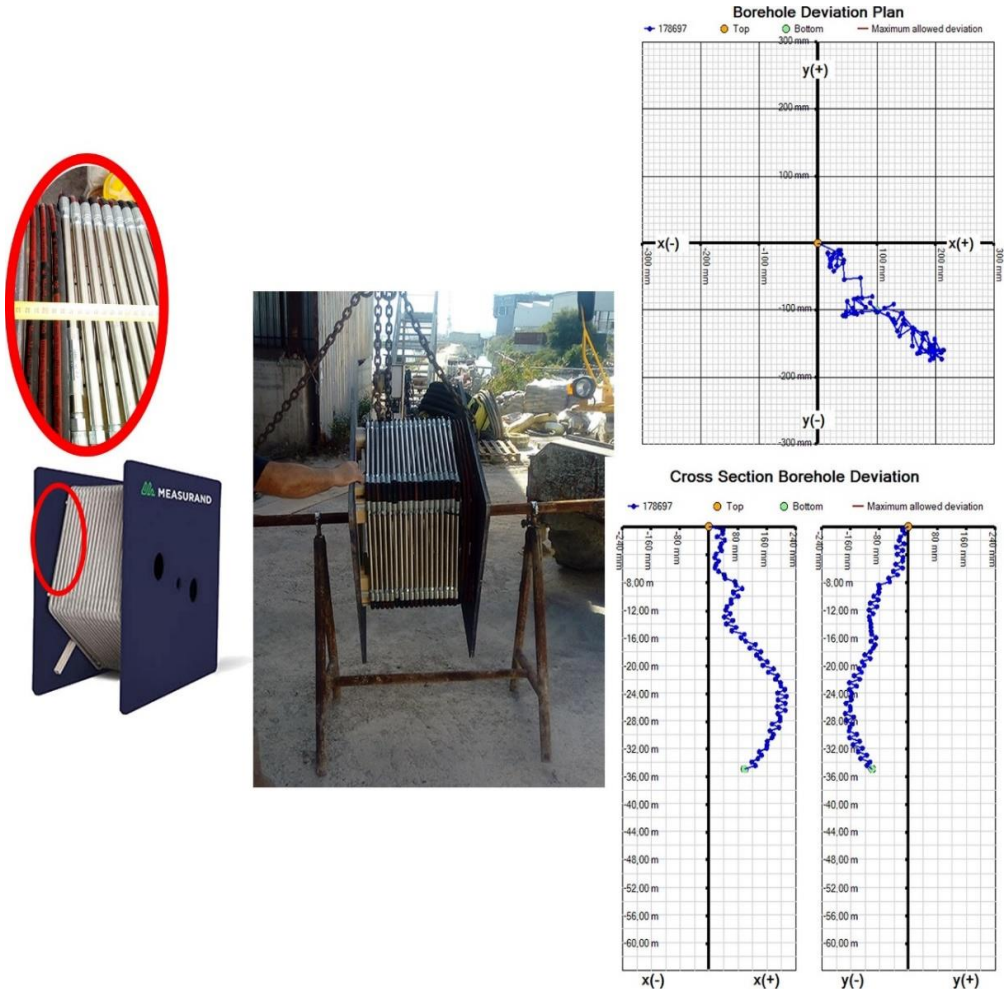

Figure 7-21: SAAScan, installation and graphic results.

The injections were performed under the caisson using tubes fitted with check valves, which were driven into the ground after drilling. The valves are rubber sleeves that cover lengths of the tube: they inflate under pressure and force the grout through the breakings preventing it from flowing back.

Grouting was performed by isolating the tube lengths by means of an inflatable double packer. In particular, as shown in Figure 7-22, the holes were ideally divided into two area: on the top area (A) the TAM method had been applied, on the bottom (B) the MPSP method had been used.

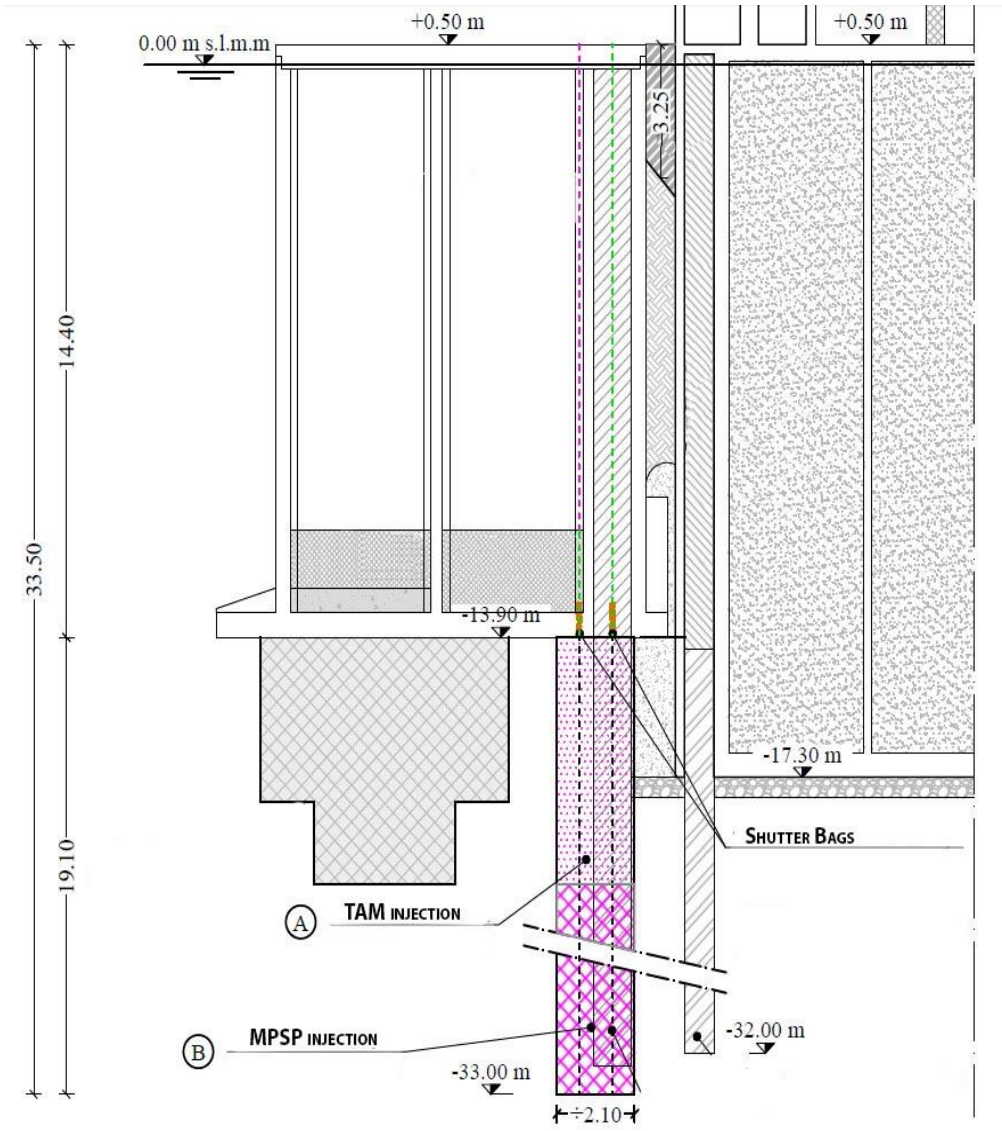

Figure 7-22: Cross section of injection treatment.

Figure 7-23 shows a shutter bags after being pumping with cement mix.

Figure 7-23: Shutter Bags after being pumping.

The cementitious and chemical mixtures were prepared and pumped by means of a specific mixing and pumping plants. As shown in Figure 7-24, two storage, doing and mixing plants were installed: one for the preparation of cement mix and the other for the chemical mixture. They included agitators, in which ready-to-inject grouts were stored and the characteristics of fluidity and homogeneity of the mixes were kept unchanged. Then pumps and injectors were fed in order to send the mixtures into the tubes and, thus, to inject the grouts into the holes. The pumping plant is shown in Figure 7-26, while Figure 7-25 shows the injection system.

Figure 7-24: Mixing plants instaled at Palermo Industrial Port.

Figure 7-25. Injection system at Palermo Industrial Port.

Figure 7-26: Pumping plant used at Palermo Industrial Port.

The whole injection system was controlled by a computerised system for automatic control, data acquisition, and automatic recording of grouting parameters: Grouting Parameter Control (GPC).

The GPC is composed by several sensors installed on the injectors (at the main plant and borehole mouth), and by a computer with software. The computerised system allows preparing a "project" that details the grouting parameters to be implemented for every single valve/stage for every hole. When the mixture is ready, the GPC send it to the injection tubes, while sensors, flow meters and digital pressure gauges measure the applied parameters in real time. These values are sent to the central system, which records and process them, and monitors grouting, by automatically controlling the operation of the injectors.

The strong point of GPC is the possibility of controlling the whole grouting process in real time. Thus, it is possible to automatically adapt injection to the geotechnical features and the data measured while working, ensuring at the same time high quality of treatment and simplified process management.

However, throughout all phases, the data were collected and analysed, in order to documents the works carried out.

Before performing the whole work, a test field was carried out in order to verify the effectiveness of the measures adopted. As shown in Figure 7-27, the first two injection of cement mixture fill the largest gaps of the soil, while the chemical mixture is able to penetrate deep down into the pores of the material as recorded in Figure 7-28.

In July 2019, all the injection activities were completed. In the following months, 54 boreholes were carried out and in each of them a pump were installed. At the end of 2019 the whole dry dock was emptied.

Figure 7-27: core drilling to evaluate the cement mixture performances.

Figure 7-28: core drilling to evaluate the chemical mixture performances.

7.8. Potential eco-friendly remediation techniques: TREVIMAT

Unequivocally the application of technologies mentioned above would drastically reduce the levee failure chance; nevertheless, the materials used, such as cement or chemical mixtures, are unsustainable and their implementation requires considerable investment.

The analyses conducted in Chapters 5 and 6 highlighted that an appropriate remediation technique should primarily have the objective of reduce the erosion process speed up by the burrowing animal activities. The levee failure due to erosion processes is a matter that needs a technology capable of reducing environmental impact at a minimum level and simultaneously one which is quick to implement, durable, and adoptable to the specific area to be protected and consolidated.

In order to take into account some sustainable remediation technique in the following sections the implementation of a geotextile is investigated. The geotextile analyzed is TREVIMAT studied and patented by GRUPPO TREVI in 80's. Nowadays, many engineering firms patented and/or applied similar technologies to reduce the surface erosion.

Trevimat is a geotextile product, consists of polypropylene technical fabrics and concrete element, thought for stabilization and protection against the erosion of natural and artificial slopes, embankments on land and sea, shorelines, seabed, riverbanks and beds, canal linings. In particular, it is used to halt erosion due to meteoric water, currents and tides.

Figure 7-29 shows the plan and the cross section of a hypothetical module. The product is characterized by distinguishing feature of the matting that has in woven loops directly into the weft of the geotextile for securing the anchorage ropes to the fabric itself. Generally, the mats are overlapping one each other. If a simple overlapping of the mats is insufficient to guarantee the TREVIMAT stability, i.e. in the case of steep slopes on in the presence of severing external dynamic stresses, it is advisable to use ropes. The ropes could be realized with plastic or galvanized steel

and may be placed in only one direction or arranged in two right-angled or diagonal directions. They are connected to the loops woven into the fabric. In rare cases and for a particular condition of the soil, the ropes may be connected to deep anchoring elements such as micropiles. Concrete elements are required for the anchorage with the soil and take different shapes and dimensions, as a function of the stability required.

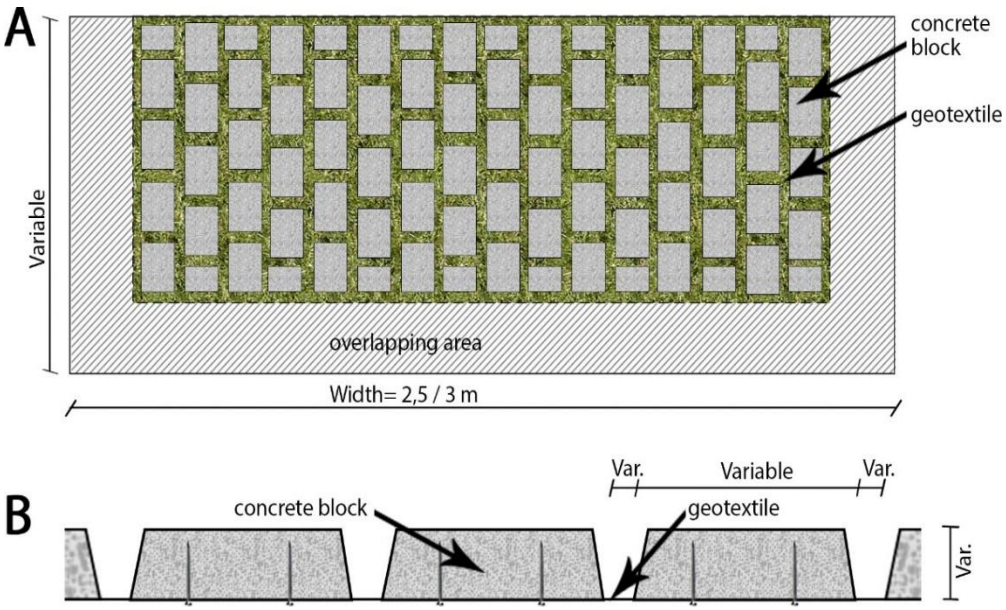

Figure 7-29: A) Trevimat plant; B) Trevimat Cross Section.

The polypropylene technical fabrics are characterized by high mechanical properties (tensile strength values, according to the various types used, of between 50 and 300 kN/m) and by suitable permeability characteristics to ensure the filtering and draining function (permeability values of between 8 and 32 lt/m2xsec). Moreover, the breaking strain is between 10% and 15%. The width of the matting is about 2.5-3 meter, while the length is variable.

The function of the concrete blocks is to provide the load required for the stabilizing operation; consequently, the design dimensions and the height of the

blocks will depend on this load. Generally, the stabilizing load ranges from 100 to 350 kg/m^2. The blocks are anchored to the sheet by means of plastic nails or some similar material which pass through the fabric so that the head remains on the side opposite the one on which the blocks are laid. For this purpose, the shank is fitted with a bulge that remains buried in the blocks during pouring. Alternatively, loops woven directly onto the matting may be used, for concrete anchoring. The concrete elements application can occur either in a prefabrication plant or in situ according to the working conditions. In order to ensure flexibility during the installation phases and to allow adaptation of the TREVIMAT to the soil surface, joints are left between the concrete elements, which could be filled with soil.

The implementation and application of this technology are actually simple. Preliminarily, anchors are provided on the sheet and the Trevimat modules are prefabricated. Figure 7-30 shows prefabricated Trevimat modules. These phases can occur in factories or on-site. After the complete concrete consolidation, the sheets are raised by means of a clamp that is hooked to the "short" ends of the sheet. In order to an assembly in situ the modules, the free joints are overlapped, and they are sewn together with propylene threads. Thanks to the simplicity of the sheet lifting, unhooking and re-hooking operations, and also to the modularity of their measurements, the configuration of the protection may be easily modified at a later date if required.

Moreover, in order to turn the Trevimat green, recesses are formed on the concrete elements and different vegetable species could be planted.

Figure 7-30: Prefabricated Trevimat modules.

7.9. Discussion and results

With the intention of finding the most successful remediation technique for the stability of earth levees weakened by burrowing animal activities, in this chapter have been presented some consolidation and sealing techniques of the soil.

The most effective technology is the CSP, described in Section 7.2, because if correctly implemented in the middle of the levee, it will create a solid barrier in reinforced concrete. As a result, not only the seepage phenomenon and the animals digging activities will be limited, but also other animal and vegetable lives.

Another interesting concrete barrier could be achieved by Jet Grouting technique. Modifying the rotation speed, it is possible to obtain a pseudo-elliptical column that reduces the consumption of concrete, as described in Section 7.3, and the amount of treated soil.

Figure 7-31 shows a simulation of the CSP (A) and Jet Grouting (B) works. However, these two techniques have to be extended to the whole levee, are very invasive, and involve an actually higher cost naturally.

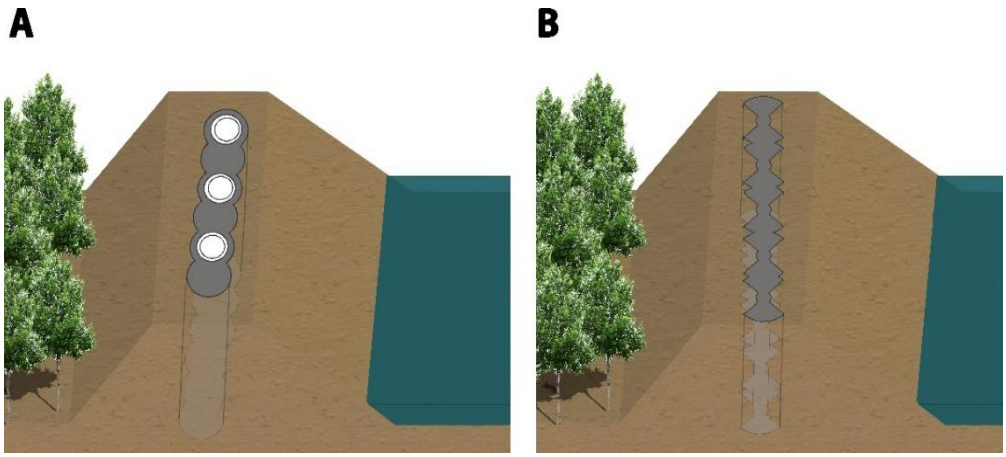

Figure 7-31: Remediation Techniques: A) CSP; B) Jet grouting.

Alternatively, micropiles (Section 7.4) and injections (Section 7.6) may be considered the most appropriate techniques to ensure the improvement of soil characteristics, intervening only in the most critical points of the levee. Specifically, micropiles increase the stability of the soil, whereas injections of cement mixtures reduce the soil permeability. Moreover, using appropriate additives, the injection techniques can preserve the plastic qualities of the soil.

However, depending on the soil type, not all technologies are equivalent as regards to solve a given problem. Indeed, as shown in Figure 7-32, the injection is profitable only for grain size more than 0.06 mm.

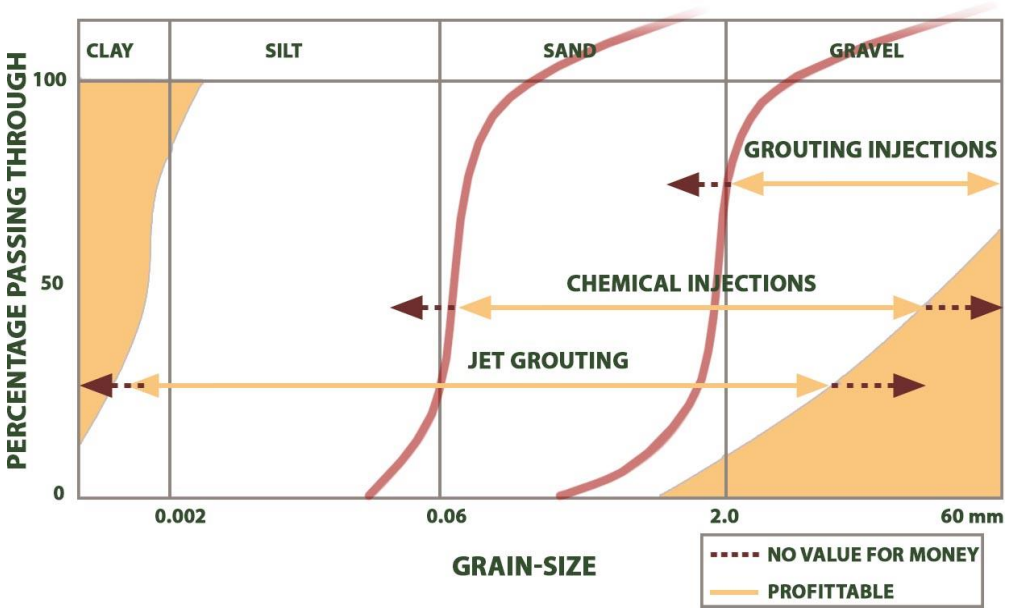

Figure 7-32: Profitability of injections or jet grouting according to soil grain size.

Furthermore, a project shall be considered satisfactory if it conceives the most efficient solution from a technical, design and economical point of view.

Taking these factors into account, it is believed that the application of Trevimat (described in Section 7.8) or similar products are probably the most suitable method

in order to increase the levee stability. It provides many advantages, such as flexibility, rapidity, maintenance, efficiency, durability, environmental impact and cost-effectiveness. Specifically, about the flexibility, this material offers the possibility of varying the permeability and resistance characteristics of the mat to easily adapt to the morphological and geotechnical characteristics of the specific soil conditions, while the weight of the concrete blocks providing the necessary stabilizing load. Moreover, the stability of the geotextile is also guaranteed by the anchoring systems. With regards to the rapidity, the possibility of using just one self-propelled crane for handling the Trevimat means that the mats can be laid quickly, even in difficult conditions and confined spaces, since the prefabrication plant of concrete blocks may locate at some distance from the job site. In connection with the maintenance, the possibility of using mats of various dimensions and the method used to connect these together, either by simple overlapping or by ropes, makes any replacement of damaged parts a quick and simple operation. The efficiency is guaranteed by the possibility of using row or grid arrangements of ropes bound to the mats and, if necessary, anchored to the ground with deep securing devise (tie-rods) or elements on the surface (beams or plates), which guarantees total stability, even on very steep slopes. The durability of this product is assured by the using of non-degenerative materials resistant to ultraviolet radiation and that makes the life of the Trevimat virtually limitless. Finally, regarding the environmental impact, both the mat and the concrete blocks can be covered by natural vegetation. In particular, the possibility of filing the empty spaces between the concrete blocks by hydroseeding or some other system makes for the rapid regeneration of the protected embankment.

Furthermore, the concrete blocks can be prefabricated with depressions suitable for the planting of all types of herbaceous plants to achieve the immediate revival of the slope. Figure 7-33 shows a simulation of what it might look like.

Figure 7-33: Hypothetical application of Trevimat to improve the earth levee stability.

Obviously, the rollout of Trevimat, or similar products, is less time-consuming and it is less complicated than the other technologies studied. Moreover, it could sufficiently effective in order to fix the problem of earth structure stability connected with the biological activities.

8. CONCLUSIONS

8.1. Summary of key results

The present dissertation aimed at contributing to the evaluation and mitigation of flood risk due to levee failures. In particular, the attention was focused on the impact of burrowing animal activities on levee stability. Such topic has received an increasing attention in the last years due to several reasons. Firstly, failure mechanisms induced by bioturbation activities seem to be unpredictable and cause catastrophic damage in flood-prone areas. Additionally, in the last years, those phenomena are increasing, and could be further worsened considering the immigration of invasive burrowing species as a consequence of climate changes. With regards to risk assessment, flood risk maps are usually developed with scarce consideration of the possible occurrence of levee failures along the river channel, and, if considered, they do not consider biological components. Finally, along with the assessment methodologies, the remediation techniques are still found not to be suitable to mitigate this kind of levee failure processes connected with burrow presence.

In the present research, a preliminary discussion on the main mechanisms that trigger levee failure was presented. In particular, the seepage phenomenon was acknowledged as one of the most common causes of levee failure all over the world. In Chapter 2, were examined the most common methodology used for assessing the seepage phenomenon. The levee attitude to undergo seepage processes without overtopping, that is its seepage vulnerability, was recognised as a key point to assess the reliability of the flood defence systems. Nevertheless, examining some past flood events, the analyses provided evidence on the fact that some levees should not have collapsed because of the given hydraulic and hydrological conditions. Consequently, some researchers started to analyse the connection between the levee failure happened and the animal burrows noted in those areas. It was widely recognized that the complex interaction between levee failure phenomena and the biota activities are fundamental to understand and manage both levee performances and animal

communities. Therefore, the importance of ecohydraulic modelling and experimentation was highlighted, an overview of burrowing animal behaviors and of burrow characteristics was presented, and the current state-of-the-art, which investigates the bioturbation impact on levee stability, was summarized.

Based on the analysed state-of-art, a Sicilian case study was considered. Specifically, the 2012 flood event occurred in the Dirillo river area was investigated. During that event, several unpredictable levee failures were registered. Thus, firstly, we assessed the main possible failure mechanisms to determine their causes; precisely, we studied overtopping with numerical simulations and seepage using analytical models. However, the analyses did not justify the flooding. Given that the chosen area was a site of burrowing animals, a field survey was performed. The goal of the levee inspections was to see the levee slope surfaces clearly, and indeed several animal burrows were identified on the landside levee slope. Unfortunately, the presence of dense vegetation did not allow to investigate properly the riverside slope. However, after a visual inspection of the activity of burrowing animals and after measuring the dimensions of the hole entrances, a Ground Penetrating Radar (GPR) survey was carried out, which allowed the depth and path of the dens to be detected. The investigation results showed that crested porcupines inhabit the burrows. The dens were not a single straight tunnel, but they were rather forked tunnels ("ψ" shaped) that connected the riverside slope to the landside slope. All burrows data measured were collected and analysed, in order to set up an experimental ecohydraulic activity and to understand the influence of burrow characteristics on the deterioration process that affect levees.

The ecohydraulic activity was performed at the Laboratory of Geography, Geology and Environment, University of Hull (UK), under the supervision of researchers specialize in the analysis of eco-hydraulic systems. The experiments aimed at contributing to the flood risk valuation in river ecosystem through the development of methodologies that considered the interactions between biological activities and levees stability. In particular, aiming at analysing the development of

surface erosion phenomenon, the surface erosion time of an undisturbed levee was compared with that of levees weakened by the presence of dens. An image analysis procedure was developed to measure the progression of morphological changes on the levee crest, as a proxy of the overall surface erosion process. Preliminary tests were performed in order to define an optimal soil composition, which allows a proper trade-off between the mean time of erosion and burrow stability. In the end, it was decided to continue the analyses using only fine sand (D_{50}=0,125 mm). The investigated burrow parameters were the following:

- burrow density: 5, 10 or 20 burrows;
- burrow length: 7 cm or 12 cm;
- vertical position: above or under water level;
- angle relative to the flow direction: 45°, 90°, or 135°.

A total of 110 experiments were conducted, keeping constant the flow characteristics.

The image analyses showed that the surface erosion increased at a large extent in levee damaged by burrows. The surface erosion of an intact levee after one hour involved the loss of 17% of the levee crest area, and this was the benchmark for the comparisons.

Primarily, the analyses proved that the erosion mechanism changes as a function of the vertical position of the burrows. The burrows above water level trigger an erosion that is from 23% to 35% of the levee crest area; it means that the erosion is increased between 35% and 106% compared to the intact levee. On the contrary, if the burrows are situated under water level, the erosion area will be between 3% and 26% of the levee crest area, and so it will be reduced compared to the benchmark.

Furthermore, the angle inclination of the burrow with respect to the flow direction seemed to have a significant influence on the erosion phenomenon. Indeed, the burrow configurations angled at 135° create the biggest eroded area. The increase is between 76% and 106% of the benchmark considering above water level configuration. For burrows angled at 45°, the eroded area is increase by 82%. The

burrows orthogonal to the flow direction have the less impact on the levee instability, indeed the increase is from 41% and 82% compared with the intact levee.

The density and length of the burrows did not show a clear trend. Moreover, the flow characteristics and the model dimensions may have affected the results. Thus, future researches would be need and should be concentrated on the development of the erosion process in the presence of burrows changing the flow parameters, and more importantly, changing flow rates to simulate a wave flood.

In any case, the physical model results enabled us to identify the main failure mechanisms playing a key role in the stability of the levees and quantifying the importance of biotic impacts on levee stability.

Additionally, the experimental activities highlighted the different development times of erosion and seepage phenomenon. When the water starts to flow on the landside, the levee is already quite eroded.

All those analyses suggest that the 2012 flood event very likely has been triggered by the presence of burrows. Indeed, the porcupine burrows were in the upper part of the levee, and their inclination was not orthogonal to the flow direction. Thus, the burrows found inside Dirillo levee were the most dangerous configurations. Their presence could have reduced the time of surface erosion, such as observed in the experimental activities, and could have caused a collapse of the levee crest. This mechanism might justify the following overtopping.

Finally, the research was also aimed at defining sustainable “restoration” techniques. In particular, collaborating with Trevi S.p.A., an overview of the know-how on the principal soil consolidation techniques was drafted. The techniques discussed, such as CPS, micropiles, injections and Jet Grouting, can consolidate different types of terrains and reduce the permeability of the soil. To identify the most suitable technology with the least environmental impact and with a good cost-effectiveness ratio, Trevimat was studied. This geotextile product, consists of polypropylene technical fabrics and concrete element, offers the possibility of increasing the resistance of the levee, without changes its soil characteristics.

Moreover, it permits an easy adaptation to different types of soil conditions. This product is the most efficient solution from a technological, design and economical point of view since it provides many advantages, such as flexibility, rapidity, maintenance, efficiency, durability, and cost-effectiveness. From an environmental point of view, it does not alter the river ecosystem and, by planting different plant species on the geotextile or the recesses onto the concrete elements, the vegetation could rapidly regenerate the levee.

In conclusion, the present research provides an increased knowledge in the field of flood risk protection from a different point of views and the results obtained suggest that this research direction is appropriate. First, the traditional approach of the study of levee failures based exclusively on hydraulic and geotechnical considerations is overcome. Indeed, the present study contributes to the understanding of the interactions between earth levee and burrowing animal activities, through a multidisciplinary approach mainly based on ecohydraulic methodology. The experimental activities results helped to highlight geometrical parameters of burrows that have a greater adverse impact on levee stability. Specifically, the physical model truly improves to understand how the burrow presence affects levee reliability, and precisely how affects surface erosion phenomena. These results are useful to support more realistic and more process-oriented approaches for the assessment of the failure mechanisms that can trigger the collapse of the river defence structures.

However, the performed experimental program represents a first step and, of course, cannot be considered exhaustive of the topics. Further investigations are recommended to achieve a complete flood risk evaluation methodology and to improve the flood hazard maps considering the bioturbation impact. In particular, other experiments should be carried out introducing further hydraulic and geotechnical variables, such as changes of water level, flow velocity, levee slope inclination, or soil composition. Additionally, new burrows geometries should be investigated (i.e. "ψ"-shaped). Anyway, the knowledge and data generated by the experimental activities can be used for the development of more reliable numerical

models, which are capable to predict levee failures, by considering the impact of animal activities.

From the monitoring point of view, the GPR survey was proved suitable to achieve a punctual reconstruction of the burrows inside the earth structures. Nevertheless, further investigations should be performed in order to reduce the analysis time and to allow frequent monitoring of the levees.

From a practical point of view, the results can provide valuable information that can contribute to the definition of proper techniques for restoration of levees. The investigation of remediation techniques suggests some suitable approaches, from different point of views. Nevertheless, further inquiries are required to understand the burrowing animals answer to the installation of a geotextile layers.

Lastly, it is clear that traditional approaches based solely on combined hydrological-hydraulic-geotechnical modelling is not enough to investigate levee failure risk, and that a more holistic and multidisciplinary methodology should be employed. Remediation techniques may also take advantage from other disciplines, such as biology and ecology, which coupled with hydrological, hydraulic and geotechnical approaches may suggest innovative and non-invasive techniques to relocate animals to areas where their activity does impact risk of flooding at a large extent.

ACKNOWLEDGEMENTS

The present work was funded through the MIUR industrial project “Dottorato Innovativo a Caratterizzazione Industriale”, whose purpose was to investigate the performance of a deteriorated earth structure.

In order to achieve the proposed objective, the present research involved various professional who contributed in different ways and whom I would like to thank. First of all, I would like to express my deep and sincere gratitude to my research supervisor, Prof. E. Foti, guidance and support, for always reminding me about the importance of this research and supporting me. Thanks to his leadership, I have learnt the importance of teamwork. Indeed, I could have not completed this research without the contribution of all the research group members. In particular, I would like to sincerely thank Rosaria (Prof. Musumeci), my “daily supervisor”, who invested quite a lot of time in me and in reading thoroughly my work, and to Prof. A. Cancelliere, for sharing his original and ambitious ideas. Moreover, I am extremely grateful to the postdocs at the University of Catania who helped me in different way. Specifically, to my office mate Laura M. Stancanelli for being the greatest colleague during all these years and for helping me at all stages of my research, especially during the experimental analyses; to David J. Peres, who dedicated time helping me with the flood event analyses; to Luca Cavallaro, who was always available to solve all my questions. Moreover, even if they are not part of the research group, I wish to acknowledge Prof. R. Grasso and Prof. M.T. Spena, for conveying me their enthusiasm for the animal studies and for helping me during the field surveys, and A. Ferrero, for giving me the opportunity to use the GPR.

I would like to thank my English supervisor, Prof. Stuart McLelland, who welcomed me to UK, gave me all the necessary help to implement my experimental activity, and had time for me. Moreover, I thank prof. Dan Parsons for the interesting conversations on my research topic, and to Brandon, Hannah, and Laura for their help in the lab. During my English period, I met many people who contributed not only to my research, but also to everything I needed, while offering a nice smile. Thus, I have

to thank Catastrophic Flows PhD students, Sergio, Bas, and Robert, the other PhD students at the University of Hull, and above all Cristina, for taking care of me whenever I felt lonely and for becoming my International English Family.

Moreover, I wish to acknowledge the significant contribution of Trevi S.p.A. for the training activities on the development of eco-friendly solution for levee remediation.

Finally, I would like to sincerely thank my reviewers, for sharing their interesting and useful comments/suggestions. Especially, I would like to express my deep gratitude to Prof. Claudio I. Meier, for investing quite a lot of time reading carefully every sentence of my work and for helping me improve my thesis, and to Prof. Luca Solari for giving me valuable advice.

LIST OF FIGURES

LIST OF TABLES

BIBLIOGRAPHY

Aller R. C., Yingst, J. Y. (1980), Relationships between microbial distributions and the anaerobic decomposition of organic matter in surface sediments of long Island Sound, USA, Marine Biology 56: 29-42, doi.org/10.1007/BF00390591;

Amori, G. and F.M. Angelici (1992). Note on the status of the crested porcupine Hystrix cristata in Italy. *Lutra*, 35:44-50;

Apel H., Merz B. & Thieken A.H.(2008) Quantification of uncertainties in flood risk assessments. International Journal of River Basin Management. 6, (2), 149–162, doi:10.1080/15715124.2008.9635344;

Arulanandan K., Perry B., (1984). Erosion in relation to filter design criteria in earth dams. Journal of Geotechnical Engineering, 109(5), 682-698. doi:10.1061/(ASCE)0733-9410(1983)109:5(682);

Barbetta, S., Moramarco, T., & Perumal, M. (2015). A Muskingum-based methodology for river discharge estimation and rating curve development under significant lateral inflow conditions. Journal of Hydrology, 554, 216–232. https://doi.org/10.1016/j.jhydrol.2017.09.022;

Bayoumi, A., & Meguid, M. A. (2011). Wildlife and safety of earthen structures: A review. Journal of Failure Analysis and Prevention, 11(4), 295–319. https://doi.org/10.1007/s11668-011-9439-y;

Bezzazi M., Khamlichi A., Parron Vera M. A., Rubio Cintas M.D., (2010) A simplified analytical modeling of the Hole Erosion Test, *American Journal of Engineering and Applied Sciences* 3(4): 765-768, doi: 10.3844/ajeassp.2010.765.768;

Black, J.A., Khan, I.U., Nakashima, K. (2019) Flood performance of earth embankment. Proceedings of the XVII ECSMGE-2019 (In press). Geotechnical Engineering foundation of the future ISBN 978-9935-9436-1-3, doi:10.32075/17ECSMGE-2019-0789;

Black, M. (1962) Models and Metaphors. Ithaca NY: Cornell University;

Blume T., Zehe E., Bronstert A. (2007) Rainfall-runoff response, event-based runoff coefficients and hydrograph separation, *Hydrological Sciences Journal*, 52:5, 843-862, doi: 10.1623/hysj.52.5.843

Bonanni G., Carli A., Casarosa N., Ceragioli N., Dell'Aiuto S., Della Maggesa M., Forti M., Matteoni S., Panocchia A., Sardi L. (2009) La rotta arginale del Serchio a Malaventre (frazione di Nodica) nel giorno di Natale 2009. Il Geologo 2010, 79, 4–19;

Camici, S., Moramarco, T., Brocca, L., Melone, F., Lapenna, V., Perrone, A., Loperte, A. (2006). On mechanisms triggering the levee failure along the Foenna stream on 1st January 2006 and which caused the flooding in the urban area of Sinalunga, Tuscany Region (Italy). A case study. *Geophys. Res*. Abstr. 12, 12037;

Camici, S., Moramarco, T., Brocca, L., Melone, F., & Lapenna, V. (2010). On mechanisms triggering the levees failure along the Foenna stream on 1st January 2006 and which caused the flooding in the urban area of Sinalunga , Tuscany Region (Italy). A case study. 12, 12037;

Camici, S., Barbetta, S., & Moramarco, T. (2017). Levee body vulnerability to seepage: the case study of the levee failure along the Foenna stream on 1 January 2006 (central Italy). Journal of Flood Risk Management, 10(3), 314–325. https://doi.org/10.1111/jfr3.12137;

Cantero-Chinchilla, Francisco Nicolás, Castro-Orgaz, Oscar and Dey, Subhasish (2019) Prediction of overtopping dike failure: sediment transport and dynamic granular bed deformation model. Journal of Hydraulic Engineering, 145 (6), 1-14, [04019021]. doi:10.1061/(ASCE)HY.1943-7900.0001608;

Carroll, P. H. (1949), Soil piping in Southeastern Arizona, in Regional Bulletin, Soil Ser., vol. 110, U.S. Dep. of Agric., Soil Conserv. Serv., Albuquerque, N. M.;

Casagrande, A. 1936. The determination of the preconsolidation load and its practical significance. In Proceedings of the 1st InternationalConference on Soil Mechanics and

Foundation Engineering, Cambridge, Mass. A.A. Balkema, Rotterdam, The Netherlands. Vol. 3, pp. 60–64;

Ciria, Ministry of Ecology, USACE (2013) The International Levee Handbook, ISBN: 978-0-86017-734-0, Number of pages: 1348;

Chlaib, H. K., Mahdi, H., Al-Shukri, H., Su, M. M., Catakli, A., & Abd, N. (2014). Using ground penetrating radar in levee assessment to detect small-scale animal burrows. Journal of Applied Geophysics, 103, 121–131. https://doi.org/10.1016/j.jappgeo.2014.01.011;

Chorley R.J., (1964) Geography and Analogue Theory. Annals Association of American Geographers, 54:127–137, doi: 10.1111/j.1467-8306.1964.tb00478.x;

Coleman, F.C., Williams S.L. (2002), Overexploiting marine ecosystem engineers: potential consequences for biodiversity. TRENDS in Ecology & Evolution. Vol. 17 n.1, 40-44;

Corsini M.T., Lovari S., Sonnino S., (1995). Temporal activity patterns of crested porcupines Hystrix cristata. *Journal of Zoology* doi: 10.1111/j.1469-7998.1995.tb01783.x;

Cosanti B., Squeglia N., Lo Presti D.C. (2011) Indagini geotecniche e analisi di stabilità degli argini del fiume Serchio dopo l'alluvione del Dicembre 2009. Proceedings of IARG 2011, Torino;

De Backer, A., Van Colen, C., Vincx, M., Degraer, S. (2010). The role of biophysical interactions within the ijzermonding tidal flat sediment dynamics. Continental Shelf Research, 30(9), 1166-1179. https://doi.org/10.1016/j.csr.2010.03.006;

Deretsky Z., (2010) Ten Ways a Levee Can Fail, National Science Foundation;

Di Prinzio, M., Bittelli, M., Castellarin, A., & Pisa, P. R. (2010). Application of GPR to the monitoring of river embankments. Journal of Applied Geophysics, 71(2–3), 53–61. https://doi.org/10.1016/j.jappgeo.2010.04.002;

Dooge J.C.I., (1973), Linear theory of hydrologic system. *US Department of Agriculture, Technical Bullletin 1468;*

FEMA. (2005). Technical Manual for Dam Owners: Impacts of Animals on Earthen Dams.pp:1-115. *Management Agency (FEMA) and the Association of State Dam Safety Officials*. FEMA 473;

Frostick L. E., Thomas R.E., Johnson M.F., Rice S.P., McLelland S.J. (eds) (2014) Users Guide to Ecohydraulic Modelling and Experimentation: Experience of the Ecohydraulic Research Team (PISCES) of the HYDRALAB Network, CRC Press/Blkema, Leiden, The Netherlands;

Green W.H., Ampt G.A. (1911) Studies on soil physics, part 1: the flow of air and water through soils. *Journal of Agricultural Science* 1911, 4, 1–24;

Grimaldi S., Petroselli, A., Tauro, F., Porfiri, M., (2012), Time of concentration: A paradox in modern hydrology, *Hydrological Sciences Journal*, 57 (2):217-228, doi: 10.1080/02626667.2011.644244;

Hagerty, D., (1992). Piping/Sapping Erosion. I: Basic considerations. *Journal of Hydraulic Engineering 117*(8), 991–1008;

Haubrock P.J., Inghilesi A.F., Mazza G., Bendoni M., Solari L., Tricarico E., (2019) Burrowing activity of *Procamnarus clarkii* on levees: analysing behaviour and burrow structure. Wetlands Ecology Menagement, 27, 497-511, doi: 10.1007/s11273-019-09674-3;

Heerden, I. (2005), Preliminary report on the performance of the New Orleans levees;

Helfrich, L. A., Parkhurst, J., & Neves, R. (2001). The Control of Burrowing Crayfish in Ponds. *Virginia Cooperative Extension*, publication 420-253;

Hobbs, H. H. III, & Lodge, D.M., (2010) Ecology and Classification of North American Freshwater Invertebrates Chapter 22. *Decapoda*, p. 901–967. Third edition. J. H. Thorp and A.P. Covich (eds.). Academic Press (Elsevier), London;

(19) (PDF) A New Genus and Species of Blind Sleeper (Teleostei: Eleotridae) from Oaxaca, Mexico: First Obligate Cave Gobiiform in the Western Hemisphere. Available from:

https://www.researchgate.net/publication/303981113_A_New_Genus_and_Species_of_Blind_Sleeper_Teleostei_Eleotridae_from_Oaxaca_Mexico_First_Obligate_Cave_Gobiiform_in_the_Western_Hemisphere [accessed May 21 2020].

Hori, T., Mohri, Y., Kohgo, Y., & Matsushima, K. (2011). Model test and consolidation analysis of failure of a loose sandy embankment dam during seepage. *Soils and Foundations*, *51*(1), 53–66. https://doi.org/10.3208/sandf.51.53;

Horlacher H.B., Bielagk U. & Heyer T. Analyse der Deichbrüchean der Elbe und Mulde während des Hochwassers (2002) im Bereich Sachsen. Research report 2005/09, Institut für Was-serbau und Technische Hydromechanik, Technische Univer-sität Dresden, 2005, 82.

Hygnstrom S. E., Timm R. M., Larson G. E.. (1994), Prevention and Control of Wildlife Damage, University of Nebraska-Lincoln. 2 vols, 4th Edition, *Cooperative Extension Division - Institute of Agriculture and Natural Resources- University of Nebraska – Lincoln; United States Department of Agriculture-Animal and Plant Health Inspection Service-Animal Damage Control; Great Plains Agricultural Council Wildlife Committee;*

Jonkman, S. N., & Vrijling, J. K. (2008). Loss of life due to floods. *Journal of Flood Risk Management*, 1(1), 43–56. https://doi.org/10.1111/j.1753-318x.2008.00006.x

Kamalzare, M., Han, T., McMullan, M., Stuetzle, C., Zimmie, T., Cutler, B., and Franklin, W. (2013) Computer Simulation of Levee Erosion and Overtopping. In: Meehan, C., Pradel, D., Pando, M.A., Labuz J.F. (eds).*Proc. Geo-Congress at Stability and Performance of Slopes and Embankments*; March 3-7, 2013, San Diego, United States. pp. 1851-1860;

Kleinhans, M. G., et al. (2014), *Quantifiable effectiveness of experimental scaling of river- and delta morphodynamics and stratigraphy*, Earth Sci. Rev.,133, 43–61, doi:10.1016/j.earscirev.2014.0;

Ko, D., & Kang, J. (2018). Experimental studies on the stability assessment of a levee using reinforced soil based on a biopolymer. Water (Switzerland), 10(8), 1–11. doi:10.3390/w10081059;

Lal M.; Mishra S.K.; Pandey A.; Pandey R.P.; Meena P.K.; Chaudhary A.; Jha R. K.; Shreevastava A.K.; Kumar Y. (2016) Evaluation of the Soil Conservation Service curve number methodology using data from agricultural plots. *Hydrogeology Journal*, v. 25, n. 1, p. 151-167. http://dx.doi.org/10.1007/s10040-016-1460-5;

Loat, R. (2009). Flood mapping in Europe – EXCIMAP. UNECE workshop on transboundary flood risk management. Geneva;

Lugeri, N., Kundzewicz, Z. W., Genovese, E., Hochrainer, S., & Radziejewski, M. (2010). River flood risk and adaptation in Europe-assessment of the present status. *Mitigation and Adaptation Strategies for Global Change*, *15*(7), 621–639. https://doi.org/10.1007/s11027-009-9211-8;

Marchi E.(1961) Sulla filtrazione attraverso gli argini fluviali. *Proceedings of VII Convegno di Idraulica e Costruzioni Idrauliche,* Palermo;

Mears BJr. 1968. *Piping*, in Fairbridge. RW (editor) – The Encyclopedia of Geomorphology, Ed. Reinhold, New York, 849-450;

Mockus, V., (1957). Use of storm and watershed characteristics in synthetic hydrograph analysis and application. *American Geophysics Union, Southwest Region Meeting, Sacramento, California;*

Masannat, Y. M. (1980), Development of piping erosion conditions in the Benson area, Arizona, U.S.A., *Quarterly Journal of Engineering Geology and Hydrogeologyl.*,13(1), 53–61, doi:10.1144/GSL.QJEG.1980.013.01.04;

Michelazzo, G., Paris, E., & Solari, L. (2016). On the vulnerability of river levees induced by seepage. *Journal of Flood Risk Management*, *11*(December 2009), S677–S686. https://doi.org/10.1111/jfr3.12261;

Michelazzo, G. (2014). Breaching of river levees : analytical flow modelling and experimental hydro-morphodynamic investigations, *PhD Dissertation* November 2013, University of Florence;

Mohamed Elmoustafa, A. (2012) Weighted normalized risk factor for floods risk assessment. *Ain Shams Engineering Journal*, 3(4), pp. 327-332. doi: 10.1016/j.asej.2012.04.001;

Morris, M., Hassan, M., Kortenhaus, A., Visser, P.J., (2009), Breaching Processes: A state of the art review. *FLOOD site Project Report, T06-06-03;*

Morris M., Dyer M. & Smith P. (2007) Management of flood embankments. A good practice review. Defra/Environment Agency Flood and Coastal Defence R&D Programme, Technical Report FD2411/TR1;

Nagy L. (2006) Estimating Dike Breach Length from Historical Data. *Periodical Civil Engineering* 50, (2), 125–138;

Nagy L., Tòth S. (2005), Detailed Technical Report on the collation and analysis of dike breach data with regards to formation process and location factors. *Technical Report, H-EURAquaLtd*., Hungary;

Oliveira P.T.S.; Nearing M.A.; Hawkins R. H.; Stone J.J.; Rodrigues D.B.B.; Panachuki E.; Wendland E. (2016) Curve number estimation from Brazilian Cerrado rainfall and runoff data. *Journal of Soil and Water Conservation*, v. 71, n. 5, p. 420 - 429. http://dx.doi.org/10.2489/jswc.71.5.420;

Ozkan S. (2003) Analytical study on flood induced seepage under river levees. *PhD Dissertation*. Louisiana State University;

Orlandini S, Moretti G., Albertson J.D., (2015) Evidence of an emerging levee failure mechanism causing disastrous floods in Italy, *Water Resources Research*, 51, 7995-8011, doi:10.1002/2015WR017426;

PAI (2004). Piano stralcio di bacino per l'Assetto Idrogeologico (P.A.I.) della Regione Siciliana;

Palladino, M. R., Barbetta, S., Camici, S., Claps, P., & Moramarco, T. (2019). Impact of animal burrows on earthen levee body vulnerability to seepage. *Journal of Flood Risk Management*, *13*(S1). https://doi.org/10.1111/jfr3.12559;

Paola, C., K. Straub, D. Mohrig, and L. Reinhardt (2009), *The unreasonable effectiveness of stratigraphic and geomorphic experiments*, Earth Sci. Rev.,97(1–4), 1–43, doi:10.1016/j.earscirev.2009.0;

Pilati N., Pepe M., Gialletti R., Moriconi F.,Beccati F., (2015) Septic Tenosynovitis Caused by Porcupine Quills: Clinical and Diagnostic Findings, Treatment, and Long-Term Outcome in Seven Horses. *Journal of Equine Veterinary Science*, Vol.35 Issue 4, 321-326, doi:10.1016/j.jevs.2015.01.012;

Pistocchi A., Zani O. & Donati F. (2004) Sul calcolo dei tempi di saturazione delle arginature. *Proceedings of XXIX IDRA Congress*, Trento (Italy), 3, 457–46;

Reichman, O.J., Smith, S.C. (1990) Burrows and burrowing behavior by mammals, Chap. 5. *Genoways, H.H.* (ed.) Current Mammalogy, pp. 197–244. Plenum Press, New York, London;

Resio, D., S. Boc, D. Ward, A. Kleinman, J. Fowler, B. Weksh, M. Mataik, P. Goodwin (2011), U.S. Army Engineer Research and Development Center: Rapid repair of levee breaches, SERRI Rep. 81000-01, Oak Ridge National Lab., Oak Ridge, Tenn;

Reuss, R.F., Schattenberg, J.W., (1972), Internal piping and shear deformation, Victor Braunig Dam.San Antonio, Texas, *Proceedings of the Specialty Conference on Performance of Earth and Erath-Supported Structures,* ASCE, Vol. I, Part.1 pp 627-651;

Reynolds J.M. (1997), An Introduction to Applied Environmental Geophysics, *Chichester: John Wiley & Sons*. ISBN 10: 0471968021 ISBN 13: 9780471968023;

Rice, S. p., Johnson, M. F., Mathers, K., Reeds, J., & Extence, C. (2016). Journal of Geophysical Research : Earth Surface fl uvial sediment transport. *Journal of Geophysical Research: Earth Surface*, *121*(5), 890–906. https://doi.org/10.1002/2015JF003726;

Roa, D. C., Shriro, M., Sitar, N., & Bray, J. D. (2014). Influence of Tree Roots and Mammal Burrowing Activity on Levee Performance : California Levee Vegetation Research Program Influence of Tree Roots and Mammal Burrowing Activity on Levee Integrity : Volume 4 . – Field Evaluation of Burrowing Animal Impacts and Effectiveness of Remedial Measures (August). doi:10.13140/RG.2.2.26069.42728;

Roper, T. J. (1992), Badger Meles meles setts - architecture, internal environment and function, *Mammal Review*, 22(1), 43–53, doi: 10.1111/j.1365-2907.1992.tb00118.x;

Roze U., (2009) The North American porcupine, *Cornel University, Ithsvs, New York 14850;*

Saadi, M., Athanasopoulos-Zekkos, A., (2013) A GIS-Enabled Approach for Assessing Damage Potential of Levee Systems Based on Underlying Geology and River Morphology. *Mathematical Problems in Engineering.* Volume 2013, 1-20, Article ID 936468, doi: 10.1155/2013/936468;

Saghaee, G., Mousa, A. A., & Meguid, M. A. (2016). Experimental evaluation of the performance of earth levees deteriorated by wildlife activities. *Acta Geotechnica*, *11*(1), 83–93. https://doi.org/10.1007/s11440-015-0373-0;

Saghaee, G., Mousa, A. A., & Meguid, M. A. (2017). Plausible failure mechanisms of wildlife-damaged earth levees: Insights from centrifuge modeling and numerical analysis. *Canadian Geotechnical Journal*, *54*(10), 1496–1508. https://doi.org/10.1139/cgj-2016-0484;

Saucier C., Howard I.L., Tom J.G. (2009) Levee breach geometries and algorithms to simulate breach closure. SERRI Report 70015-001, US Department of Homeland Security Science and Technology Directorate;

Seed, R. B., Bea, R. G., Athanasopoulos-Zekkos, A., Boutwell, G. P., Bray, J. D., Cheung, C., Cobos-Roa, D., Harder Jr. L. F., Moss, R. E. S., Pestana, J. M., Riemer, M. F.,Rogers,J. D. Storesund, R.,Vera-Grunauer,X.andWartman, J. (2008) New Orleans and Hurricane Katrina.III: The 17th Street Drainage Canal. *Journal of Geotechnical and Geoenvironmental*. 134:740-761;

Sellmeijer, J. (1988). On the mechanism of piping under impervious structures. *PhD Dissertation.* University of Technology Delft;

Sherard, J. L., Decker, R. S., Ryker, N. L.(1972) Piping in earth dams of dispersive clay. *Proc., Specialty Conf. on Performance of Earth and Earth Supported Structures,* Vol. 1, Part 1, ASCE, NewYork, 589–626;

Taccari, M. L., & Van Der Meij, R. (2016). Investigation of the influence of animal burrowing on the failure of the levee of San Matteo along the Secchia river. *E3S Web of Conferences*, *9*, 1–6. https://doi.org/10.1051/e3sconf/20160919001;

Taccari, M. L., & Van Der Meij, R. (2016). Study of the effect of burrows of European Badgers (Meles meles) on the initiation of breaching in dikes. E3S Web of Conferences, 7. https://doi.org/10.1051/e3sconf/20160703001;

Terzaghi, K., R. B. Peck, and G. Mesri (1996),Soil Mechanics in Engineering Practice, 3rd ed., 592 pp., John Wiley, N. Y;

Terzaghi, K.., (1929). Effect of minor geologic details on the safety of dams. *Geotechnical Special Publication* No. 118, Volume 1, 118(1), pp.39–54;

Tocchetto G., (2000) Indagine sulla struttura delle tane di Nutria Myocastor Coypus (Molina, 1782) e loro impatto sulle arginature dei corsi d'acqua. *III Convegno faunisti veneti*;

Toschi A., (1965) FAUNA D'ITALIA - Vol. VII. MAMMALIA: Lagomorpha - Rodentia - Carnivora - Ungulata - Artiodactyla – Cetacea, *edizioni Calderini*.

Vleck, D. (1979), The energy cost of burrowing by the pocket gopher. *Thomomys bottae*, *Physiological Zoology.*, 52(2), 122–136, doi: 10.1086/physzool.52.2.30152558;

Yang C.T., Wang L.K., (2015) Advances in water resources engineering, *Handbook of Environmental Engineering Series, Vol. 14, Springer* ISBN 9783319385501;

Winterwerp, J.C., Van Kesteren, W. G. M. (2004). Introduction to the Physics of Cohesive Sediment in the Marine Environment. *Developments in Sedimentology Serie n.56* doi:10.1017/S0016756806211944;

Woods C.A. (1973) Erethizon dorsatum, Mammal Species, 29 *American Society of Mammalogists*, doi: 10.2307/3504036;

Zhu HY, Jia SF (2004) Uncertainty in the spatial interpolation of rainfall data. *Progress in Geography* 23(2):34–42.

La borsa di dottorato è stata cofinanziata con risorse del
Programma Operativo Nazionale Ricerca e Innovazione 2014-2020 (CCI 2014IT16M2OP005),
Fondo Sociale Europeo, Azione I.1 “Dottorati Innovativi con caratterizzazione Industriale”

UNIONE EUROPEA
Fondo Sociale Europeo